To the Graduate Council:

I am submitting herewith a dissertation written by Ronald Lewis Clouse entitled "The Mathematical Modeling and Validation of Gas Flow Processes in Large Industrial Facilities." I have examined the final copy of this dissertation for form and content and recommend that it be accepted in partial fulfillment of the requirements for the degree of Doctor of Philosophy, with a major in Mechanical Engineering.

R. L. Young, Major Professor

We have read this dissertation
and recommend its acceptance:

Roy J. Schulz

Roy A. Crawford

James W. Cunning

Accepted for the Council:

Vice Provost
and Dean of the Graduate School

THE MATHEMATICAL MODELING AND VALIDATION OF GAS FLOW PROCESSES IN LARGE INDUSTRIAL FACILITIES

A Dissertation

Presented for the

Doctor of Philosophy

Degree

The University of Tennessee, Knoxville

Ronald Lewis Clouse

August 1990

DEDICATION

This dissertation is dedicated to my parents, William McKinley and Lena Clouse -- whose formal education included only the eighth and fourth grades, respectively -- but whose faith and confidence in me never faltered, not once.

ACKNOWLEDGMENTS

I am deeply indebted to many people for their support during my academic career that has spanned portions of six decades. First, I am reminded of my first grade teacher, Miss Blanche Kirk, who made a tremendous, positive impression on my life. Memories of those early years also include Mr. O. M. Brown who walked some twelve miles daily, in all types of weather, to teach at Fredonia Elementary.

Dr. R. L. Young, under whom I took my first graduate course some 27 years ago, has provided constant inspiration. He will undoubtedly be remembered as one of the greatest educators that the university has ever had. Dr. J. W. Cunningham, my ex-supervisor and one of the most technically talented men I have ever known, has provided support and encouragement for many years.

I am also indebted to my wife, Diane, and children, Mrs. Renee Holt and Miss Mysty Clouse. Too often they were without a husband and father, but they did so without a single complaint.

Last, but certainly not least, I humbly recognize and acknowledge all the support from my parents, William McKinley and Lena Clouse, who are 92 and 83 years old, respectively. I earnestly pray that they are physically able to attend the graduation ceremonies.

God bless all of you!

ABSTRACT

The activation of large, industrial facilities characterized by gas pumping and conditioning equipment may require that facility operators be trained and control system hardware and software be activated via a computer system hosting a simulation of the various gas flow processes within the facility. The mathematical relationships represented by the simulation must be kept quite simple because the simulation must execute in "real time." The requirement for a high degree of accuracy for the mathematical model may also be present thus compounding an already challenging problem.

The new Aeropropulsion Systems Test Facility (ASTF) at the Arnold Engineering Development Center in Tennessee is an example of such a facility. All of the gas flow processes within this facility were mathematically modeled and a large portion of the facility was simulated in real time utilizing an off-the-shelf minicomputer as a part of the facility activation and operator training. In the portions of the facility where "near steady-state" conditions exist, the development was relatively straightforward. However, in areas where transient phenomena occur, many challenges were successfully overcome without the necessity of resorting to partial differential equations in spatial coordinates and time -- a technique that would have surely negated the possibility of a real time simulation. Although many problems were encountered along the way, the Automatic Test Control System -- the system that controls test conditions in ASTF -- was

successfully activated and the operators were trained prior to the initial operation of the facility.

This dissertation presents a summary of the math modeling project for the ASTF. A conscientious attempt has been made throughout the presentation to keep all the material as general as possible such that the tailoring of methods and techniques to other, similar facilities will be minimal.

TABLE OF CONTENTS

CHAPTER		PAGE
1.	INTRODUCTION	1
2.	BRIEF DESCRIPTION OF THE AEROPROPULSION SYSTEMS TEST FACILITY (ASTF)	5
	2.1 Overview	5
	2.2 The Air Supply System	8
	2.3 The Exhaust System	11
	2.4 Subsystems	14
	2.5 The Automatic Test Control System (ATCS)	21
3.	THE MATHEMATICAL MODELS	24
	3.1 General	24
	3.2 Subsystems	37
	3.3 Systems	60
4.	VALIDATION	98
	4.1 General	98
	4.2 ASTF Validation	104
5.	A METHODOLOGY FOR THE DEVELOPMENT OF MATH MODELS AND SIMULATIONS	129
	5.1 Background	129
	5.2 Brief Review of the Modeling and Simulating Process	131
	5.3 The Methodology	133

CHAPTER PAGE

5.4 Application of Methodology at the AEDC 153

5.5 Application to Other Development Efforts 153

5.6 Summary 154

6.0 SUMMARY AND RECOMMENDATIONS 156

BIBLIOGRAPHY 160

VITA 162

LIST OF FIGURES

FIGURE		PAGE
2.1-1	The Aeropropulsion Systems Test Facility (ASTF) .	6
2.2-1	Air Supply System Schematic - ASTF	9
2.3-1	Exhaust System Schematic - ASTF	12
2.4.4-1	Typical Turboexpander Arrangement	17
2.4.4-2	Turboexpander Radial Vane Mechanism	18
2.4.5-1	Test Area Layout	19
2.5-1	Valves Controlled by ATCS	22
3.1.1-1	Example of the Lumped Parameter Technique	27
3.1.1-2	Lumped Parameter Representation of ASTF	28
3.2.1-1	Schematic of Compressor or Exhauster	41
3.2.1-2	Generic Plots of Compressor or Exhauster, Mathematical Model	46
3.2.2.1-1	Schematic of Butterfly Valve Installation	47
3.2.3.2-1	Turboexpander Quantities of Importance - Original Assessment	56
3.3.2.3-1	Schematic for Isothermal - Adiabatic Flow Example	69
3.3.2.3-2	"Isothermal/Adiabatic" Comparison - Pressure . .	70
3.3.2.3-3	"Isothermal/Adiabatic" Comparison - Mass Flowrate	71
3.3.2.3-4	"Isothermal/Adiabatic" Comparison - Temperature	72
3.3.2.5-1	Effect of Mixing on Outlet Temperature	79

FIGURE PAGE

3.3.2.5.1-1 The "N Sub-Volume Technique:" Single Inlet-Single Outlet 81

3.3.2.5.2-1 The "N Sub-Volume Technique:" Dual Inlets - Single Outlet 85

3.3.2.5.3-1 The "N Sub-Volume Technique:" Dual Inlets - Single Outlet with Stub-offs 91

3.3.2.5.3-2 The "N Sub-Volume Technique:" Dual Inlets - Single Outlet with Stub-offs — Summary 97

4.1.1-1 Relationship Among System, Model, Simulation, and V&V 99

4.1.2-1 Flow Chart for Subsystem Validation 101

4.1.3-1 Hierarchy of Validation Using ASTF as an Example . . . 103

4.2.2.1-1 "N Sub-Volume Technique" Validation - Case 1 - N = 1 111

4.2.2.1-2 "N Sub-Volume Technique" Validation - Case 2 - N = 1 112

4.2.2.1-3 "N Sub-Volume Technique" Validation - Case 3 - N = 1 113

4.2.2.1-4 "N Sub-Volume Technique" Validation - Case 4 - N = 1 114

4.2.2.2.1-1 Duct Metal Temperature Measurement Locations . . . 116

FIGURE PAGE

4.2.2.2.2-1 Example - Heat Transfer Validation - Initial Comparison 118

4.2.2.2.4-1 Heat Transfer Validation - Case 1 123

4.2.2.2.4-2 Heat Transfer Validation - Case 2 124

4.2.2.2.4-3 Heat Tranfer Validation - Case 3 125

4.2.2.2.4-4 Heat Transfer Validation - Case 4 126

5.3.2-1 Summary of Work Phases, Documentation, Reviews and Audits 140

5.3.5-1 Steps in Model and Simulation Development 144

5.3.10-1 MSDP Table of Contents 148

NOMENCLATURE

A	Area
a	Speed of sound in an ideal gas
c	Specific heat
C_F	Valve flow coefficient
D	Diameter
f	Darcy-Weisbach friction factor
g_c	Universal gravitation constant
h	Convective heat transfer coefficient
h_{fg}	Heat of vaporization for water
K	Equivalent pressure loss coefficient; constant
k	Thermal conductivity
L	Length
M	Mass; Mach number
m	Mass flowrate
N	Compressor speed total number of subvolumes
N_C	Corrected speed
Nu	Nusselt number
P	Pressure
Pr	Prandtl number
Q	Heat transfer rate
R	Specific gas constant
Re	Reynolds number
s	Duct wall thickness
SH	Specific humidity

T	Temperature
t	Time
u	Internal energy
V	Volume; velocity
γ	Ratio of constant pressure to constant volume specific heats
η	Efficiency; effectiveness
Δ	Difference
δ	Pressure to reference pressure ratio
ρ	Density
ϕ	Valve angle
θ	Temperature to reference temperature ratio
μ	Absolute viscosity

Subscripts

1,2,...n,j	Station number locations
A	Volume A
a	Atmosphere
B	Volume B; bulk
c	Compressor; cell; corrected
cd	Compressor discharge
D	Design point
d	Design; duct
e	Equivalent
f	Fluid; film
g	Gas

i	ith subvolume; ith station number
j	jth subvolume; jth station number
m	Metal
min,max	Minimum; maximum
o	Stagnation
p	Constant pressure
ref	Reference
s	Static; surface
sp	Setpoint
t	Vena contraction location; turbine
v	Volume; venturi
w	Wall; water

Superscripts

'	Station number location
.	Time rate of change
-	Average value

CHAPTER 1

INTRODUCTION

In the current era of aggressive competition, in both the domestic as well as the foreign arenas, there is an ever increasing need to increase productivity while reducing operational costs of capital facilities. A very effective method to meet this requirement is automation of such facilities. In many facilities, especially those characterized by transient or unsteady gas flow pumping and conditioning requirements, automatic control systems can be developed and tested, and the facility operators trained, via computer simulations. The risk and cost of using the actual facility for these types of activities are, in many cases, unacceptably high. The computer simulations are required to execute in "real time" thereby necessitating the use of simple, yet accurate, mathematical relationships.

In general, the overall objective of the math modeling efforts is to provide the mathematical relationships for development of the various computer simulations of the gas flow processes within these types of industrial facilities. The relationships must be of sufficient fidelity to ensure that the resulting simulations can be used for one or more of the following purposes:

a Training of the facility operators,

b. Hardware-in-the-loop testing of the control system(s),

c. Performance testing of the control algorithms,

d. Accurately estimating facility capabilities to meet specific operational requirements.

Items a and b set the requirement for a real time simulation.

The need for a real time simulation typically imposes a great challenge to the modeling effort: The mathematical relationships must be kept as simple as possible to minimize computational resources but yet meet accuracy requirements which may be very tight. Fortunately, the tremendous advances in digital computational state-of-the-art over the last ten to fifteen years have resulted in the capability to simulate relatively large and complex facilities utilizing standard off-the-shelf minicomputers. For the example facility used in this dissertation, an SEL 32/67® minicomputer was utilized. This is a 32 bit machine rated at four mips (AEDC estimate) with two mbytes of main memory. The simulation consisted of 10,600 lines of FORTRAN source code with an execution cycle time of 50 ms.

This dissertation presents a summary of the math modeling program for the Air Force Aeropropulsion Systems Test Facility (ASTF) -- the largest test facility of its kind in the Free World--located at the Arnold Engineering Development Facility (AEDC) in Tennessee. Even though ASTF is unique, many of the gas flow processes are very similar to those found in other industrial facilities and are therefore directly applicable to other modeling efforts. A conscientious attempt has been made to keep the presentation at a general level such that the tailoring required for other applications is minimal.

A brief description of the ASTF is presented in Chapter 2. The Automatic Test Control System (ATCS)--the system which controls test conditions in ASTF and the system for which the mathematical relationships were primarily developed--is included in the description. The modeling methods and techniques, together with the models for ASTF components common to some other industrial facilities, are developed and discussed in Chapter 3. Of particular importance is the treatment of unsteady gas flow processes in facility ducting. Another area that receives emphasis is the application of dimensional analysis, a simple, yet powerful technique for modeling many facility components. The results of the validation effort are presented in Chapter 4. Although validation of the total system was not completed, sufficient experimental data were obtained to validate several portions of the model. The "lessons learned" portion of the modeling effort is summarized in Chapter 5 in the form of a methodology for the successful development of mathematical models and computer simulations. The methodology is believed to be generally applicable to essentially any modeling and simulating project. Chapter 6 presents the summary and recommendations.

The author of this dissertation technically supervised the math modeling and simulating team throughout essentially all the development period from 1977 to 1988. In addition, his direct personal contributions included the development of most of the mathematical models discussed in Chapter 3, the writing of the model validation specifications and active participation in the experimental data acquisition and

analysis (Chapter 4), and the development of the modeling and simulating methodology (Chapter 5).

CHAPTER 2

BRIEF DESCRIPTION OF THE AEROPROPULSION SYSTEMS TEST FACILITY (ASTF)

2.1 Overview

The ASTF (Figure 2.1-1) is a unique national facility designed to test aircraft propulsion systems in true mission environments without leaving the ground [1][1]. The ASTF is the newest addition to the AEDC Engine Test Facility (ETF), which has been established as the United States Air Force (USAF) center of expertise for turbine engine testing. Located on a 57 acre site, the ASTF is an open-circuit test facility with two test cells, each 28 feet in diameter and 60 feet long [1]. Total rated electrical power is in the order of 450 MW and the total cooling water flow rate capability is almost 400,000 gpm.

For convenience in identifying the various geographical areas and functions associated with the ASTF, not only in this description, but also throughout the remainder of this document, two gas flow systems are defined (Figure 2.1-1b):

a. The air supply system - That portion of the facility from the compressor atmospheric inlets to the test cells, inclusive, and

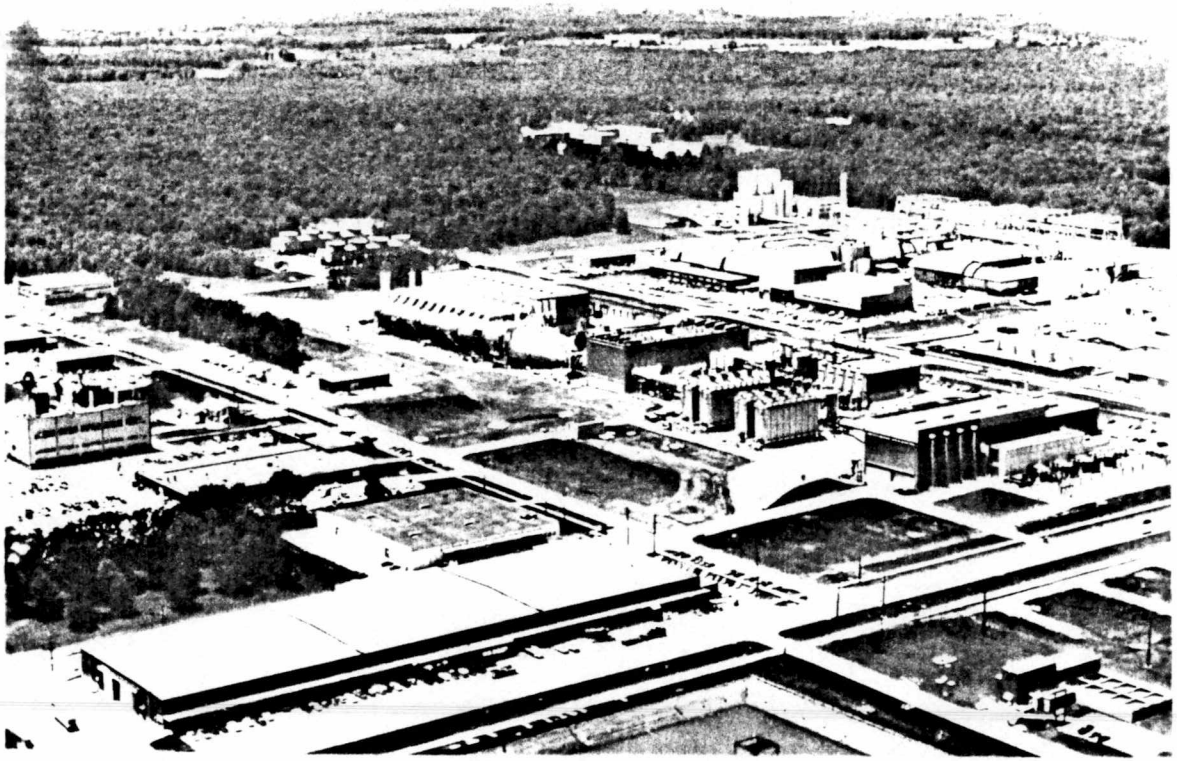
b. The exhaust system - That portion of the facility from the test cell discharge to the vacuum pumps (exhausters), atmospheric exhaust, inclusive.

---

[1]Numbers in brackets refer to similarly numbered references in the Bibliography.

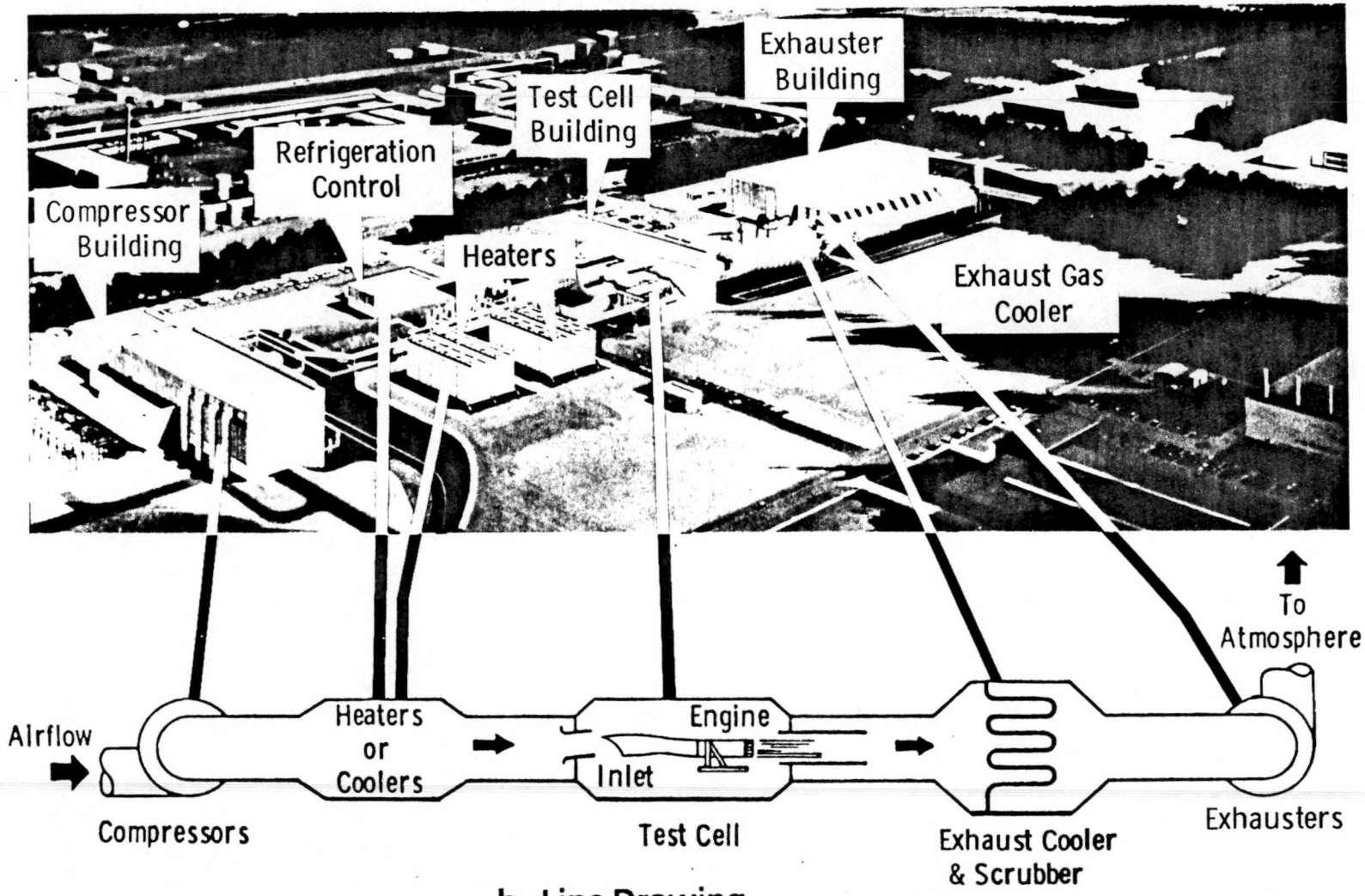
Arnold Engineering Development Center

An Air Force Systems Command Test Facility



a. Aerial View

Figure 2.1-1 The Aeropropulsion Systems Test Facility (ASTF)



b. Line Drawing

Figure 2.1-1 The Aeropropulsion Systems Test Facility (ASTF)

In addition to the gas flow systems, there is a control system--the ATCS--that was important to the math modeling program. Each of these systems and the following, pertinent gas flow subsystems,

a. Air Supply Compressors

b. Air Supply Coolers

c. Air Supply Heaters

d. Turboexpanders

e. Venturi

f. Exhaust Compressors

g. Exhaust Coolers

h. Configuration and Control Valves

are briefly described in this chapter.

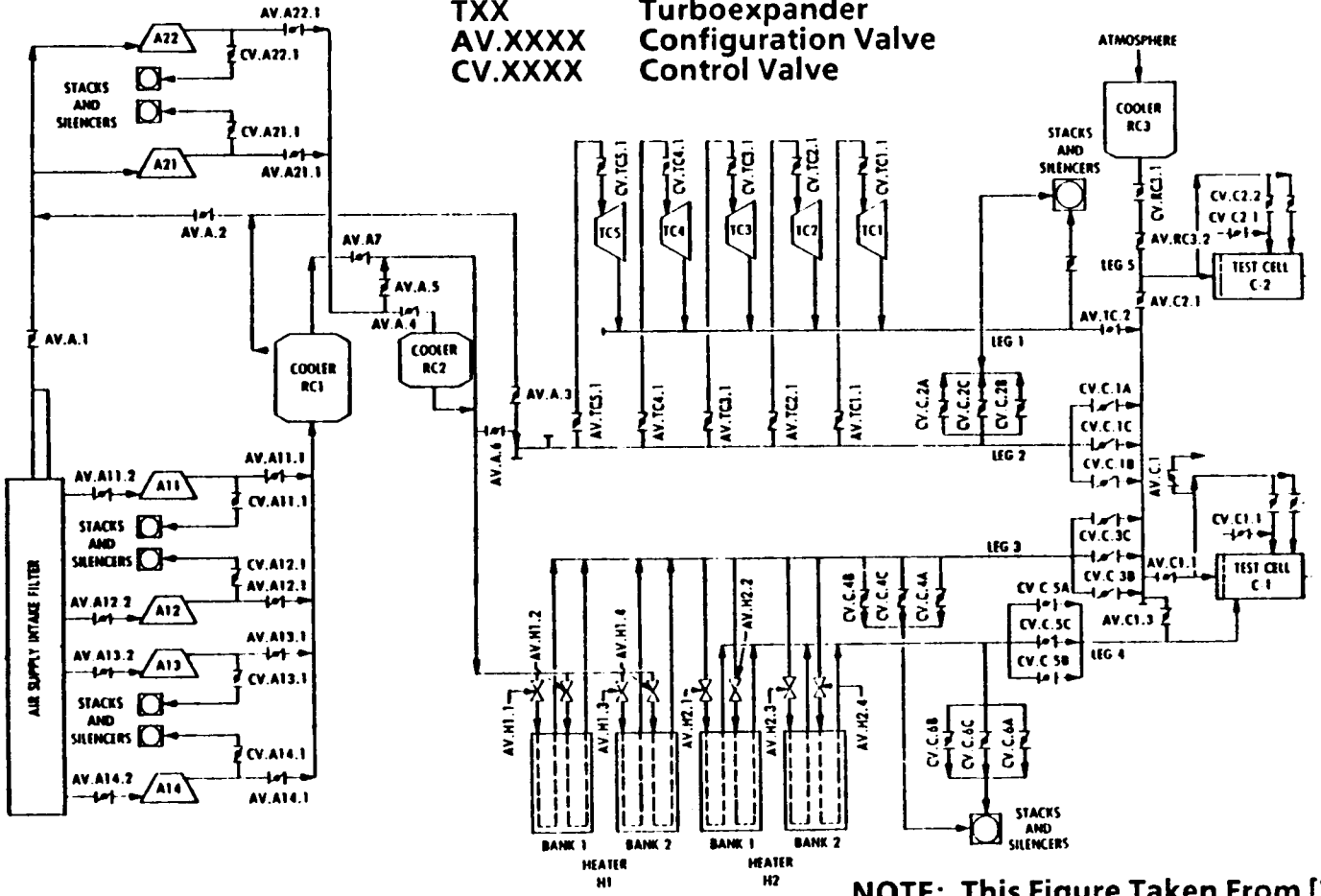
2.2 The Air Supply System

The ASTF air supply system is designed to provide conditioned air to the test cell using the compressors, coolers, heaters, and turbo-expanders (Figure 2.2-1).

The air supply compressors can be configured in a parallel one-stage operating mode to provide discharge pressure up to 50 psia or in a parallel-series operating mode to attain discharge pressures up to 150 psia. The airflow capacities for these operating modes are 1,450 lbm/sec and 1,050 lbm/sec, respectively [2]*.

After being pumped from atmosphere by the air supply compressors,

*The ASTF capabilities presented in this chapter are from the work of Polce.



NOTE: This Figure Taken From [2].

Figure 2.2-1 Air Supply System Schematic - ASTF

the air passes through an air cooler(s) for dehumidification and temperature conditioning. The air may then be delivered to the test cell area by as many as four different flow paths or legs. Each of the flow paths allows for different temperature conditioning capabilities.

Leg 1 operation allows for expansion of the air to temperatures as low as -100°F using the turboexpanders.

Leg 2 operation provides no further thermal conditioning of the air (-24°F to 300°F).

Leg 3 operation can deliver air at temperatures as high as 650°F through heater H-1.

Leg 4 provides for a special purpose capability by receiving air that has been heated by H-1 and H-2 in series to a maximum heater discharge temperature of 1,200°F. Leg 4 can only be used after a special duct has been installed in the C-1 inlet plenum.

An additional special purpose capability for the air supply area is the operation of leg 5 with atmospheric cooler RC3. RC3 is intended for use with only test cell C-2 and was designed to be used primarily for testing high bypass ratio turbofan engines at subatmospheric inlet pressure.

The valves in the air supply area include configuration valves (AV.XXXX) and fast response control valves (CV.XXXX). The configuration valves are used for establishing air supply compressor configurations and appropriate flow paths to the mixing header. The air supply system control valves near the compressors are used to control compressor discharge pressure or compressor pressure ratio. The remaining

control valves are used for controlling pressure or mass flow rate in the various legs supplying the mixing header and for controlling cooling and secondary air into the test cells.

There are two test cells, cell C-1 and cell C-2, which are designed for testing large turbojet and turbofan engines, respectively. In addition, both test cells have the basic facility features required for free-jet testing. The process air from the supply legs enters the common mixing header typically through legs 1, 2, and 3 where it can be mixed to attain the desired test cell inlet conditions of pressure and temperature. The air then flows from the mixing header to either C-1 or C-2 through flow straighteners and a multiple venturi airflow measuring system before being ingested by the test article.

Alternate air supply flow paths are available to cell C-1 and cell C-2 after reconfiguring the valving to use leg 4 and leg 5, respectively. Only C-1 can be used with leg 4 while only C-2 can be used with leg 5. Either of these legs can be operated in parallel with any or all of the other three air supply legs.

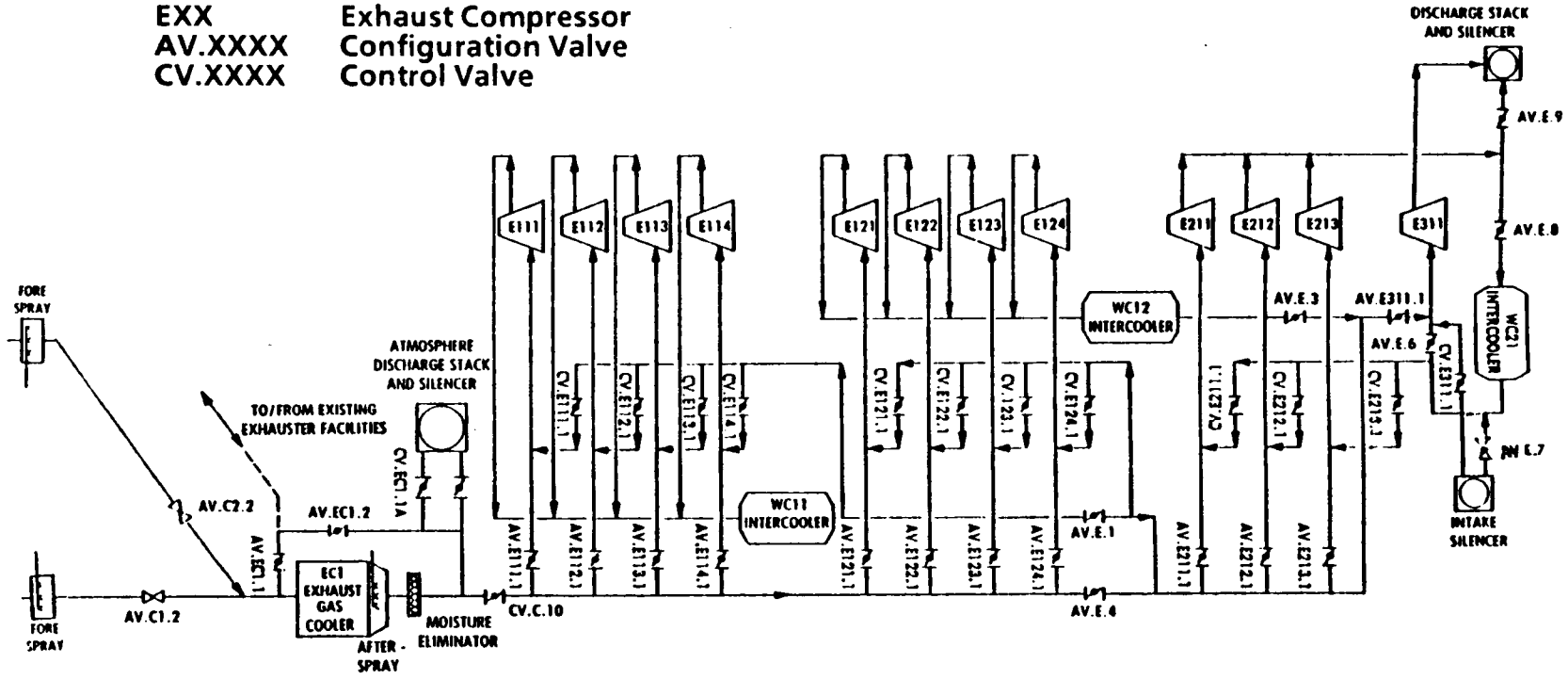
The test cell cooling flow can be extracted from the plenum area upstream of the venturi system or taken from atmosphere before flowing into the test cell to provide cooling for test instrumentation and the test article.

2.3 The Exhaust System

The test article exhaust gas and test cell cooling flow pass through a constant area ejector prior to being cooled directly with water sprays and indirectly by exhaust gas cooler EC1 (Fig. 2.3-1).

LEGEND:

EXX	Exhaust Compressor
AV.XXXX	Configuration Valve
CV.XXXX	Control Valve



NOTE: This Figure Taken From [2].

Figure 2.3-1 Exhaust System Schematic - ASTF

The exhaust gas is further spray cooled before being throttled with the primary exhaust control valve CV.C.10. The gas from the discharge of CV.C.10 then enters the exhaust plenum of the exhauster area. An alternate exhaust flow path is available when the pressure in the exhaust ducting is sufficiently above atmospheric pressure such that the flow can be discharged to atmosphere through valves CV.EC1.1A and CV.EC1.1B.

The ASTF exhaust system is designed to pump exhaust gas from the test cells to the surrounding atmosphere. Contained within the exhaust system are 12 identical exhaust gas compressors and three compressor intercoolers plus the associated configuration and control valves. Four of the exhaust gas compressors are configured for high exhaust plenum pressures (above 5 psia) and the remaining eight for lower pressure service. The exhaust gas compressors can be configured by the associated valving to attain one-stage, two-stage, or three-stage compressor configurations discharging to atmosphere. The intercoolers remove the heat of compression for protecting the latter exhaust gas compressor stages from excessive inlet temperatures.

The valves in the exhaust area consist of configuration valves (AV.XXXX) and control valves (CV.XXXX). The configuration valves allow for configuring the exhaust gas compressors to attain a one-stage, two-stage, or three-stage configurations. The control valves are used to control test cell pressure and compressor inlet pressure or compressor pressure ratio.

2.4 Subsystems

2.4.1 Air Supply Compressors. Each of the four, identical, axial flow first-stage air supply compressors (Figure 2.2-1, page 8) has a design inlet volumetric capacity of 278,000 CFM and a pressure ratio of 3.19. Each of the two, identical, axial, second-stage compressors has a design inlet volumetric capacity of 173,000 CFM and a pressure ratio of 3.19. Each of the six compressors is driven by a 3600 rpm synchronous electric motor [2].

2.4.2 Air Supply Coolers. Cooler RC1 performs aftercooling and dehumidification for the airflow from the first-stage compressors. It consists of a cylindrical shell 42-feet in diameter and 152-feet long which contains four stages of cooling and one stage of reheat [2]. The design capabilities of each stage at 1100 lbm/sec of airflow are shown below:

Stage	Inlet Air Temperature (°F)	Discharge Air Temperature (°F)	Discharge Specific Humidity (Grains/lbm Dry Air)
1	322	90	75.8
2	90	38	12
3	38	0	2
4	0	-24	0.5
5	-24	+200	0.5

Cooler RC2 performs aftercooling and dehumidification for the second-stage air supply compressors. It consists of a cylindrical shell 32-feet in diameter and 79-feet long which contains two stages of cooling. There are two operating modes for this cooler. When the

second-stage compressors are operating in a single-stage configuration, the first-stage of RC2 is designed to cool the airflow (350 lbm/sec) from the two second-stage compressors from 325 to 90°F and 76 grains/lbm dry air. The second-stage of RC2 cools the flow down to 38°F and 12 grains/lbm dry air. When the second-stage compressors are operating in a two-stage configuration (1100 lbm/sec) only the first-stage of cooler RC2 is normally in operation because the air has already been dehumidified by cooler RC1. In this case, cooler RC2 cools the total flow (1100 lbm/sec) down to 100°F.

Cooler RC3 is located in atmospheric Leg 5. This cooler consists of a concrete structure which is approximately 47-feet wide by 51-feet long by 52-feet high. RC3 has only one stage of cooling with the design capability of cooling 1440 lbm/sec to 38°F and 35 grains/lbm dry air [2].

2.4.3 Air Supply Heaters. ASTF contains two indirect fired heaters, H-1 and H-2. Each of the two outer structures for each heater, which transports the flue gases, is approximately 90-feet long by 22-feet wide by 60-feet high. Heater H-1 was designed to deliver 1100 lbm/sec of airflow to the test cell at 630°F via Leg 3. Heater H-2 is a second-stage heater only, utilizing the discharge air from heater H-1. Heater H-2 was designed to deliver 1100 lbm/sec of airflow to the test cell at 1020°F via Leg 4.

2.4.4 Turboexpanders. The five, identical, radial flow turboexpanders supply very cold air to the test cell via leg 1 (Figure 2.2-1, page 8). Each turboexpander is designed to cool 288 lbm/sec of airflow from

-6 to -108°F at an inlet pressure of 38 psia and a discharge pressure of 12.8 psia [2]. Each turboexpander (Fig. 2.4.4-1) can be operated at off-design conditions to produce large deviations from design discharge temperature by varying mass flow rate and discharge pressure. A single-stage centrifugal compressor is coupled to the shaft of each turboexpander for power absorption purposes. Each compressor simply takes air in from atmosphere, compresses it, and discharges it back to atmospheric through a stack. Off-design control is provided by a hydraulically actuated, radial vane mechanism which functions as a control valve (Figure 2.4.4-2).

2.4.5 Venturi. A critical-flow multiple venturi subsystem is installed upstream of each test cell to accurately measure air flow rate (Fig. 2.4.5-1). The subsystem for test cell C-1 consists of a bulkhead with nine venturis, each with a throat diameter of 1.39 feet. Bulkhead penetrations are available (and blanked-off) for up to 16 additional venturis as future needs may dictate. Test cell C-2 has thirty-six venturis with penetrations available for an additional 13.

2.4.6 The Exhaust Compressors. There are 12, identical axial flow exhaust compressors (Figure 2.3-1, page 11). Eight are first-stage units, E111 through E114 and E121 through E124; three are second-stage units, E211 through E213, and one is a third-stage unit, E311. These units can be configured into a multiplicity of configurations with the limitation that the first-stage units cannot be used in single-stage operation to atmosphere due to power limitations. Each unit is driven by a 3600 rpm synchronous motor through a reduction gear to 2290 rpm.

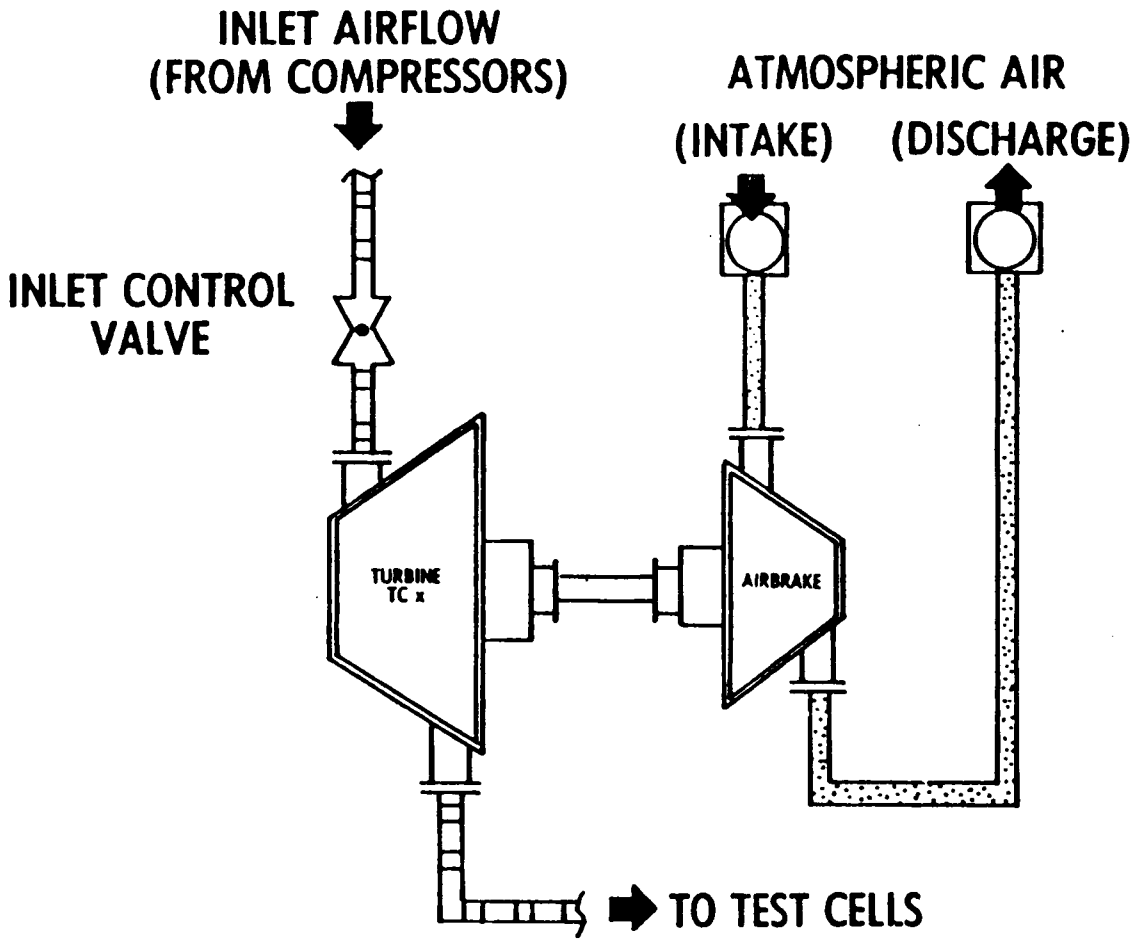


Figure 2.4.4-1 Typical Turboexpander Arrangement

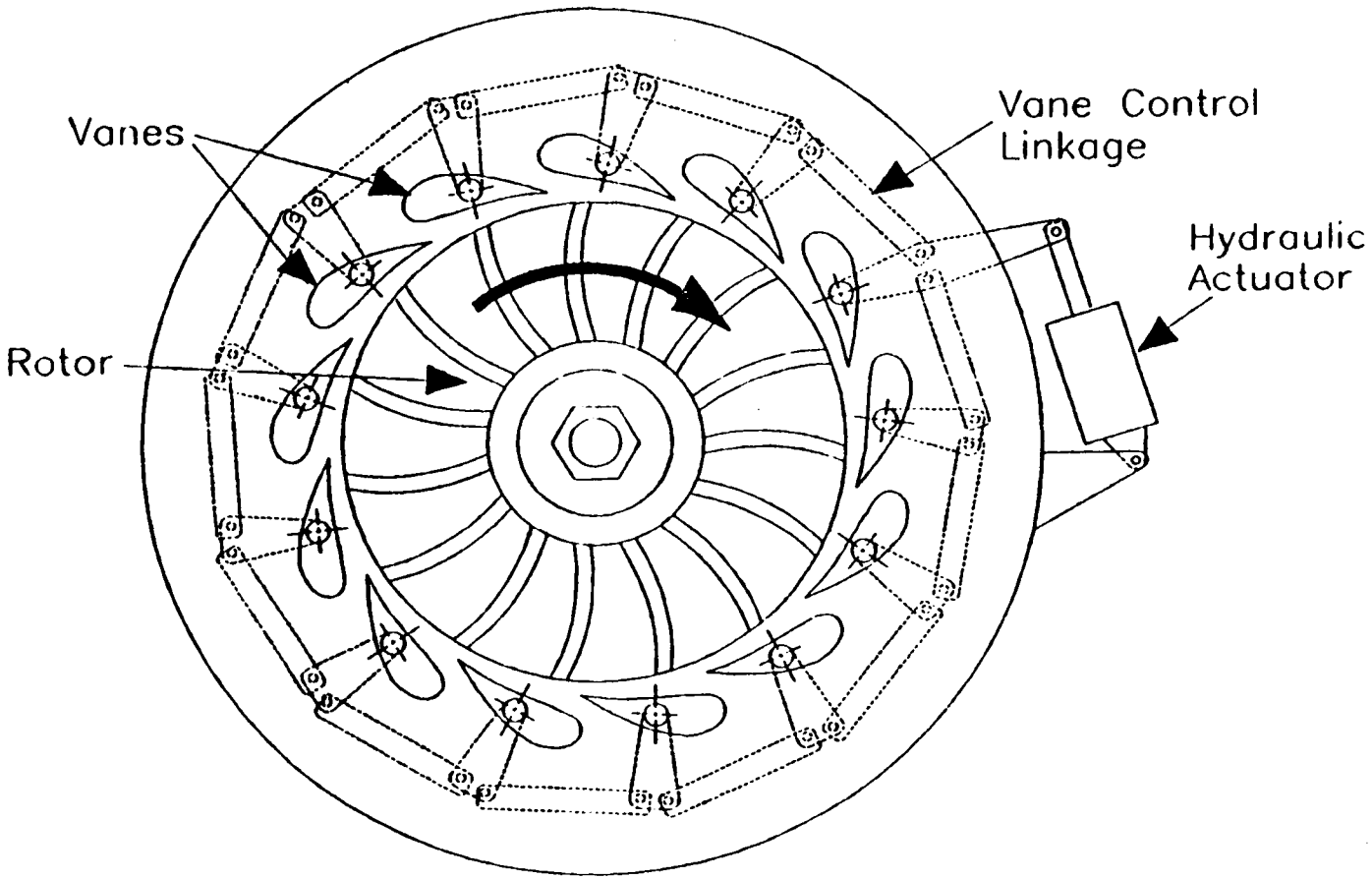


Figure 2.4.4-2 Turboexpander Radial Vane Mechanism

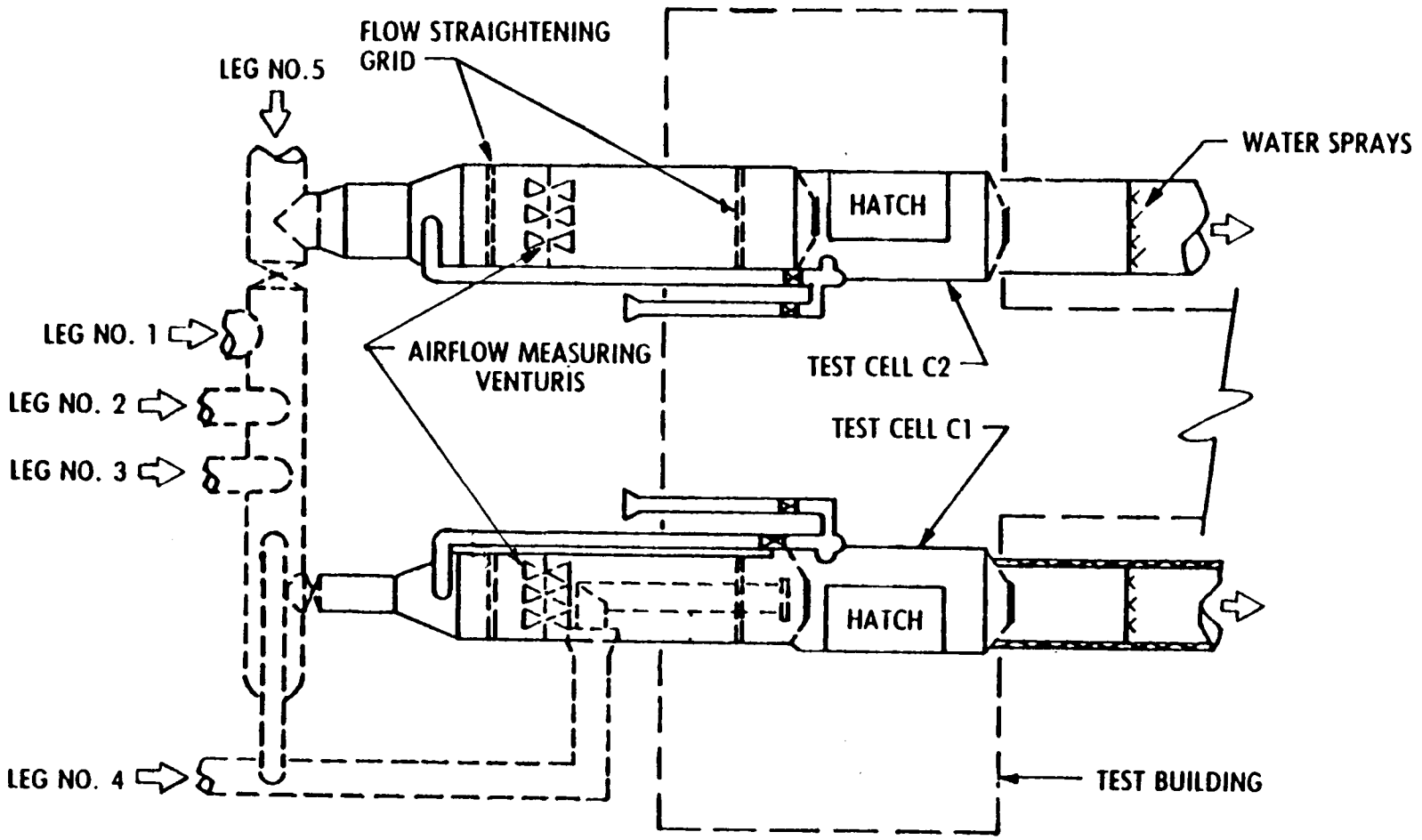


Figure 2.4.5-1 Test Area Layout

Each unit is rated at 1,000,000 CFM at a pressure ratio of 3.5 and an inlet temperature of 100°F based on dry air design considerations [2].

2.4.7 Exhaust Coolers. Intercoolers are provided downstream of all first- and second-stage exhaust compressors (Figure 2.3-1, page 11). Intercoolers WC11 and WC12 service the first-stage units and WC21 services the second-stage units. WC11 and WC12 are 62-feet long and 46-feet in diameter while WC21 is approximately 51-feet long and 35-feet in diameter. All intercoolers are water-to-gas units that cool the gas from temperatures approaching 500°F [2]. Some dehumidification can occur; therefore, all units are equipped with mist separators aft of the cooling coils.

Cooler EC1 is a 65-foot-diameter tube-and-shell heat exchanger with water flow in the tubes and gas flow in the shell. In addition, direct water spray injection capability exists both upstream and downstream of the unit. For test cell C-1 operation, the upstream sprays are activated for gas temperatures in excess of 2500°F. For test cell C-2 operation, upstream spray cooling is employed when gas temperatures exceed 600°F as the C-2 discharge ducting is not water jacketed. EC1 is designed to cool 1860 lbm/sec of exhaust gases from 2500°F to 350°F at 2.92 psia. The aft sprays are capable of further cooling to 100°F [2].

2.4.8 Configuration and Control Valves. There is a total of 110 configuration and control valves in ASTF. All of the valves with the exception of the turboexpander inlet valves and the isolation valves downstream of the test cells are of the butterfly type. Configuration

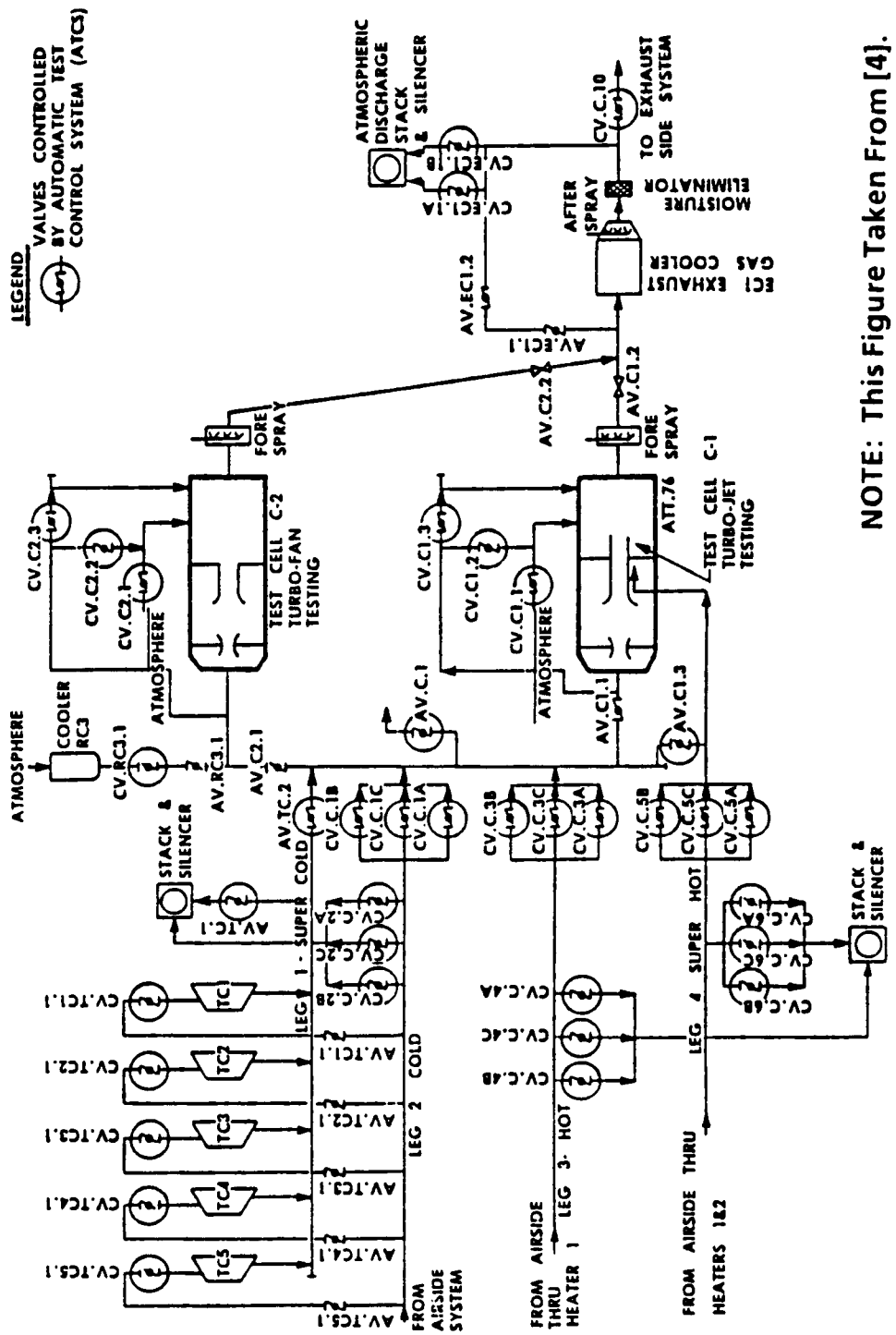
valves, designated by the "AV" prefix (Figures 2.2-1 and 2.3-1, pages 8 and 11), are isolation valves being normally fully open or closed, and provide the ability to establish certain air supply, test area and exhaust configurations. Most of the configuration valves are electric driven and have relatively slow stroke times that vary from 20 to 60 seconds. These valves range in size from 3.5- to 32-feet in diameter [2].

Control valves, designated by the "CV" prefix (Figures 2.2-1 and 2.3-1), typically control pressure or mass flow rate throughout the facility. Almost all of the control valves are hydraulic actuated with relatively fast stroke times that are primarily in the range of from 1 to 10 seconds. These valves vary from 1.5- to 15-feet in diameter [2].

2.5 The Automatic Test Control System (ATCS)

One of the unique capabilities built into ASTF is extensive controllability of simulated flight conditions. By properly manipulating 38 high response control valves, the facility can be made to simulate flight conditions ranging from straight and level to the maximum performance maneuvers of the latest military aircraft [3].

The computer control system which commands these valves and provides the facility with its unique controllability is the ATCS. Figure 2.5-1 identifies the valves controlled by the ATCS [4]. In order to satisfy its purpose, ATCS must have complete authority over the 38 valves it controls. However, this great authority also enables ATCS, in the event of a malfunction, to inflict serious damage on the propulsion system under test, which may be a multi-million dollar



NOTE: This Figure Taken From [4].

Figure 2.5-1 Valves Controlled by ATCS

prototype. For this reason, great care was taken to enhance the reliability of the ATCS. For example, it is housed in a triple redundant fault tolerant computer system and the software was developed under the rigid discipline of several MIL-standards.

The required reliability of the ATCS also demanded that the system be checked out and the operators trained with a technique that did not involve the actual facility. The technique utilized to meet this requirement involved interfacing the ATCS to a "real time" digital simulation -- a technique often referred to as "hardware-in-the-loop" testing. All the facility from points upstream of the supply bleed valves to atmospheric and the turboexpander inlets to a point in the exhaust header downstream of CV.C.10 was simulated.

CHAPTER 3

THE MATHEMATICAL MODELS

3.1 General

The successful mathematical modeling and real time simulation of even a relatively small portion of a facility as large as ASTF demands that the mathematical model be kept quite simple. Since, in most cases, the flow can be treated as one-dimensional, the temptation is to formulate and solve sets of partial differential equations in time and distance along the duct for the various ASTF ducting segments. Not only would a model and simulation with spatial dependency have been very expensive to produce, but the required computational resources for real time simulation would have been prohibitive. Based on previous experience with the modeling of a smaller, yet functionally similar facility, it was assumed that such an approach would not be required. Many simplifying, yet acceptable techniques and assumptions, were made throughout the course of the modeling effort. The first was the implementation of the "lumped parameter technique."

3.1.1 The Lumped Parameter Technique. The transportation of various gases in many, if not most, industrial process facilities occurs at low Mach numbers. This is primarily due to the fact that pumping equipment is more costly than ducting. In other words, large pressure losses associated with small, less expensive, ducting cannot be tolerated because the associated cost and operational power expenses of the compressor systems are unjustifiably high. Low Mach number flow

simplifies the modeling process in that large axial pressure gradients in the ducting typically do not exist. In addition, the low velocities often produce low inside heat transfer coefficients thereby minimizing the heat transfer rates and associated axial temperature gradients.

The absence of large axial pressure and temperature gradients and the lack of a requirement to track pressure waves often leads to the concept of "collecting up" the pressure losses and temperature changes and "lumping" them at points, periodically, along the ducting -- hence the name "lumper parameter technique." At all other locations the flow can be considered to be frictionless and adiabatic. Furthermore, the pressure losses and heat transfer rates are computed independently of each other with the equations being basically steady state in nature with time dependent inputs. The general limitations of this technique are discussed in [5], with the primary limitation being a "low" Mach number. Although this reference does not identify "low" in a quantitative sense, various modeling efforts at AEDC down through the years have indicated that a Mach number up to at least 0.2 is acceptable.

In the lumped parameter technique the spatial dependency in the equation sets is eliminated and the resulting differential equations become ordinary in the single independent variable time. The points where pressure losses and heat transfer are calculated are a matter of convenience and accuracy. Convenience in that the analyst or designer can select those locations in the facility where the values of variables are needed and accuracy in that the greater the number of lumps the more accurate the calculations.

Under the lumped parameter assumption, a typical portion of an industrial facility might appear as shown in Figure 3.1.1-1. In this example, the portion of the facility is broken up into three volumes V_1, V_2, and V_3 all of which are frictionless and adiabatic. There are correspondingly three locations where pressure loss and heat transfer rate are computed.

The lumped parameter representation of the example facility used in this study -- the ASTF -- is shown in Figure 3.1.1-2. The pressure loss and heat transfer symbology has been omitted for clarity.

3.1.2 Other Simplifying Assumptions at the Facility Level

3.1.2.1 Pressure Losses. The lumped pressure losses for a straight section of constant area ducting can be approximated using the normal Fanno relationships with time dependent inputs. However, in a facility as large as ASTF, these relationships are computationally burdensome and additional simplifications were sought.

As a worst case example, a duct segment for the ASTF mathematical model can be assigned the following characteristics:

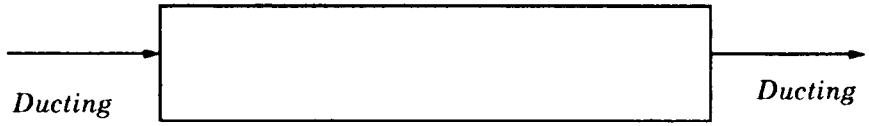
L_e = 4000 ft (equivalent length)

D_e = 10 ft

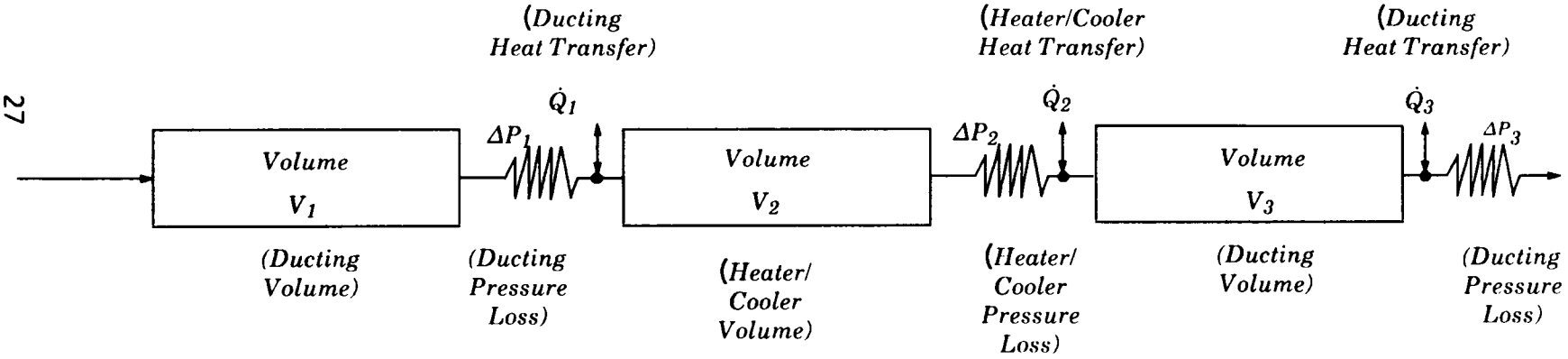
f = 0.01

M_1 = 0.1

The "equivalent length" is the length of ducting plus the straight duct equivalent of other pressure loss mechanisms such as internal duct hardware and elbows. (In a strict sense, the Fanno relationships



a) Actual Facility Schematic (Partial)



b) Lumped Parameter Representation

Figure 3.1.1-1 Example of The Lumped Parameter Technique

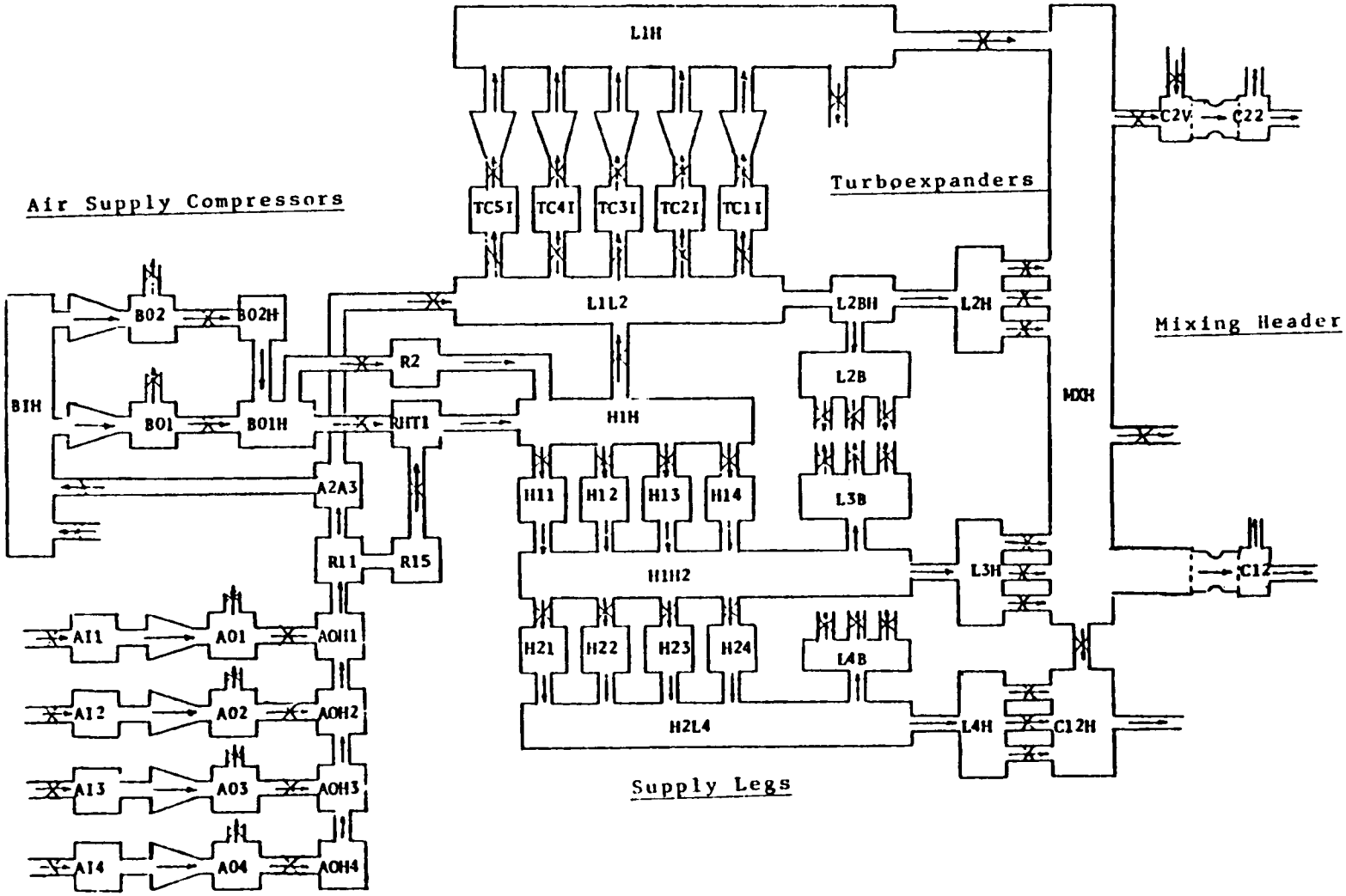


Figure 3.1.1-2 Lumped Parameter Representation of ASTF

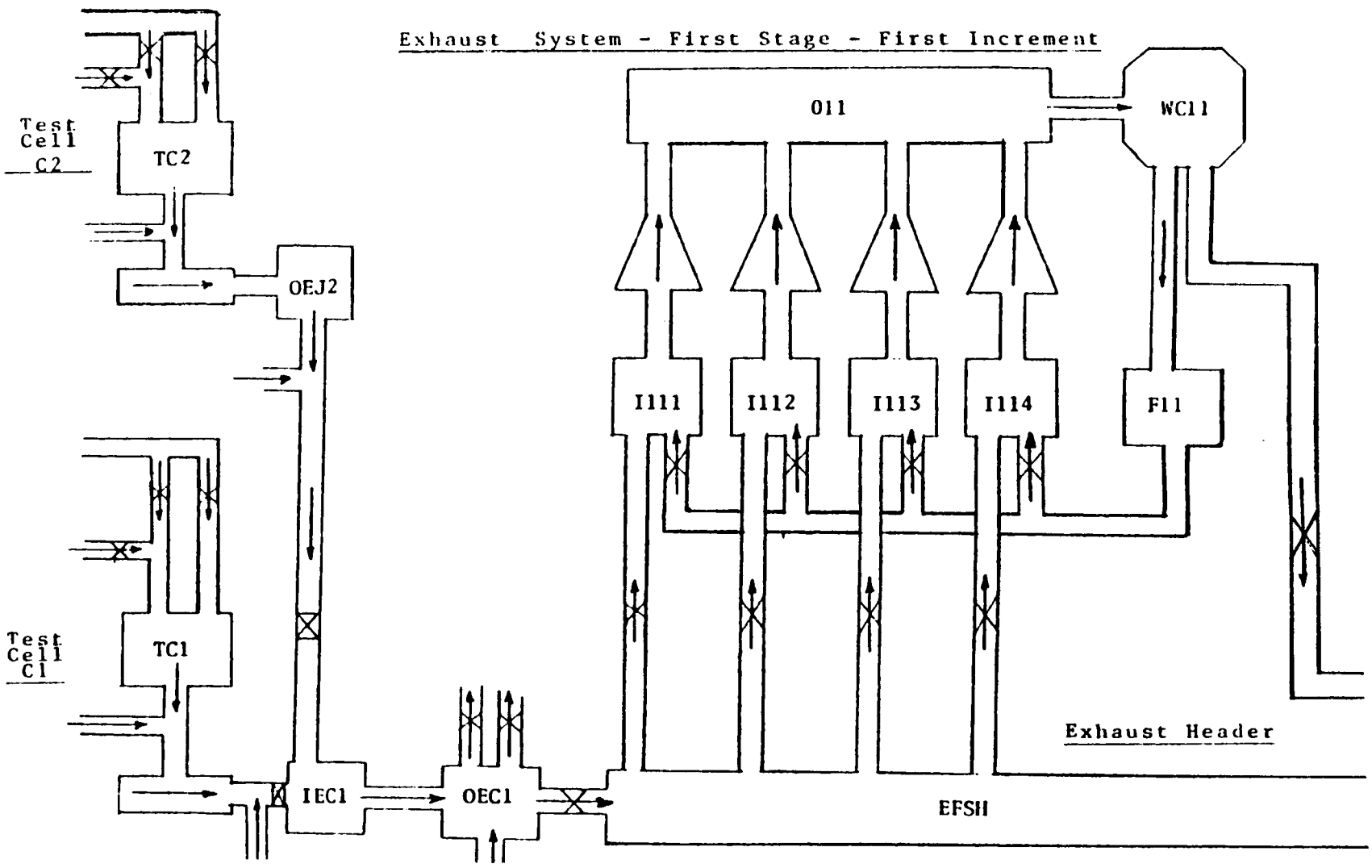


Figure 3.1.1-2 Lumped Parameter Representation of ASTF - continued

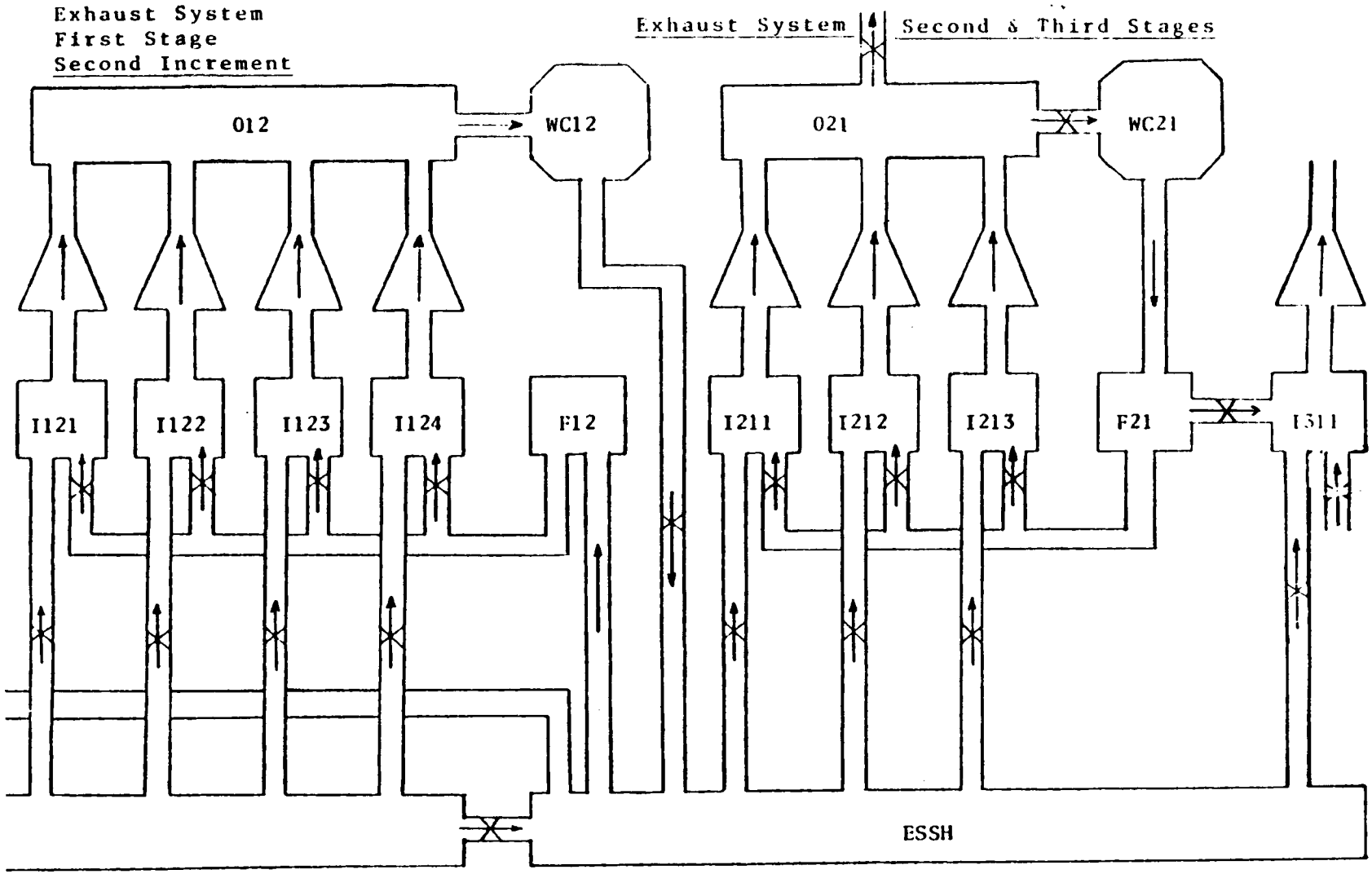


Figure 3.1.1-2 Lumped Parameter Representation of ASTF - concluded

cannot be applied to anything other than straight ducting; however, this approach is deemed sufficiently accurate for the purposes of this illustration.) The "exact" theoretical solution for Fanno Flow is given by [6]

$$\frac{f(x^*-x_1)}{D_e} = \frac{\gamma+1}{2\gamma}\ell n\left[\frac{\frac{\gamma+1}{2}M_1^2}{1+\frac{\gamma-1}{2}M_1^2}\right] + \frac{1}{\gamma}\left[\frac{1}{M_1^2}-1\right]. \qquad (3.1.2.1\text{-}1)$$

For $M_1 = 0.1$ and $\gamma = 1.4$,

$$f(x^* - x_1)/D_e = 66.922.$$

But,

$$\frac{f(x_2-x_1)}{D_e} = 4.0.$$

Therefore, by subtraction

$$\frac{f(x^*-x_2)}{D_e} = 62.922.$$

When Equation (3.1.2.1-1) is written and solved for M_2, the result is

$$M_2 = 0.103.$$

The resulting loss in total pressure is given by

$$\frac{P_{o_2}}{P_{o_1}} = \frac{M_1}{M_2}\left[\frac{1+\frac{\gamma-1}{2}M_2^2}{1+\frac{\gamma-1}{2}M_1^2}\right]^{\frac{\gamma+1}{2(\gamma-1)}}.$$

For $M_1 = 0.1$ and $M_2 = 0.103$, the resulting total pressure ratio is

$$\frac{P_{o_2}}{P_{o_1}} = 0.97122$$

or

$$\frac{P_{o_1} - P_{o_2}}{P_{o_1}} = 0.02878 .$$

This represents the "exact" solution for an adiabatic flow in a constant area duct with friction for the inlet conditions previously assigned.

A simplified approach for lumping the pressure losses at a point will now be developed and compared to the exact theoretical solution. From elementary hydraulics, for incompressible flow, [7], the equation for loss in total pressure in a fluid flow system is given by

$$\Delta P_o = \frac{f L_e}{D_e} \frac{\rho V^2}{2 g_c} .$$

Substitution of V = Ma, the definition of Mach number, ρ = Ps/RTs and the isentropic pressure ratio relationship results in

$$\Delta P_o = \frac{f L_e}{D_e} \frac{\rho M^2 a^2}{2 g_c}$$

$$= \frac{f L_e}{D_e} \frac{P_s}{R T_s} \frac{M^2 \gamma g_c R T_s}{2 g_c}$$

$$= \frac{f L_e}{D_e} \frac{\gamma}{2} P_s M^2$$

or,

$$P_{o_1} - P_{o_2} = \frac{f L_e}{D_e} \frac{\gamma}{2} \frac{P_{s_1}}{P_{o_1}} P_{o_1} M_1^2$$

or,

$$\frac{P_{o_1} - P_{o_2}}{P_{o_1}} = \frac{fLe}{D_e} \frac{\gamma}{2} \left[1 + \frac{\gamma - 1}{2} M_1^2\right]^{-\frac{\gamma}{\gamma - 1}} M_1^2. \qquad (3.1.2.1\text{-}2)$$

For $M_1 = 0.1$, $\gamma = 1.4$, and $f\ L_e/D_e = 4.0$, as before, Equation (3.1.2.1-2) gives

$$\frac{P_{o_1} - P_{o_2}}{P_{o_1}} = 0.02781$$

Comparison to the previous "exact" solution shows that

$$\frac{\Delta P_{o_{exact}}}{\Delta P_{o_{approx}}} = \frac{0.02878}{0.02781} = 1.034.$$

The approximate result is within 3.4 percent of the exact theoretical solution even in this worst case example. Alternately, the Mach number at station 2 could be used in the computations. For $M_2 = 0.103$

$$\frac{P_{o_1} - P_{o_2}}{P_{o_1}} = 0.02892.$$

The resulting error is

$$\frac{\Delta P_{o_{exact}}}{\Delta P_{o_{approx}}} = \frac{0.02878}{0.02892} = 0.995$$

or, -0.5 percent.

Either answer is within the accuracy threshold of the ASTF model and for many, if not most, industrial facilities. The overriding point

to be made here is that not only can the pressure loss be lumped at a point, and Equation (3.1.2.1-2) be utilized, but it can be lumped at any point, of convenience. This important finding was used repeatedly throughout the ASTF model.

3.1.2.2 Heat Transfer. As noted previously the velocity of the flow in the ASTF as well as many other industrial facilities is low. This typically produces low inside heat transfer coefficients for the ducting which, in turn, results in low heat transfer rates. A very simple approach for calculating heat transfer rates and resulting changes in gas temperature was also developed and implemented.

The worst case example in the ASTF air supply system upstream of the mixing valves -- the portion of the facility where heat transfer rates are low -- can be represented by

$$\dot{m} = 500 \text{ lbm/sec}$$

$$T_{B_1} = 1160°R$$

$$D = 9 \text{ ft}$$

$$L = 100 \text{ ft}$$

$$T_W = 460°R$$

As discussed in Chapter 4, the time constant for most of the ASTF ducting is in the order of hours and days; therefore, the assumption of a constant wall temperature for this illustration is justified. The "exact" solution is given by [8]

$$Q = \dot{m} c_p \left(T_{B_2} - T_{B_1} \right) = h A_S \left[\frac{T_{B_2} - T_{B_1}}{\ell n \dfrac{T_w - T_{B_1}}{T_w - T_{B_2}}} \right] \qquad (3.1.2.2\text{-}1)$$

where

$$Re_{D_1} = \frac{\rho VD}{\mu}\Big)_1 = \frac{4m}{\pi D\mu} = 3.6 \times 10^6 .$$

$$Nu_{D_1} = 0.023\ (Re_d)^{0.8}(Pr)^{1/3} = 3560 \qquad [8]$$

$$h = Nu_{D_1}\frac{k}{d} = 10.2\ \frac{btu}{hr\,ft^2\,°F} .$$

It is recognized that heat transfer coefficient, h, will change slightly in the direction of flow, but in this illustration, it is assumed constant. Equation (3.1.2.2-1) can be solved for T_{B_2} to yield the "exact" answer of

$$T_{B_2} = 1114.80°R.$$

If all the heat transfer is lumped at the longitudinal center of the ducting segment, where the convective temperature difference is assumed to be $(T_{B_1} + T_{B_2})/2$, then

$$m c_p\left(T_{B_2} - T_{B_1}\right) = h A\left(T_w - \frac{T_{B_1} + T_{B_2}}{2}\right).$$

By some algebraic manipulation, this equation can be shown to result in

$$T_{B_2} = \frac{T_w + \left(\frac{m c_p}{h A_s} - 0.5\right)\left(T_{B_1}\right)}{\left(\frac{m c_p}{h A_s} + 0.5\right)} \qquad (3.1.2.2\text{-}2)$$

which yields, for the specific example above,

$$T_{B_2} = 1114.77°R.$$

The difference in the two temperatures is essentially zero. In order to conserve computational resources, while maintaining reasonable accuracy, the slightly less complex equation (Equation 3.1.2.2-2) was used in the ASTF model.

For most of the ASTF ducting and internal hardware, the convective ΔT from the air to the wall is much less than the example just cited. Leg 2, for example, has a maximum ΔT of about 125°F. In the exhaust system downstream of CV.C.IO, the maximum ΔT is less than that for Leg 2 (except in the short duct segments from the exhauster discharges to the intercoolers). In all of these areas the gas flow was treated as adiabatic.

The portion of the ASTF between the mixing valves and the inlets to the test cells has a high heat transfer rate. In the original theoretical model (prior to validation) Equation (3.1.2.2-2) with theoretically determined values of h for axisymmetric flow, together with a constant wall temperature assumption, were used. (This turned out to be woefully inadequate. (See Chapter 4 - Validation). In fact, this represented the only serious error in the original theoretical math model.)

3.1.2.3 Miscellaneous. A few additional, miscellaneous, simplifying assumptions were made at the facility level. The first involved the determination and tracking of total and static parameters. Most of the gas flow in ASTF occurs at very low subsonic Mach numbers, as is the

case in many other industrial plants. In those portions of the facility where the Mach number is less than 0.1, static values of pressure and temperature were assumed equal to their corresponding total or stagnation values. Since the values of the pressure and temperature ratios at M = 0.1, γ = 1.4 are

$$\frac{P_s}{P_o} = 0.99303$$

$$\frac{T_s}{T_o} = 0.99800$$

the resulting errors were very small. For locations where the Mach number is greater than 0.1, for example, in the venturi and diffuser, a strict accounting of the differences was imposed.

Another assumption used throughout the ASTF model was that the gas could be treated as "ideal" or "perfect" and the perfect gas equation of state is used. A check of the compressibility factor, Z, at selected locations in the facility revealed that Z is approximately equal to one at all locations. In the exhaust system, when spray cooling is employed, the gases are treated as mixtures of ideal gases and the gas properties are calculated accordingly. Where needed, thermal conductivity and viscosity were permitted to be temperature dependent.

3.2 Subsystems

There can be many different subsystems in a typical industrial facility. The ASTF is no exception. However, in order to present the

most meaningful information, only those subsystems that are most common to other facilities are presented herein. These are

Compressors and Exhausters (Vacuum pumps or exhaust compressors),

Butterfly Valves,

Turboexpanders,

Heaters,

Coolers, and

Venturis.

(Ducting, which is perhaps the most common facility component, is addressed in the subsequent section, 3.3 "Systems".) Each of the mathematical models for these subsystems is presented in turn.

3.2.1 Compressors and Exhausters. One of the most powerful, yet very simple techniques for modeling gas pumping equipment, such as compressors and exhausters, as well as a host of other industrial equipment is the "principle of dimensional homogeneity" -- more commonly referred to as "dimensional analysis". E. Buckingham in his famous paper "Model Experiments and the Forms of Empirical Equation" [9], written some 75 years ago, comprehensively describes the fundamentals of this technique and illustrates its application with several very practical examples. Perhaps no one could have stated the principle any more concisely than Buckingham himself:

> "...By means of this principle it may easily be shown that any equation
>
> $$F(Q_1, Q_2, \ldots Q_n) = 0 \qquad (1)$$
>
> describing a relation among the n different kinds of quantity Q1, Q2,...Qn is always reducible to the form
>
> $$f(\Pi_1, \Pi_2, \ldots \Pi_{n-k}) = 0, \qquad (2)$$

in which each of the variables Π represents a dimensionless product of the form

$$\Pi = Q^{a}_{1} Q^{b}_{2} \ldots Q^{n}_{n}; \tag{3}$$

k is the number of independent fundamental units needed in specifying the units of the n kinds of quantity; and f is some unknown function to be found by experiment.

A dimensionless quantity is one of which the numerical value does not change when the sizes of the fundamental units alter, so long as the relations between the derived and the fundamental units are kept unchanged. The simplest example of such a quantity is the ratio of two quantities of the same kind; the ratio of two lengths, for instance, does not depend on the unit we adopt for measuring lengths. Another simple example is the expression

$$\frac{Dg}{S^2} \text{ or } D\,g\,S^{-2},$$

in which D is the diameter of a fly wheel, S its peripheral speed, and g the acceleration of gravity. The numerical value of this product, in any particular case, will be the same whether measured by an American using feet and seconds or by a European using meters and seconds, and either of them might change from seconds to minutes without affecting his numerical result, if he changed his derived units of speed and of acceleration accordingly."

Of course, this theorem subsequently became known as the "Buckingham Pi Theorem."

In the conclusions of this paper, Buckingham emphasized some extremely important points:

"...The method is not a *theoretical* one in the ordinary sense, - there is nothing hypothetical about it. It is purely algebraic and tells us with certainty, that if certain quantities and no others are connected by a physical relation, the equation which describes the relation must be reducible to a certain form: the only chance of mistake is in overlooking some essential factor in the problem. Since the process of reasoning is purely mathematical, we cannot, of course, get out at the end any more than we put in at the beginning when we use our physical common-sense and experience to write down the original list of variables for the problem in hand. But we get out what we put in in a form which often makes it much more available than when it went in."

With regard to overlooking some essential factor in the problem, one could include every different quantity that could be thought of in the dependency in order to make sure the results are valid. However, this would complicate the problem enormously as data must be taken to evaluate the variations of each quantity. The key is to analyze the problem in enough detail to feel reasonably confident that all the important parameters are included. If there is any reasonable doubt about a particular parameter, it should be included.

When the Buckingham Pi Theorem is applied to a compressor or exhauster, operating in steady state, as shown in Figure 3.2.1-1, the following results:

$$F_1 (m, P_{o1}, RT_{o1}^{*}, N, D, P_{o2}) = 0.$$

The fundamental units for these quantities are:

$$m - \frac{M}{t}$$

$$P_{o_1} - \frac{M}{Lt^2}$$

$$RT_{o_1} - \frac{L^2}{t^2}$$

*In this study, the M-L-t fundamental units are used rather than M-L-t-T. This requires that temperature always appear in combination with the specific gas constant.

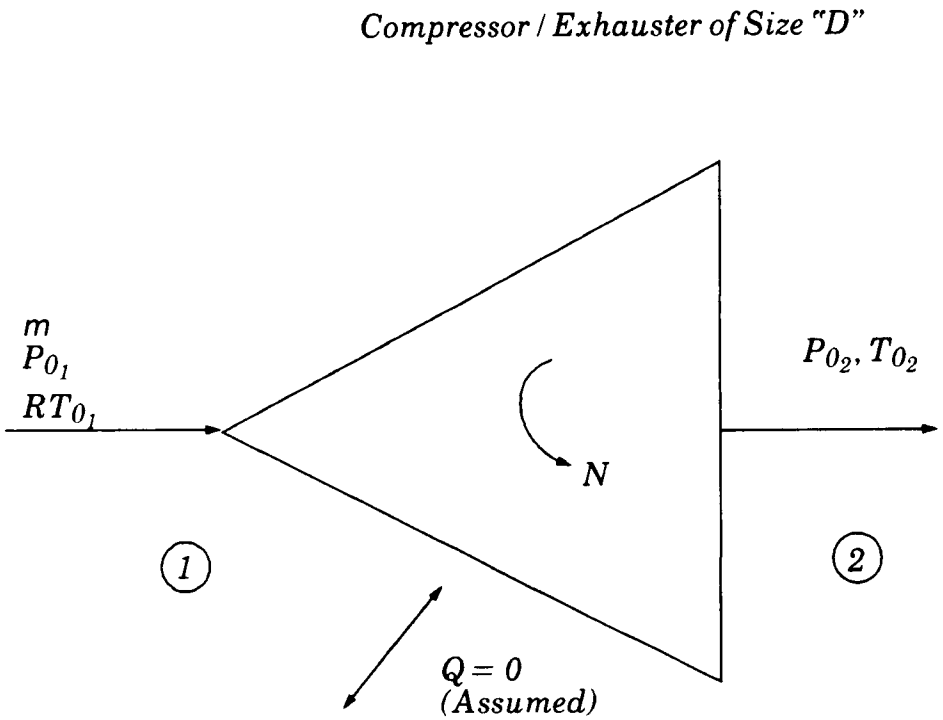


Figure 3.2.1-1 Schematic of Compressor or Exhauster

$$N - \frac{1}{t}$$

$$D - L$$

$$P_{o_2} - \frac{M}{Lt^2}.$$

With six separate kinds of quantities, n = 6, and three fundamental units, k = 3, there will be n-k=3 dimensionless groupings. We shall choose P_{O2}, D and N as quantities having, collectively, all fundamental units and then operate, in turn, on each of the others as shown below. But first, by inspection,

$$\Pi_1 = P_{o_2}/P_{o_1}$$

Solving for Π_2 results in:

$$\Pi_2 = P_{o_2}{}^x D^y N^z (RT_{o_1})$$

$$\Pi_2 = \left(\frac{M}{Lt^2}\right)^x (L)^y \left(\frac{1}{t}\right)^z \frac{L}{t^2}$$

L: -x + y + 2 = 0

M: x = 0

t: -2x - z - 2 = 0.

These three algebraic expressions yield:

x = 0

y = -2

z = -2.

Therefore,

$$\Pi_2 = D^{-2} N^{-2} RT_{o_1} = \frac{RT_{o_1}}{D^2 N^2}$$

or,

$$\Pi_2 = = \frac{\sqrt{RT_{o_1}}}{DN}.$$

Similarly,

$$\Pi_3 = P_{o_2}{}^x D^y N^z (m) = \left(\frac{M}{Lt^2}\right)^x (L)^y \left(\frac{1}{t}\right)^z \frac{M}{t}$$

L: -x + y = 0

M: x + 1 = 0

T: -2x - z - 1 = 0,

which yields

x = -1

y = -1

z = 1.

Therefore,

$$\Pi_3 = P_{o_2}{}^{-1} D^{-1} N\, m = \frac{mN}{P_{o_2} D}.$$

Since the product of Pi groupings is in itself a Pi grouping, it is convenient to express Π_3 as

$$\Pi_3 = \frac{mN}{P_{o_2} D} (\Pi_1)(\Pi_2) = \frac{mN}{P_{o_2} D} \left(\frac{P_{o_2}}{P_{o_1}} \right) \left(\frac{\sqrt{R T_{o_1}}}{ND} \right) = \frac{m \sqrt{R T_{o_1}}}{P_{o_1} D^2}$$

Therefore,

$$F_2 \left(\frac{P_{o_2}}{P_{o_1}}, \frac{\sqrt{R T_{o_1}}}{ND}, \frac{m \sqrt{R T_{o_1}}}{P_{o_1} D^2} \right) = 0$$

or,

$$\frac{P_{o_2}}{P_{o_1}} = F_3 \left(\frac{\sqrt{R T_{o_1}}}{ND}, \frac{m \sqrt{R T_{o_1}}}{P_{o_1} D^2} \right).$$

When the second dependent variable, T_{o_2}, is introduced, the result is obviously

$$\Pi_4 = T_{o_2} / T_{o_1}.$$

Therefore,

$$F_4 \left(\frac{T_{o_2}}{T_{o_1}}, \frac{\sqrt{R T_{o_1}}}{ND}, \frac{m \sqrt{R T_{o_1}}}{P_{o_1} D^2} \right) = 0$$

or,

$$\frac{T_{o_2}}{T_{o_1}} = F_5 \left(\frac{\sqrt{R T_{o_1}}}{ND}, \frac{m \sqrt{R T_{o_1}}}{P_{o_1} D^2} \right).$$

If the specific gas constant is, indeed, a constant, if all machines are the same physical size, and since the reciprocal of any grouping is a valid grouping, then

$$\frac{P_{o_2}}{P_{o_1}} = F_6\left(\frac{N}{\sqrt{T_{o_1}}}, \frac{m\sqrt{T_{o_1}}}{P_{o_1}}\right)$$

and

$$\frac{T_{o_2}}{T_{o_1}} = F_7\left(\frac{N}{\sqrt{T_{o_1}}}, \frac{m\sqrt{T_{o_1}}}{P_{o_1}}\right).$$

If all important quantities have been included, the data should plot, without significant scatter, on plots similar to those shown in Figure 3.2.1-2. The surge line has been added in Figure 3.2.1-2 because for the example used in this study, the ASTF, all compressors and exhausters are axial machines and are therefore characterized by the surging phenomena.

3.2.2 Butterfly Valves

3.2.2.1 Dimensional Analysis. Figure 3.2.2.1-1 shows, schematically, a butterfly valve installed in a typical duct segment. Application of the First Law of Thermodynamics for steady adiabatic flow of an ideal gas results in

$$T_{o_2} = T_{o_1}.$$

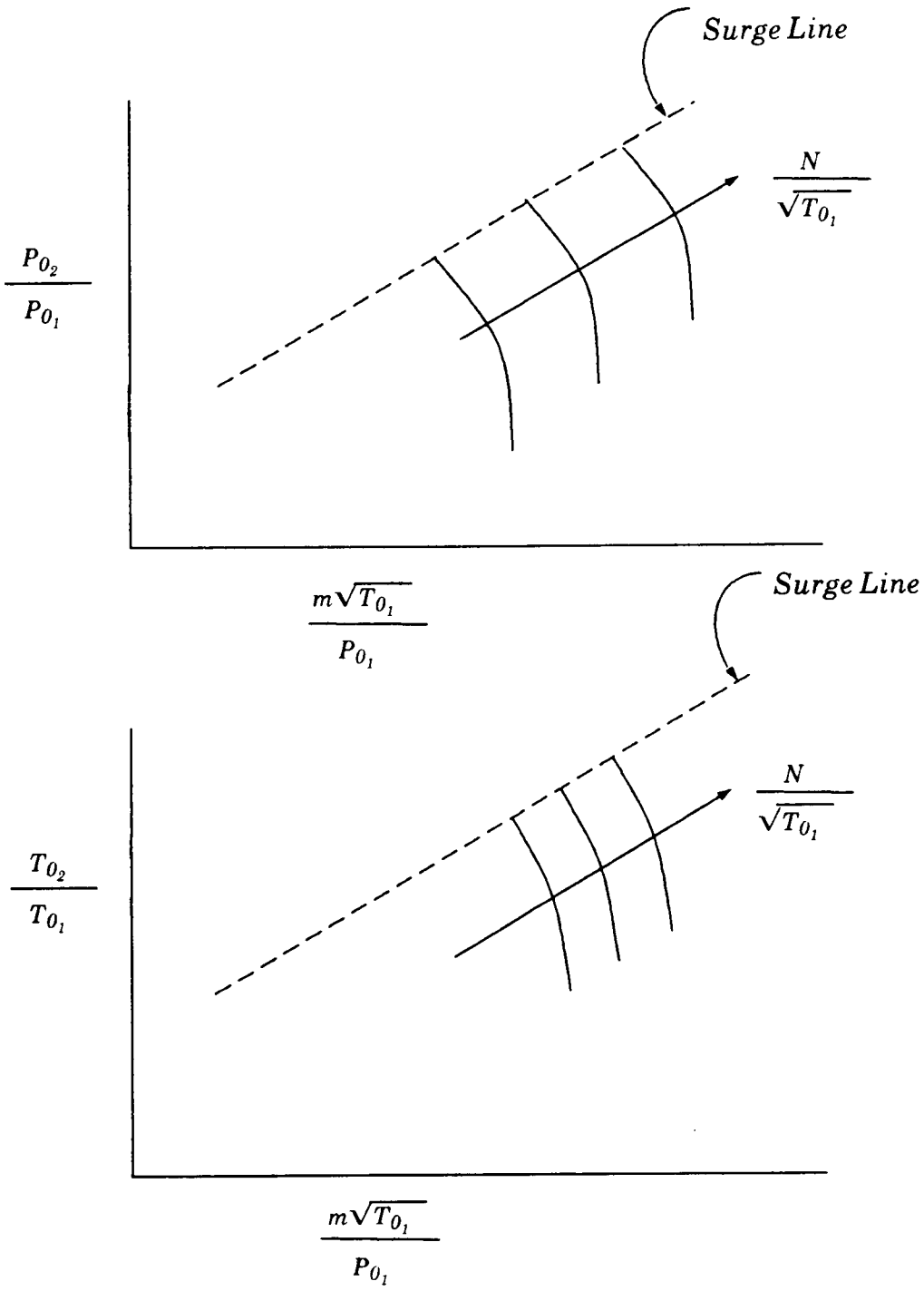


Figure 3.2.1-2 Generic Plots of Compressor or Exhauster, Mathematical Model

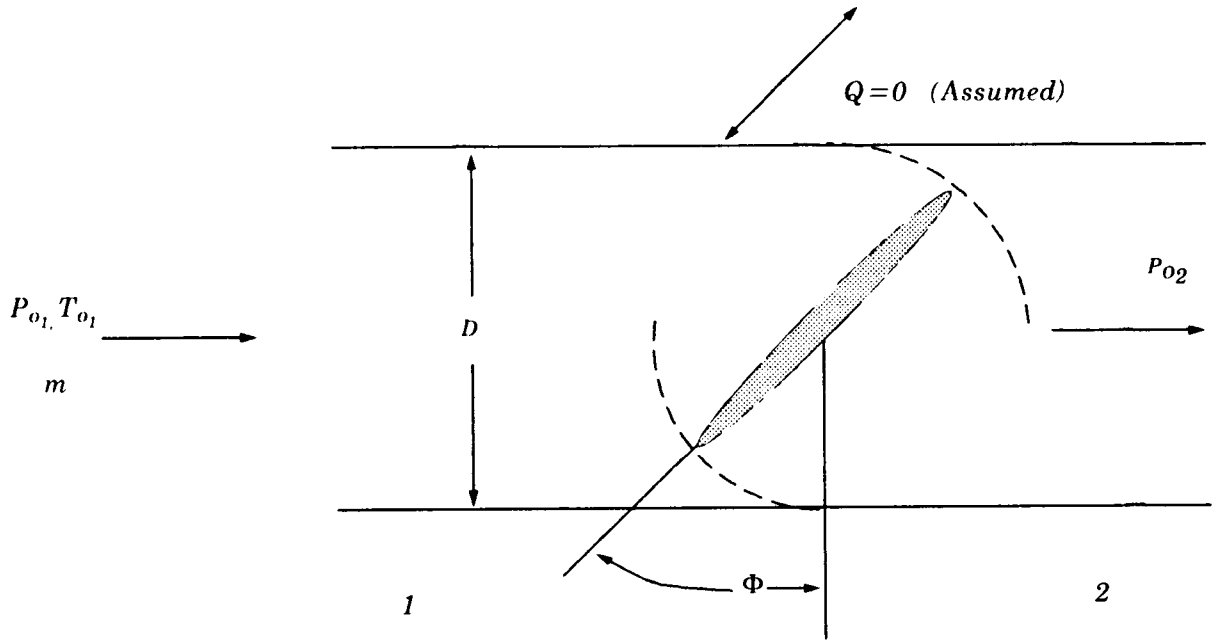


Figure 3.2.2.1-1 Schematic of Butterfly Valve Installation

Application of the Buckingham Pi Theorem yields

$$F_1(P_{o_1}, RT_{o_1}, P_{o_2}, m, \phi, D) = 0.$$

With n = 6; k = 3, there will be three dimensionless groupings. By inspection,

$$\Pi_1 = \frac{P_{o_2}}{P_{o_1}}$$

and,

$$\Pi_2 = \phi \qquad (Radians).$$

Let

$$\Pi_3 = P_{o_1}{}^x (RT_{o_1})^y D^z m$$

$$\Pi_3 = \left(\frac{M}{Lt^2}\right)^x \left(\frac{L}{t^2}\right)^y L^z \frac{M}{t}.$$

Then,

L: -x + 2y + z = 0

M: x + 1 = 0

t: -2x - 2y - 1 = 0.

From which,

x = -1

y = 1/2

z = -2.

Therefore,

$$\Pi_3 = (P_{o_1})^{-1} (RT_{o_1})^{1/2} D^{-2} m,$$

or

$$\Pi_3 = \frac{m\sqrt{RT_{o_1}}}{P_{o_1} D^2}.$$

Therefore,

$$F_2\left(\frac{P_{o_2}}{P_{o_1}}, \frac{m\sqrt{RT_{o_1}}}{P_{o_1} D^2}, \Phi\right) = 0$$

or

$$\frac{P_{o_2}}{P_{o_1}} = F_3\left(\frac{m\sqrt{RT_{o_1}}}{P_{o_1} D^2}, \Phi\right).$$

3.2.2.2 Derivation from Fundamentals. An alternate technique for defining the flow through a butterfly valve is to obtain the functional relationship by the direct application of the laws of continuity, energy and momentum. As is discussed later, in order to keep the relationship manageable in terms of utilization in a real time simulation some limiting assumptions must be employed.

Consider the same system as defined previously (Figure 3.2.2.1.1-1). Stations 1 and 2 are remote locations upstream and downstream of the valve disc, respectively. Establish a third station, called "t", where the flow achieves a minimum cross section. (This is the vena contraction location and is not the "mechanical area" between the valve

disc extremity and the duct wall.) At this location the flow is given by

$$m = \rho_t A_t V_t$$

$$= \frac{P_{s_t}}{RT_{s_t}} A_t M_t \left(\gamma g_c RT_{s_t}\right)^{1/2}$$

$$= \left(\frac{\gamma g_c}{R}\right)^{1/2} A_t M_t P_{s_t} \left(T_{s_t}\right)^{-1/2}$$

$$= \left(\frac{\gamma g_c}{R}\right)^{1/2} A_t M_t \frac{P_{s_t}}{P_{o_t}} P_{o_t} \left(\frac{T_{o_t}}{T_{s_t}}\right)^{1/2} \frac{1}{\left(T_{o_t}\right)^{1/2}}.$$

But,

$$\frac{T_{o_t}}{T_{s_t}} = \left(\frac{P_{o_t}}{P_{s_t}}\right)^{\frac{\gamma-1}{\gamma}}$$

so that

$$m = \left(\frac{\gamma g_c}{R}\right)^{1/2} A_t M_t \frac{P_{s_t}}{P_{o_t}} P_{o_t} \left(\frac{P_{o_t}}{P_{s_t}}\right)^{\frac{\gamma-1}{2\gamma}} \frac{1}{\left(T_{o_t}\right)^{1/2}}.$$

Assuming isentropic flow from Station 1 to Station t ($P_{ot} = P_{o1}$) and applying the First Law of Thermodynamics for steady, adiabatic flow of an ideal gas between the same two station numbers ($T_{ot} = T_{o1}$) gives:

$$m = \left(\frac{\gamma g_c}{R} \right)^{1/2} \frac{P_{o_1} A_t M_t}{\left(T_{o_1} \right)^{1/2}} \frac{P_{s_t}}{P_{o_1}} \left(\frac{P_{o_1}}{P_{s_t}} \right)^{\frac{\gamma - 1}{2\gamma}} .$$

Now assume that $P_{st} = P_{o2}$. This is equivalent, in incompressible flow, to the pressure loss in a sudden expansion with $A_2/A_t = \infty$. Then,

$$m = \left(\frac{\gamma g_c}{R} \right)^{1/2} \frac{P_{o_1} A_t M_t}{\left(T_{o_1} \right)^{1/2}} \frac{P_{o_2}}{P_{o_1}} \left(\frac{P_{o_1}}{P_{o_2}} \right)^{\frac{\gamma - 1}{2\gamma}}$$

$$= \left(\frac{\gamma g_c}{R} \right)^{1/2} \frac{P_{o_1} A_t M_t}{\sqrt{T_{o_1}}} \left(\frac{P_{o_1}}{P_{o_2}} \right)^{\frac{\gamma - 1}{2\gamma}} \qquad (3.2.2.2\text{-}1)$$

All gas flow parameters are now expressed in terms of conditions at stations 1 and 2, which can be measured, except for M_t. The task now is to express M_t in terms of Station 1 and 2 parameters. In general,

$$\frac{P_o}{P_s} = \left(1 + \frac{\gamma - 1}{2} M^2 \right)^{\frac{\gamma}{\gamma - 1}} .$$

Solving for M results in

$$M = \left(\frac{2}{\gamma - 1} \right)^{1/2} \left[\left(\frac{P_s}{P_o} \right)^{\frac{1 - \gamma}{\gamma}} - 1 \right]^{1/2} .$$

Applying this equation to Station t, recalling that $P_{st} = P_{o2}$ and $P_{ot} = P_{o1}$ yields:

$$M_t = \left(\frac{2}{\gamma - 1} \right)^{1/2} \left| \left(\frac{P_{o_2}}{P_{o_1}} \right)^{\frac{1-\gamma}{\gamma}} - 1 \right|^{1/2}$$

Substitution into Equation (3.2.2.2-1) produces

$$m = \left(\frac{\gamma g_c}{R} \right)^{1/2} \left(\frac{2}{\gamma - 1} \right)^{1/2} \frac{P_{o_1} A_1}{\left(T_{o_1} \right)^{1/2}} \left(\frac{P_{o_2}}{P_{o_1}} \right)^{\frac{\gamma+1}{2\gamma}} \left| \left(\frac{P_{o_2}}{P_{o_1}} \right)^{\frac{1-\gamma}{\gamma}} - 1 \right|^{1/2}$$

or,

$$m = \left(\frac{2\gamma g_c}{(\gamma - 1)R} \right)^{1/2} \frac{P_{o_1} A_t}{\sqrt{T_{o_1}}} \left| \left(\frac{P_{o_2}}{P_{o_1}} \right)^{\frac{2}{\gamma}} - \left(\frac{P_{o_2}}{P_{o_1}} \right)^{\frac{\gamma+1}{\gamma}} \right|^{1/2}. \qquad (3.2.2.2\text{-}2)$$

This relationship now needs to be extended to incorporate the choking phenomena. Choking will occur when, for γ = 1.4,

$$\frac{P_{s_t}}{P_{o_t}} = 0.528$$

But, $P_{st} = P_{o2}$ and $P_{ot} = P_{to1}$. Therefore,

$$\frac{P_{s_t}}{P_{o_t}} = \frac{P_{o_2}}{P_{o_1}}$$

At the choked condition, again for γ = 1.4,

$$\left[\left(\frac{P_{o_2}}{P_{o_1}}\right)^{\frac{2}{\gamma}} - \left(\frac{P_{o_2}}{P_{o_1}}\right)^{\frac{\gamma+1}{\gamma}}\right]^{1/2} = 0.256.$$

Therefore, Equation (3.2.2.2-2) can be written as follows:

$$m = \left(\frac{2\gamma g_c}{(\gamma-1)R}\right)^{1/2} \frac{P_{o_1} A_t}{\sqrt{T_{o_1}}} f\left(\frac{P_{o_2}}{P_{o_1}}\right)$$

where

$$f\left(\frac{P_{o_2}}{P_{o_1}}\right) = \left[\left(\frac{P_{o_2}}{P_{o_1}}\right)^{\frac{2}{\gamma}} - \left(\frac{P_{o_2}}{P_{o_1}}\right)^{\frac{\gamma+1}{\gamma}}\right]^{1/2}.$$

If,

$$0.528 \geq \frac{P_{o_2}}{P_{o_1}} > 0$$

then,

$$f\left(\frac{P_{o_2}}{P_{o_1}}\right) = 0.256 \ (for \gamma = 1.4).$$

In many, if not most, industrial facilities, stations 1 and 2 will be at locations where the flow has a very low Mach number. Under such conditions, static parameters are approximately equal to total or stagnation parameters and the stagnation parameter subscripting in the above relationships can be dropped.

The same problem now exists that typically is present in flow through orifices. That is, the area at the minimum flow cross section, A_t, is unknown. The solution selected for use in this study is very similar to the solution to the orifice problem -- use the "mechanical area" as defined previously and adopt a flow coefficient, C_F, to account for the differences. This flow coefficient may differ from a constant value, however, and may be a function of valve angle, pressure ratio, etc. The final equation, then, is

$$m = C_F\left(\frac{2\gamma g_c}{(\gamma-1)R}\right)^{1/2} \frac{P_{o_1} A_m}{\sqrt{T_{o_1}}} f\left(\frac{P_{o_2}}{P_{o_1}}\right). \qquad (3.2.2.2\text{-}3)$$

where

$$f\left(\frac{P_{o_2}}{P_{o_1}}\right) = \left[\left(\frac{P_{o_2}}{P_{o_1}}\right)^{\frac{2}{\gamma}} - \left(\frac{P_{o_2}}{P_{o_1}}\right)^{\frac{\gamma+1}{\gamma}}\right]^{1/2}.$$

If

$$0.528 \geq \frac{P_{o_2}}{P_{o_1}} > 0$$

then

$$f\left(\frac{P_{o_2}}{P_{o_1}}\right) = 0.256 \quad (\textit{for}\ \gamma = 1.4).$$

There are two limiting assumptions in the above derivation. The first, that of isentropic flow from Station 1 to t, is usually not serious. Some pressure loss is sure to occur, but this loss is believed to be small. The second assumption, $P_{st} = P_{o2}$ is more serious. It is likely to be accurate at low subsonic flow conditions but may produce unacceptable errors as compressibility effects become pronounced near the choked point.

3.2.3 Turboexpanders

3.2.3.1 Manufacturer's Model. In the example facility utilized in this study -- the ASTF -- the manufacturer supplied a mathematical model of the airflow processes within the five identical turboexpanders. However, considerable uncertainty existed with regard to the model accuracy due to the prediction of physically impossible results over a portion of the operational envelope. To alleviate this concern, an additional model was developed utilizing dimensional analysis.

3.2.3.2 Dimensional Analysis. Figure 3.2.3.2-1 shows the various quantities believed to be of importance in the performance of the turboexpanders. (A description of the turboexpanders utilized in this study is contained in Chapter 2.) The associated dimensions are as follows:

Pressures	M/Lt^2
Temperatures	L^2/t^2
Mass Flow Rates	M/t
Diameters	L
Vane Angle	Dimensionless

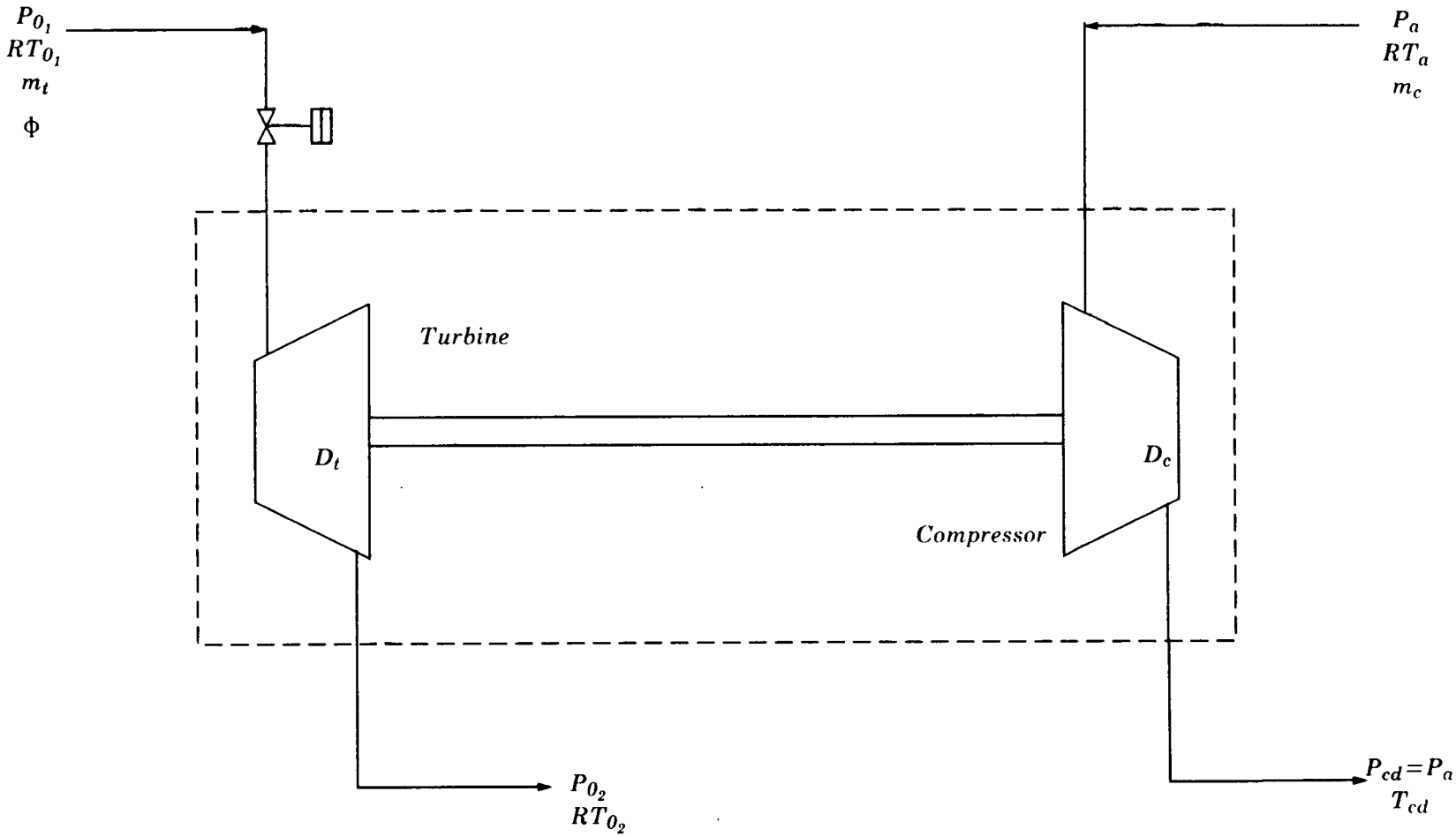


Figure 3.2.3.2-1 Turboexpander Quantities of Importance—Original Assessment

Separating the various quantities into the categories of independent and dependent quantities yields:

Independent	Dependent
P_{o1}	m_t
RT_{o1}	m_c
D_t	RT_{o2}
Φ	P_{cd}
P_{o2}	T_{cd}
P_a	
RT_a	
D_c	

Therefore,

$$m_t = g_1(P_{o1}, RT_{o1}, D_t, \Phi, P_{o2}, P_a, RT_a, D_c)$$

$$m_c = g_2(P_{o1}, RT_{o1}, D_t, \Phi, P_{o2}, P_a, RT_a, D_c)$$

$$\vdots$$

$$T_{cd} = g_5(P_{o1}, RT_{o1}, D_t, \phi, P_{o2}, P_a, RT_a, D_c)$$

and,

$n = 13$
$k = 3$ } 10 Dimensionless Groups

Application of dimensional analysis for the dependent quantities of interest produced the following results:

$$\Pi_1 = \Phi$$

$$\Pi_2 = \frac{m_t \sqrt{R T_{o_1}}}{P_{o_1} D_t^2}$$

$$\Pi_3 = \frac{T_{o_2}}{T_{o_1}}$$

$$\Pi_4 = \frac{P_{o_2}}{P_{o_1}}$$

$$\Pi_5 = \frac{\rho_{c_1}}{\rho_{t_1}}$$

$$\Pi_6 = \frac{D_t}{D_c} = constant,$$

or,

$$\frac{m_t \sqrt{R T_{o_1}}}{P_{o_1} D_t 2} = g_6\left(\frac{P_{o_2}}{P_{o_1}}, \frac{\rho_{c_1}}{\rho_{t_1}}, \Phi\right)$$

$$\frac{T_{o_2}}{T_{o_1}} = g_7\left(\frac{P_{o_2}}{P_{o_2}}, \frac{\rho_{c_1}}{\rho_{t_1}}, \Phi\right).$$

3.2.4 Heaters and Coolers. The mathematical models for the heaters and coolers (with the exception of cooler EC1) are quite simple. Because these subsystems are located in portions of the facility that operated in the "near steady state" mode and because each subsystem has

a very large thermal capacitance, the temperature model simply assumes that the discharge temperature is equal to the control system setpoint value. Pressure losses are computed using

$$\Delta P = K \frac{\rho_1 V_1^2}{2g_c} \qquad (3.2.4\text{-}1)$$

where the resistance coefficient, K, is calculated from manufacturer's specification data.

Cooler EC1 is modeled by dividing the 30 tube rows into 12 groups, each group having different tube and fin geometries. All tube rows within each group are lumped as are the tube temperatures, exit water temperatures and gas temperatures. Various other assumptions and approximations are made including uniform gas temperature and velocity distribution across the shell. The specific equations for EC1 are not presented herein, because, as is noted in Chapter 4, insufficient data are available for validation.

3.2.5 Venturi. Previous work at AEDC indicates that the mass flowrate through an air flow metering venturi can be expressed as

$$m = \frac{P_1 A}{\sqrt{T_1}} f\left(\frac{P_2}{P_1}\right) \qquad (3.2.5\text{-}1)$$

where $f(P_2/P_1)$ varies depending primarily on the specific design. Equation (3.2.5-1) represents the ASTF model where $f(P_2/P_1)$ was

approximated using experimental data from similar venturi subsystems in the Engine Test Facility.

The venturi heat transfer was modeled using Equation (3.1.2.2-2), page 35),

$$T_{B_2} = \frac{T_w + \left(\frac{m c_p}{hA} - 0.5\right)\left(T_{B_1}\right)}{\left(\frac{mc_p}{hA} + 0.5\right)},$$

and a lumped parameter differential equation for the metal temperature of

$$\frac{dT_m}{dt} = \frac{Q}{c_m M_m},$$

where

$$Q = m c_p\left(T_{B_2} - T_{B_1}\right).$$

3.3 Systems

Subsystems are typically connected together by interconnecting duct segments to form systems. There are two gasflow process systems in ASTF -- the air supply and the exhaust. Thermodynamically, these duct segments may be viewed as rigid vessels with unsteady flow simultaneously occurring at both the inlet and discharge. The conditions therefore change with respect to both time and distance. As discussed in Section 3.1, to obtain the "exact" analytical solutions would require the development and solution of many sets of partial differential equations for a large industrial facility. It was

recognized that the required real time simulation could never be achieved if the "exact" models were utilized. The primary goal for the modeling team, as was the case throughout the entire project, was to develop models of sufficient accuracy to meet the validation criteria but yet relatively simple in terms of mathematical complexity.

This section examines in detail unsteady flow of an ideal gas from primarily a thermodynamic viewpoint. Elementary concepts of either flow into or out of a rigid vessel are covered first, briefly, as an introduction to the general case of unsteady flow at both the inlet and outlet. The solution of most of the cases presented requires knowledge of the gas temperature within the thermodynamic system. The assumption that the bulk temperature within the system is equal to the outlet temperature is made and the adequacy of this assumption is analyzed in detail. Finally, a modeling technique is presented which overcomes the shortcomings of the temperature assumption.

3.3.1 Elementary Concepts

3.3.1.1 Flow Into a Vessel Initially Evacuated. Consider first a rigid vessel, initially evacuated, with flow, not necessarily steady, into the vessel. The thermodynamic system is defined as the fluid within the vessel. This particular case is treated extensively in the literature [e.g. 10] and is included here because this most elementary case is used as a foundation upon which more complex examples are identified and solved. The First Law of Thermodynamics in integral format can easily be shown to be

$$Q = M_2 u_2 - \int (h_o \, dM)_{in.} .$$

If the system is assumed adiabatic and if the flow is from a constant enthalpy reservoir, the solution is

$$u_2 = h_{o_{in.}} .$$

The result is in harmony with technical intuition, as the internal energy in the system is simply the internal energy plus the "flow work" of the entering stream. For an ideal gas, the result reduces to

$$T_2 = \gamma T_{o_{in.}}$$

This result is often surprising when first encountered because, for air at standard conditions, the final temperature of the system is 727°R (267°F). If the final temperature were experimentally determined the result would be somewhat lower primarily because it is difficult to construct as adiabatic container. However, the actual measured temperature for many practical systems should be quite high, approaching the calculated value.

3.3.1.2 Flow Into a Vessel Containing Initial Mass. Consider now a slightly more complicated case -- one in which some fluid initially exists in the vessel. The first law is

$$Q = M_2 u_2 - M_1 u_1 - \int (h_o \, dM)_{in.}$$

If the system is adiabatic and the flow is from a constant enthalpy reservoir, the equation reduces to

$$M_2(u_2 - h_{o_{in.}}) - M_1(u_1 - h_{in}) = 0$$

Introducing relationships for enthalpy, h = u + RT, specific gas constant, R = c_p - c_v, and the equation of state, followed by algebraic manipulation, yields the final result [11]

$$T_2 = \frac{c_p P_2 T_{o_{in.}}}{c_v(P_2 - P_1) + c_p P_1 \left(\frac{T_{o_{in.}}}{T_1}\right)}$$

(Note that if the vessel is initially evacuated, P_1 = 0, the result reduces to $T_2 = \gamma T_{in.}$)

3.3.1.3 Flow Out of a Vessel at Constant Rate. For constant mass flow rate out of a vessel, the first law can be written in differential form (neglecting the kinetic energy term at the discharge) as

$$-(m\,h)_{out} = \frac{d}{dt}(Mu)$$

which, by employing the equation of state and the relationship u = c_vT, reduces to

$$\frac{dP}{dt} = -\frac{\gamma R}{V}(mT)_{out}.$$

Even with the introduction of conservation of mass, without additional information, this equation cannot be solved. If it is assumed,

however, that T = T_{out}*, then

$$\frac{dP}{P} = -\frac{\gamma\, m_{out}}{M}\, dt.$$

Introducing conservation of mass

$$M = M_{init} - m_{out}\, t\,,$$

simplifying, and then integrating yields

$$\frac{P}{P_{init}} = exp\ \gamma\left[\ell n\left(1 - \frac{m_{out}\, t}{M_{init}}\right)\right]$$

which is equivalent to

$$\frac{P}{P_{init}} = \left(1 - \frac{m_{out}\, t}{M_{init}}\right)^{\gamma}.$$

The corresponding temperature relationship is

$$\frac{T}{T_{init}} = \left(1 - \frac{m_{out}\, t}{M_{init}}\right)^{\gamma-1}.$$

By comparing the pressure and temperature ratios it can be easily seen that

$$\frac{T}{T_{init}} = \left[\frac{P}{P_{init}}\right]^{\frac{\gamma-1}{\gamma}}$$

---

*The assumption T = T_{out} is examined in detail in Section 3.3.2.4.

and the process is isentropic. This is another somewhat surprising result, as an isentropic assumption was not explicitly made.

3.3.2 The General Cases.

3.3.2.1 Adiabatic Flow. Most systems have unsteady flows simultaneously occurring at both the inlet and outlet. If it is assumed that the system is adiabatic with no shaft work, the first law in differential form can be expressed as

$$(mh)_{in} = (mh)_{out} + \frac{d}{dt}(Mu).$$

But, for an ideal gas with constant specific heats, the derivative reduces to

$$\frac{d}{dt}(Mu) = \frac{d}{dt}\left[\frac{PV}{RT} c_v T\right] = \frac{c_v V}{R}\frac{dP}{dt}$$

and

$$(mh)_{in} = m_{in} c_p T_{in}; \quad (mh)_{out} = m_{out} c_p T_{out}.$$

The first law then becomes

$$m_{in} c_p T_{in} = m_{out} c_p T_{out} + \frac{c_v V}{R}\frac{dP}{dt}$$

or,

$$\frac{dP}{dt} = \frac{\gamma R}{V}\left(m_{in} T_{in} - m_{out} T_{out}\right).$$

As was previously the case, even with the introduction of conservation of mass, this equation cannot be solved without additional information. If it is further assumed that

$$T = T_{out} ,$$

where T is the bulk or "mixing cup" temperature, then

$$\frac{dP}{dt} = \frac{\gamma R}{V}\left(m_{in} T_{in} - m_{out} T\right). \qquad (3.3.2.1\text{-}1)$$

The conservation of mass equation becomes

$$\frac{dM}{dt} = m_{in} - m_{out} , \qquad (3.3.2.1\text{-}2)$$

where

$$M = \frac{PV}{RT} . \qquad (3.3.2.1\text{-}3)$$

Equations (3.3.2.1-1), (3.3.2.1-2), and (3.3.2.1-3) in three unknowns (P, T, and M) completely define the state of the system for the adiabatic case. When the specific variations in mass flow rates and inlet temperatures are introduced, the equations are nonlinear and usually cannot be integrated analytically.

3.3.2.2 Isothermal Flow. Differentiation of the equation of state with respect to time yields the solution for the isothermal case:

$$P = MRT/V$$

$$\frac{dP}{dt} = \frac{RT}{V}\frac{dM}{dt}$$

where

$$\frac{dM}{dt} = m_{in} - m_{out}.$$

Therefore,

$$\frac{dP}{dt} = \frac{RT}{V}(m_{in} - m_{out}).$$

For the isothermal case, the first law reduces to

$$Q_{sys} + (mh)_{in} = (mh)_{out} + \frac{d}{dt}(Mu)$$

or,

$$Q = m_{out}c_pT_{out} - m_{in}c_pT_{in} + \frac{c_vV}{R}\frac{dP}{dt}.$$

Since $T_{in} = T_{out} = T$ (isothermal throughout),

$$Q = c_pT_{in}\left(m_{out} - m_{in}\right) + \frac{c_vV}{R}\frac{dP}{dt}.$$

But, $c_p - c_v = R$ or $R/c_v = \gamma - 1$. The first law becomes

$$Q = c_pT_{in}\left(m_{out} - m_{in}\right) + \frac{V}{(\gamma-1)}\frac{dP}{dt}.$$

This represents the heat transfer that must occur to maintain isothermal conditions within the system.

3.3.2.3 Special Adaptations. The question is sometimes asked, "What happens if the system is both adiabatic and isothermal?" Of course, this is an impossible situation as shown in the preceding derivations. However, a very practical, approximate application results from this theoretically invalid approach. Additionally, computational resources are significantly reduced because it eliminates one equation in each equation set. Under isothermal conditions, the adiabatic equation becomes:

$$\frac{dP}{dt} \approx \frac{\gamma RT}{V}\left(m_{in} - m_{out}\right),$$

where

$$T = T_{in} = T_{out}.$$

This equation coupled with the conservation of mass completely defines the state of the system.

A comparison of the results of this theoretically erroneous, isothermal case was made to the results of the theoretically valid, adiabatic case for a typical duct segment in ASTF. A schematic of the physical configuration is shown in Figure 3.3.2.3-1. At time equal to zero, a step decrease was introduced into the discharge valve area sufficient in magnitude to produce a 10 percent increase in the pressure within the duct segment. This is considered to be a worst case situation for most of the ASTF ducting. The results are presented in Figures 3.3.2.3-2 through 3.3.2.3-4. As was expected, no errors were

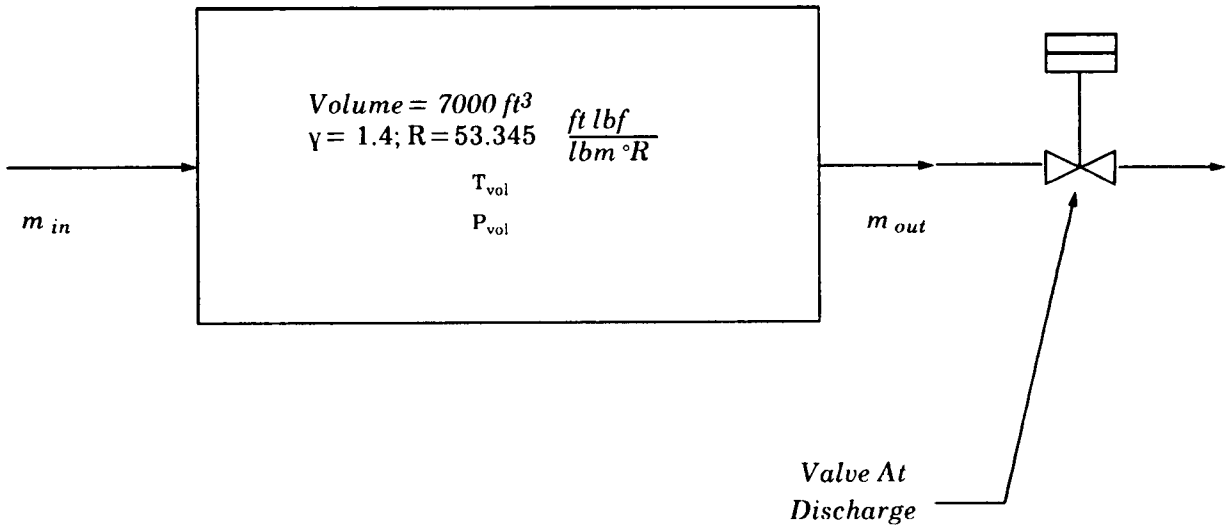


Figure 3.3.2.3-1 Schematic for Isothermal--Adiabatic Flow Example

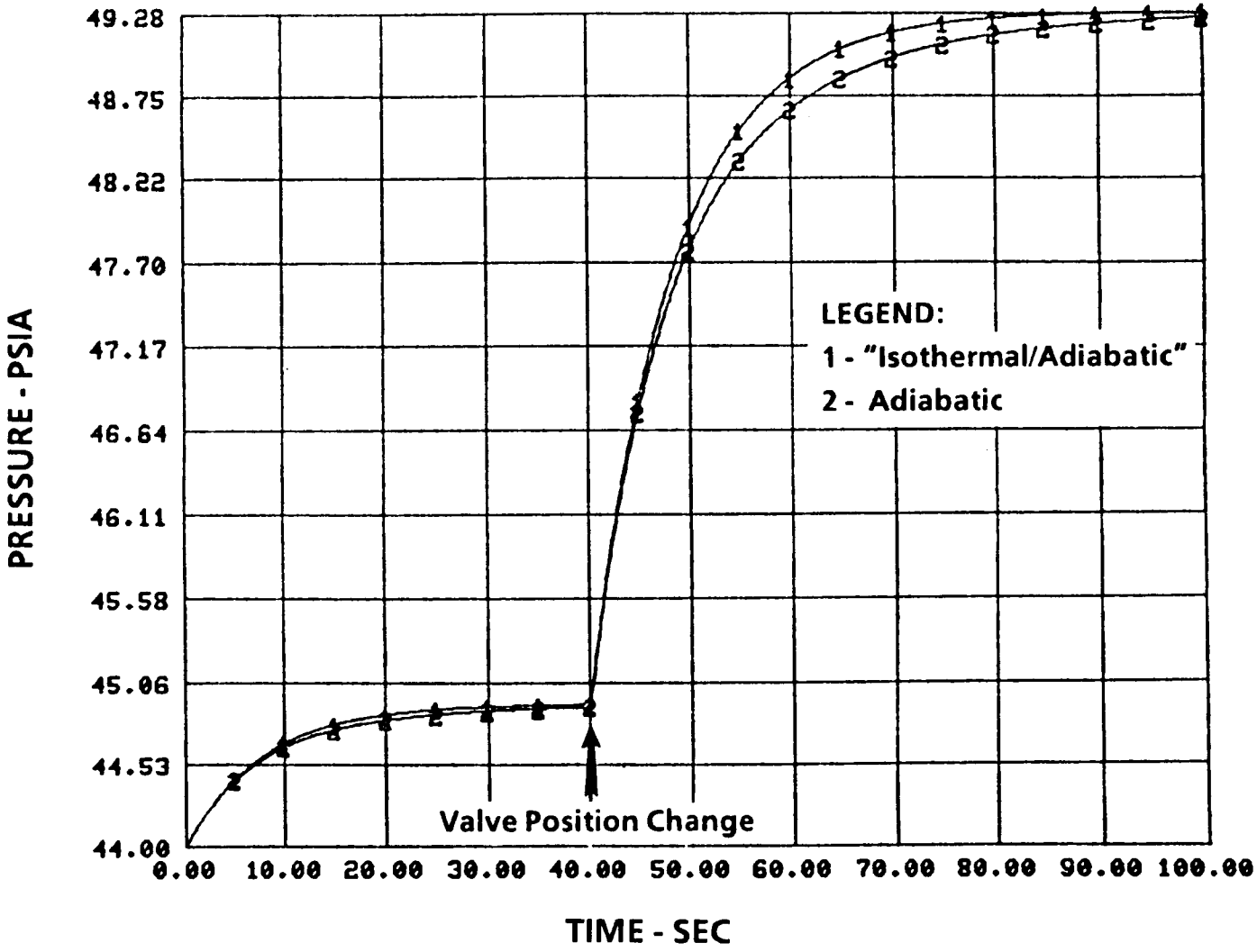


Figure 3.3.2.3-2 "Isothermal/Adiabatic"Comparison - Pressure

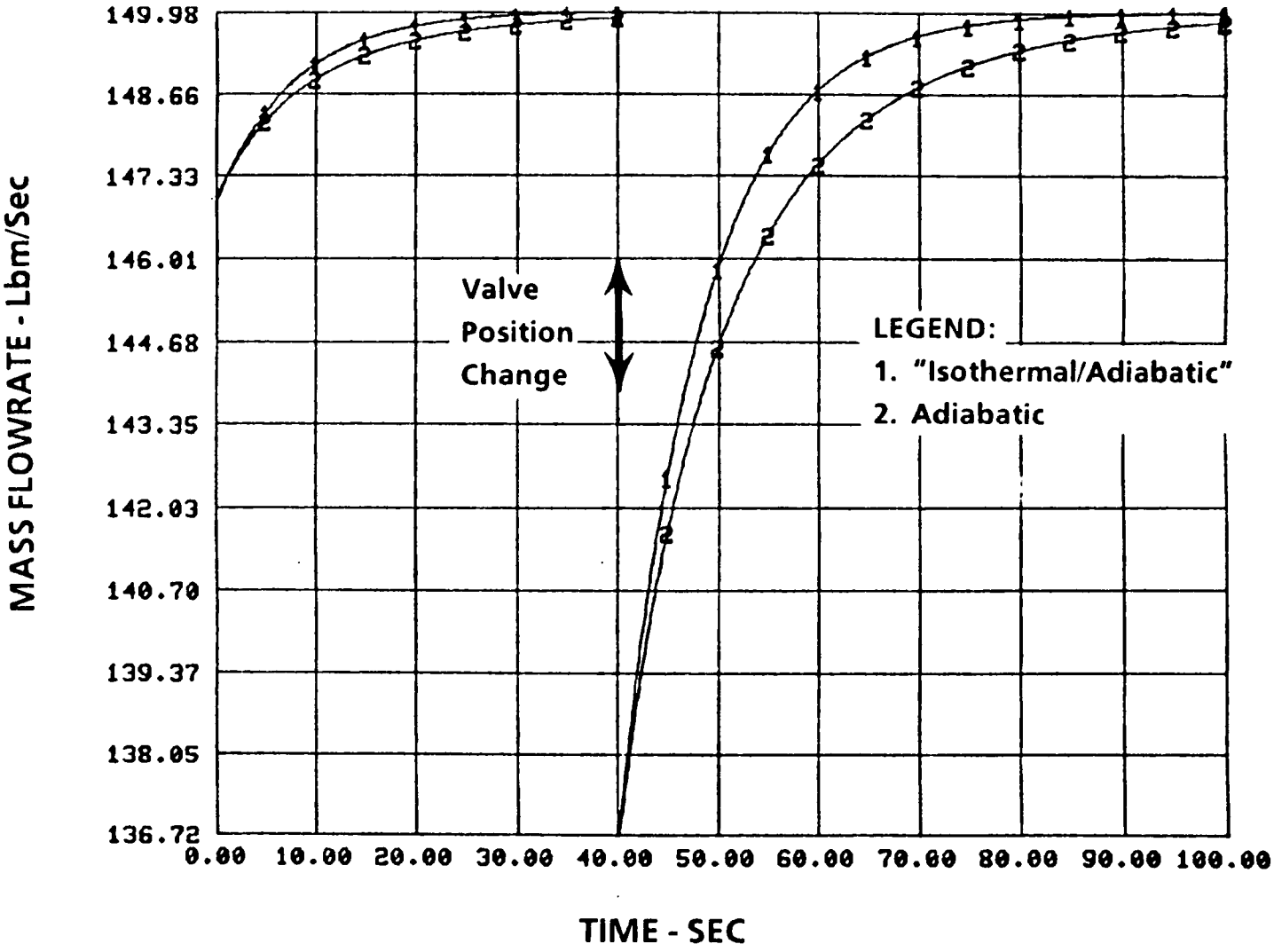


Figure 3.3.2.3-3 "Isothermal/Adabatic" Comparison - Mass Flowrate

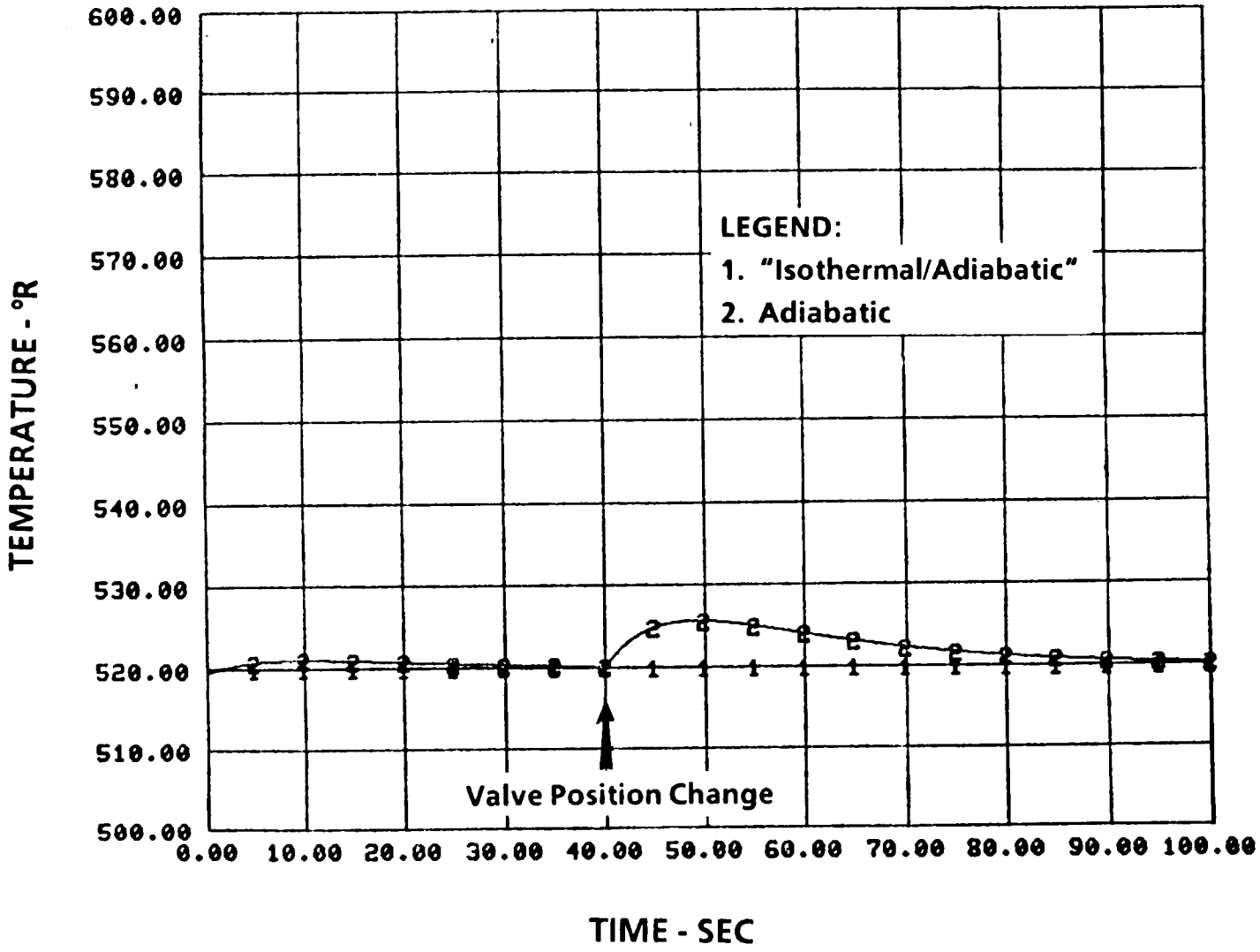


Figure 3.3.2.3-4 "Isothermal/Adiabatic" Comparison - Temperature

introduced into the steady-state solutions. In what was somewhat surprising, the differences in the unsteady solutions were very small. The maximum errors for the invalid isothermal case were as follows:

Pressure - 0.4%

Discharge Mass Flowrate - 0.8%

Temperature - 1.2%

The explanation for these small differences is that not much heat transfer is required to keep the system in the isothermal state for these conditions. The important point to be made here, however, is that these errors were certainly considered to be well within the model accuracy requirements. Therefore, many duct segments were treated as both adiabatic and isothermal even though this is a theoretically invalid approach. The savings in simulation execution time contributed toward the overall goal of achieving a real time simulation. Even in applications where a real time simulation was not required, project costs were reduced due to simpler programming and verification tasks.

3.3.2.4 The Validity of the $T_{out} = T$ Assumption. In general, the temperature out of the system is never equal to the bulk or "mixing cup" temperature within the system. There can be cases however, where this assumption represents a reasonable approximation to the actual situation.

The difference between the two temperatures can be determined as follows. The first law for unsteady, zero shaft work flow of an ideal gas can be written as

$$Q + m_{in} c_p T_{in} = m_{out} c_p T_{out} + \frac{c_v V}{R} \frac{dP}{dt} .$$

Solving for T_{out} gives

$$T_{out} = \frac{1}{c_p m_{out}} \left[Q + m_{in} c_p T_{in} - \frac{c_v V}{R} \frac{dP}{dt} \right] . \qquad (3.3.2.4\text{-}1)$$

The bulk temperature is given by

$$T = \frac{PV}{MR} . \qquad (3.3.2.4\text{-}2)$$

Subtracting Equation (3.3.2.4-2) from (3.3.2.4-1) produces

$$T_{out} - T = \frac{Q}{c_p m_{out}} + \frac{m_{in}}{m_{out}} T_{in} - \frac{V}{\gamma R m_{out}} \frac{dP}{dt} - \frac{PV}{MR}$$

Dividing both sides by T yields

$$\frac{T_{out} - T}{T} = \frac{Q}{c_p m_{out} T} + \frac{m_{in} T_{in}}{m_{out} T} - \frac{V}{\gamma R T m_{out}} \frac{dP}{dt} - 1 .$$

Therefore, for T_{out} to be within a small fraction δ of T,

$$\frac{Q}{c_p m_{out} T} + \frac{m_{in} T_{in}}{m_{out} T} - \frac{V}{\gamma R T m_{out}} \frac{dP}{dt} = 1 \pm \delta \qquad (3.3.2.4\text{-}3)$$

It is obvious that for adiabatic, steady-state conditions, $\delta = 0$, and $T_{out} = T$, exactly.

In industrial facilities that operate in the "near steady-state" mode, an order of magnitude analysis may be helpful in assessing the relative importance of the three terms in Equation (3.3.2.4-3). The following orders are applicable:

$$T \sim T_{in}, \text{ and}$$

$$m_{out} \sim m_{in}.$$

It is immediately recognized that

$$\frac{m_{in} T_{in}}{m_{out} T} \sim 1, and$$

$$\frac{V}{\gamma R T m_{out}} \left(\frac{dP}{dt} \right) \sim 0.$$

The heat-transfer rate, even in near steady-state conditions, can be high such that

$$\frac{Q}{c_p m_{out} T} \sim 1.$$

Therefore, in general, for near steady-state facilities

$$\frac{Q}{c_p m_{out} T} + \frac{m_{in} T_{in}}{m_{out} T} \sim 1 \pm \delta.$$

For the example used in the study -- the ASTF -- the order of the first term can be shown quantitatively. For the worst case operating conditions in the air supply and exhaust systems at locations remote from the test cell*, the calculated steady-state heat transfer rates

*As is shown later, heat transfer between the mixing valves and the test cell inlets is high.

are shown in Table 3.3.2.4-1, together with other important parameters. It is recognized that the unsteady rate will differ from those in steady state; however, for an order of magnitude determination, they are herein assumed equal. The values of the first term in Equation (3.3.2.4-3) are:

Case 1: $Q = 798$ BTU/sec

$T \approx T_{out} \approx T_{in} = 436°R$

$m_{out} = 500$ lbm/sec

$$\frac{Q}{c_p m_{out} T} = 0.015.$$

Case 2: $Q = -5232$ BTU/sec

$T \approx 1160°R$

$m_{out} = 500$ lbm/sec

$$\frac{Q}{c_p m_{out} T} = 0.0376.$$

Case 3:

$$\frac{Q}{c_p m_{out} T} = 0.0376.$$ (Same as Case 2)

Case 4: $Q = 120$ BTU/sec

$T \approx 540°R$

$m_{out} = 500$ lbm/sec

$$\frac{Q}{c_p m_{out} T} = 0.019.$$

Table 3.3.2.4-1 Worst Case Operating Conditions for Heat Transfer (Steady State)

Case No.	$\dot{m}_{air}$ lbm/sec	P_1 psia	T_1 °R	T_2 °R	$_1\Delta T_2$ °R	$_1\Delta T_2/T_1$ %	Q BTU/sec
1	500	40	436	442.7	+6.7	+1.52	798
2	500	40	1160	1116.4	-43.6	-3.76	-5232
3	500	130	1160	1116.4	-43.6	-3.76	-5232
4	500	130	540	541.0	+1	+0.19	120

Notes: 1) Straight duct segment of length equal to 100 feet.

2) Excludes the ASTF Test Area where heat transfer rates are much higher.

The heat transfer term is approximately zero, even under worst case conditions. Therefore, the assumption of adiabatic flow for the ASTF air supply and exhaust ducting (exclusive of the "test area") is considered acceptable with regard to the assumption that $T_{out} \approx T$.

3.3.2.5 The "N-Sub-volume Technique". There are many cases, in general, where the assumption of $T_{out} = T$ is not a good approximation. For example, when a temperature change is made at the inlet to a duct segment, the resulting temperature at the duct discharge as a function of time can, in general, be considerably different from the inlet variation. Consider the situation presented in Figure 3.3.2.5-1. At time t_o, a step input is made at the inlet. (This is approximated, for example in ASTF, when the ATCS setpoint for the Leg 3 control valve cluster is stepped toward the open position and the setpoint for the Leg 2 control valve cluster is stepped toward the closed position.) As the flow is swept through the ducting (the transport time in ASTF may be as long as 30-45 seconds), some degree of mixing with the air already in the ducting will typically occur. The mechanisms responsible for this mixing include induced swirling at the inlet, valve induced turbulence and the presence of other internal hardware such as screens and grids. The step input is therefore degraded by longitudinal mixing. Two extremes exist. First, if the entering flow is totally mixed with the air in the volume, the outlet temperature will vary as per the "total mixing" curve in Figure 3.3.2.5-1. Second, if no mixing occurs, the step input is replicated at the discharge after

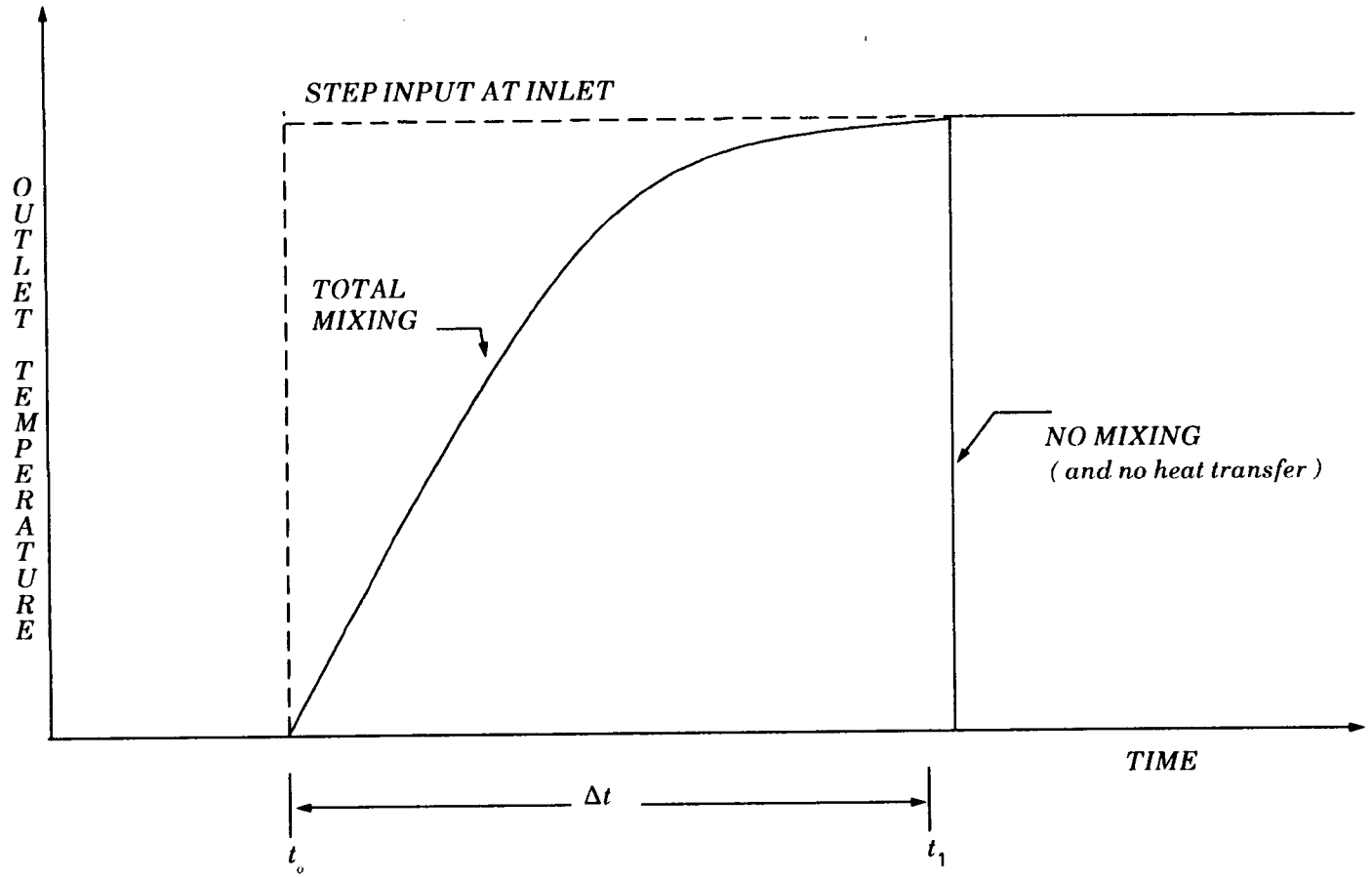


Figure 3.3.2.5-1 Effect of Mixing on Outlet Temperature

the transport time, Δt. In reality, the discharge temperature-time profile will lie somewhere between these two extremes.

A technique was developed to minimize the error introduced by the assumption that $T_{out} = T$. The technique involves dividing up the duct segment into an arbitrary number, N, of equal sub-volumes, effective only for temperature, in each of which $T_{out} = T$ is assumed. By making N sufficiently large, the outlet temperature from each sub-volume approaches the temperature within that volume.

3.3.2.5.1 Single Inlet-Single Outlet. Consider a duct segment as shown in Figure 3.3.2.5.1-1. The segment has been divided up into the sub-volumes as indicated. If the system is assumed adiabatic, based on the results of Section 3.3.2.1, the time rate of change of pressure in the i^{th} sub-volume can be written as

$$\frac{dP_i}{dt} \equiv \dot{P}_i = \frac{\gamma R}{V_i}\left(m_{i-1}T_{i-1} - m_i T_i\right).$$

But for the entire volume, V,

$$\dot{P} = \frac{\gamma R}{V}\left(m_{in}T_{in} - m_{out}T_{out}\right).$$

Because pressure losses are lumped at a point outside the duct segment, there is one and only one pressure throughout the segment. Therefore,

$$P_i = P,$$

and

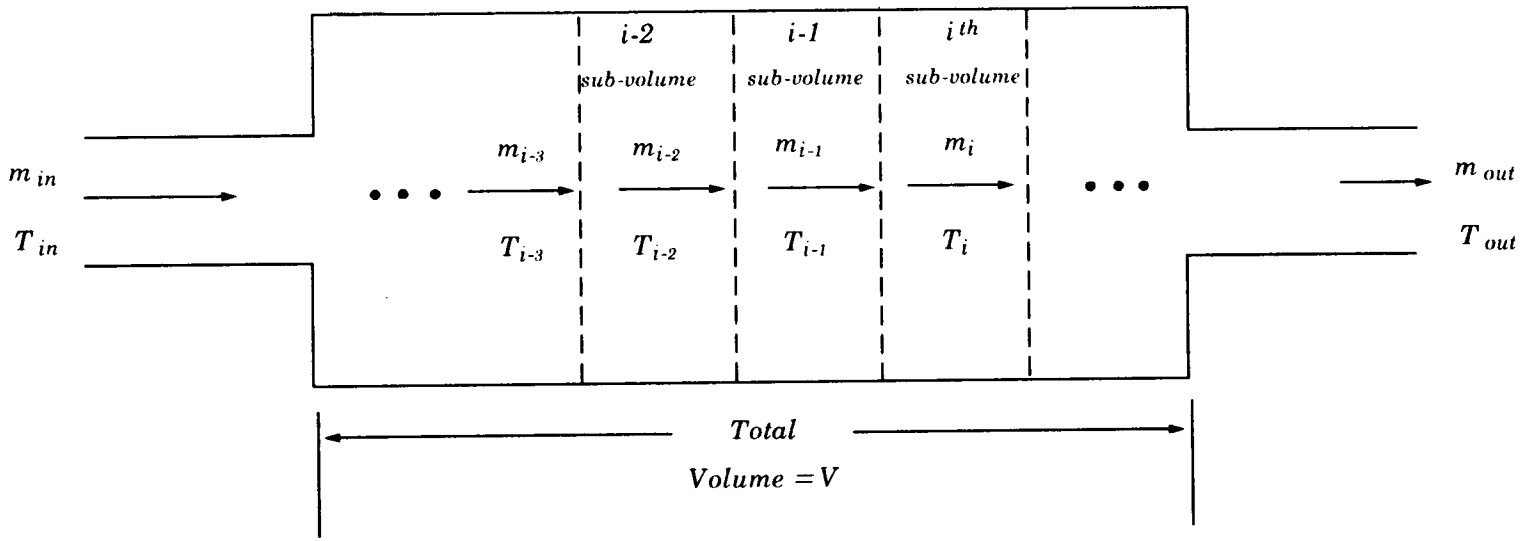


Figure 3.3.2.5.1-1 The "N Sub-Volume Technique:"
Single Inlet-Single Outlet

$$\frac{1}{V_i}\left(m_{i-1}T_{i-1} - m_i T_i\right) = \frac{1}{V}\left(m_{in}T_{in} - m_{out}T_{out}\right),$$

or,

$$m_i T_i = m_{i-1}T_{i-1} - \frac{V_i}{V}\left(m_{in}T_{in} - m_{out}T_{out}\right)$$

For the i-1 and i^{th} sub-volume combined

$$\dot{P}_{(i-1)+i} = \frac{\gamma R}{V_i + V_{i-1}}\left(m_{i-2}T_{i-2} - m_i T_i\right)$$

Equating again to the equation for P yields

$$\frac{1}{V_i + V_{i-1}}\left(m_{i-2}T_{i-2} - m_i T_i\right) = \frac{1}{V}\left(m_{in}T_{in} - m_{out}T_{out}\right)$$

or,

$$m_i T_i = m_{i-2}T_{i-2} - \frac{V_i + V_{i-1}}{V}\left(m_{in}T_{in} - m_{out}T_{out}\right)$$

Similarly for the i-2, i-1 and i sub-volumes combined,

$$\frac{1}{V_i + V_{i-1} + V_{i-2}}\left(m_{i-3}T_{i-3} - m_i T_i\right) = \frac{1}{V}\left(m_{in}T_{in} - m_{out}T_{out}\right)$$

or,

$$m_i T_i = m_{i-3}T_{i-3} - \frac{V_i + V_{i-1} + V_{i-2}}{V}\left(m_{in}T_{in} - m_{out}T_{out}\right)$$

By simply extending this derivation to the duct inlet, it can easily be seen that

$$m_i T_i = m_{in} T_{in} - \frac{V_i + V_{i-1} + \ldots + V_1}{V} \left(m_{in} T_{in} - m_{out} T_{out} \right) \qquad (3.3.2.5.1\text{-}1)$$

If all sub-volumes are equal in volume, then

$$V_i + V_{i-1} + \ldots + V_1 = i\, V_i$$

and

$$V = N\, V_i,$$

where N is the total number of sub-volumes within V. Substitution into Equation (3.3.2.5.1-1) yields:

$$m_i T_i = m_{in} T_{in} - \frac{i V_i}{N V_i} \left(m_{in} T_{in} - m_{out} T_{out} \right)$$

But,

$$\left(m_{in} T_{in} - m_{out} T_{out} \right) = \frac{\dot{P} V}{\gamma R}.$$

Therefore,

$$m_i T_i = m_{in} T_{in} - \frac{i}{N} \frac{\dot{P} V}{\gamma R},$$

or,

$$m_i = m_{in} \frac{T_{in}}{T_i} - \frac{i}{N T_i} \frac{\dot{P} V}{\gamma R}.$$

3.3.2.5.2 Dual Inlets-Single Outlet. Consider now the slightly more complicated case illustrated in Figure 3.3.2.5.2-1. The i^{th} sub-volume nomenclature is associated with volume A; the j^{th} nomenclature with Volume B. Applying the results of the previous derivation to Volume A, it can easily be shown that:

$$m_{A_i} = \frac{1}{T_{A_i}} \left[m_{A_{i-1}} T_{A_{i-1}} - \frac{V_i}{V_A} \left(m_c T_c - m_A T_A \right) \right]$$

$$m_{A_i} = \frac{1}{T_{A_i}} \left[m_{A_{i-2}} T_{A_{i-2}} - \frac{V_i + V_{i-1}}{V_A} \left(m_c T_c - m_A T_A \right) \right]$$

$$m_{A_i} = \frac{1}{T_{A_i}} \left[m_{A_{i-3}} T_{A_{i-3}} - \frac{V_i + V_{i-1} + V_{i-2}}{V_A} \left(m_c T_c - m_A T_A \right) \right]$$

$$\vdots$$

$$m_{A_i} = \frac{1}{T_{A_i}} \left[m_c T_c - \frac{V_i + V_{i-1} + V_{i-2} + \ldots + V_1}{V_A} \left(m_c T_c - m_A T_A \right) \right].$$

For equal sub-volumes,

$$m_{A_i} = \frac{1}{T_{A_i}} \left[m_c T_c - \frac{i}{N_A} \left(m_c T_c - m_A T_A \right) \right].$$

where N_A is the total number of sub-volumes into which Volume A has been subdivided. But, using

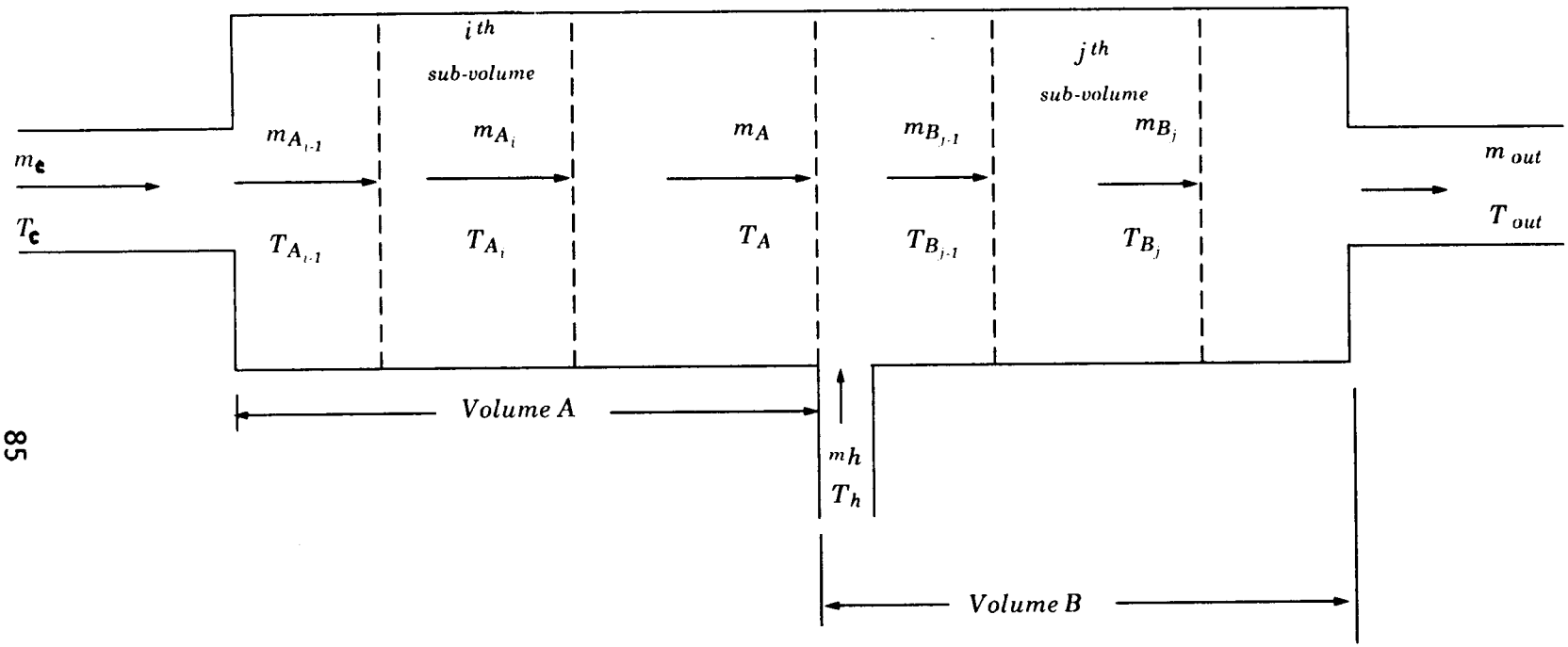


Figure 3.3.2.5.2-1 The "N Sub-Volume Technique:"
Dual Inlets-Single Outlet

$$P_A = \frac{\gamma R}{V_A}\left(m_c T_c - m_A T_A\right)$$

or,

$$\left(m_c T_c - m_A T_A\right) = \frac{\dot{P}_A V_A}{\gamma R}$$

the final result is

$$m_{A_i} = \frac{1}{T_{A_i}}\left[m_c T_c - \frac{i}{N_A}\frac{\dot{P}_A V_A}{\gamma R}\right].$$

The complete set of equations for the i^{th} sub-volume is

$$\dot{M}_{A_i} = m_{A_{i-1}} - m_{A_i} \qquad (i = 1 \text{ to } N_A)$$

$$T_{A_i} = \frac{P_A V_{A_i}}{R M_{A_i}} \qquad (i = 1 \text{ to } N_A)$$

$$m_{A_i} = \frac{1}{T_{A_i}}\left[m_c T_c - \frac{i}{N_A}\frac{\dot{P}_A V_A}{\gamma R}\right]. \qquad (i = 1 \text{ to } N_A)$$

For Volume B, it can be seen by inspection that the equation set reduces to

$$\dot{M}_{B_j} = m_{B_{j-1}} - m_{B_j} \qquad (j = 1 \text{ to } N_B)$$

$$T_{B_j} = \frac{P_B V_{B_j}}{R M_{B_j}} \qquad (j = 1 \text{ to } N_B)$$

$$m_{B_j} = \frac{1}{T_{B_j}} \left[m_A T_A + m_h T_h - \frac{j}{N_B} \frac{\dot{P}_B V_B}{\gamma R} \right]. \qquad (j = 1 \text{ to } N_B)$$

In order to ensure the complete understanding of the preceding equations, assume that each of the Volumes A and B is subdivided into three equal sub-volumes. The complete set of equations becomes (since $\dot{P}_A = \dot{P}_B = \dot{P}$):

$$\dot{M}_{A_1} = m_c - m_{A_1}$$

$$T_{A_1} = PV_{A_1}/R\,M_{A_1}$$

$$m_{A_1} = \left[m_c T_c - \dot{P} V_A / 3\gamma R \right] \frac{1}{T_{A_1}}$$

$$\dot{M}_{A_2} = m_{A_1} - m_{A_2}$$

$$T_{A_2} = PV_{A_2}/R\,M_{A_2}$$

$$m_{A_2} = \left[m_c T_c - 2\dot{P} V_A / 3\gamma R \right] \frac{1}{T_{A_2}}$$

$$\dot{M}_{A_3} = m_{A_2} - m_{A_3}$$

$$T_{A_3} = PV_{A_3}/R\,M_{A_3}$$

$$m_A = \left[m_c T_c - \dot{P} V_A/\gamma R \right] \frac{1}{T_{A_3}}$$

$$\dot{M}_{B_1} = m_A - m_{B_1}$$

$$T_{B_1} = PV_{B_1}/R\,M_{B_1}$$

$$m_{B_1} = \left[m_A T_A + m_h T_h - \dot{P} V_B/3\gamma R \right] \frac{1}{T_{B_1}}$$

$$\dot{M}_{B_2} = m_{B_1} - m_{B_2}$$

$$T_{B_2} = PV_{B_2}/R\,M_{B_2}$$

$$m_{B_2} = \left[m_A T_A + m_h T_h - 2\dot{P} V_B/3\gamma R \right] \frac{1}{T_{B_2}}$$

$$\dot{M}_{B_3} = m_{B_2} - m_{out}$$

$$T_{B_3} = PV_{B_3}/R\,M_{B_3}$$

$$m_{out} = \left[m_A T_A + m_h T_h - \dot{P} V_B / \gamma R \right] \frac{1}{T_{B_3}}$$

In a typical industrial facility application, the following variables are usually known:

$$m_c, T_c, m_h, T_h, and\, m_{out}.$$

Therefore, the above set of 18 independent equations have precisely 18 unknowns and thus a solution is possible.

The equation set can be further simplified by the elimination of $m_A T_A$. Note that

$$m_A T_A = m_c T_c - \frac{\dot{P}_A V_A}{\gamma R}$$

So, that with $\dot{P}_A = \dot{P}_B = \dot{P}$,

$$m_{B_j} = \frac{1}{T_{B_j}} \left[m_c T_c + m_h T_h - \frac{\dot{P}}{\gamma R} \left(V_A + \frac{j}{N_B} V_B \right) \right] \frac{1}{T_{B_3}}.$$

3.3.2.5.3 Dual Inlets-Single Outlet with "Stub-offs". It is not unusual in certain operational configurations to have duct segments that are effective for pressure changes within the system but not effective

for temperature transport lag. These are "dead-headed" or "stub-off" duct segments, open to the system under consideration, but through which no gas flows. This situation is shown schematically in Figure 3.3.2.5.3-1. Although only two stub-offs are shown here, any number could be present.

Applying the results of Section 3.3.2.1 for adiabatic flow in the i^{th} sub-volume of Volume A,

$$\dot{P}_{A_i} = \frac{\gamma R}{V_{A_i} + V'_{A_i}} \left(m_{A_{i-1}} T_{A_{i-1}} - m_{A_i} T_{A_i} \right)$$

where V'_{A_i} is the volume of the stub-off. But, for the entire volume

$$\dot{P}_A = \frac{\gamma R}{V_A + V'_{A_i}} \left(m_c T_c - m_A T_A \right).$$

Since $\dot{P}'_{A_i} = \dot{P}_A$ (assuming the restriction into V'_{A_i} is not severe),

$$\frac{1}{V_{A_i} + V'_{A_i}} \left(m_{A_{i-1}} T_{A_{i-1}} - m_{A_i} T_{A_i} \right) = \frac{1}{V_A + V'_{A_i}} \left(m_c T_c - m_A T_A \right)$$

or,

$$m_{A_i} = \frac{1}{T_{A_i}} \left[m_{A_{i-1}} T_{A_{i-1}} - \frac{V_{A_i} + V'_{A_i}}{V_A + V'_{A_i}} \left(m_c T_c - m_A T_A \right) \right].$$

In a manner similar to the preceding derivations,

$$m_{A_i} = \frac{1}{T_{A_i}} \left[m_{A_{i-2}} T_{A_{i-2}} - \frac{V_{A_i} + V_{A_{i-1}} + V'_{A_i}}{V_A + V'_{A_i}} \left(m_c T_c - m_A T_A \right) \right]$$

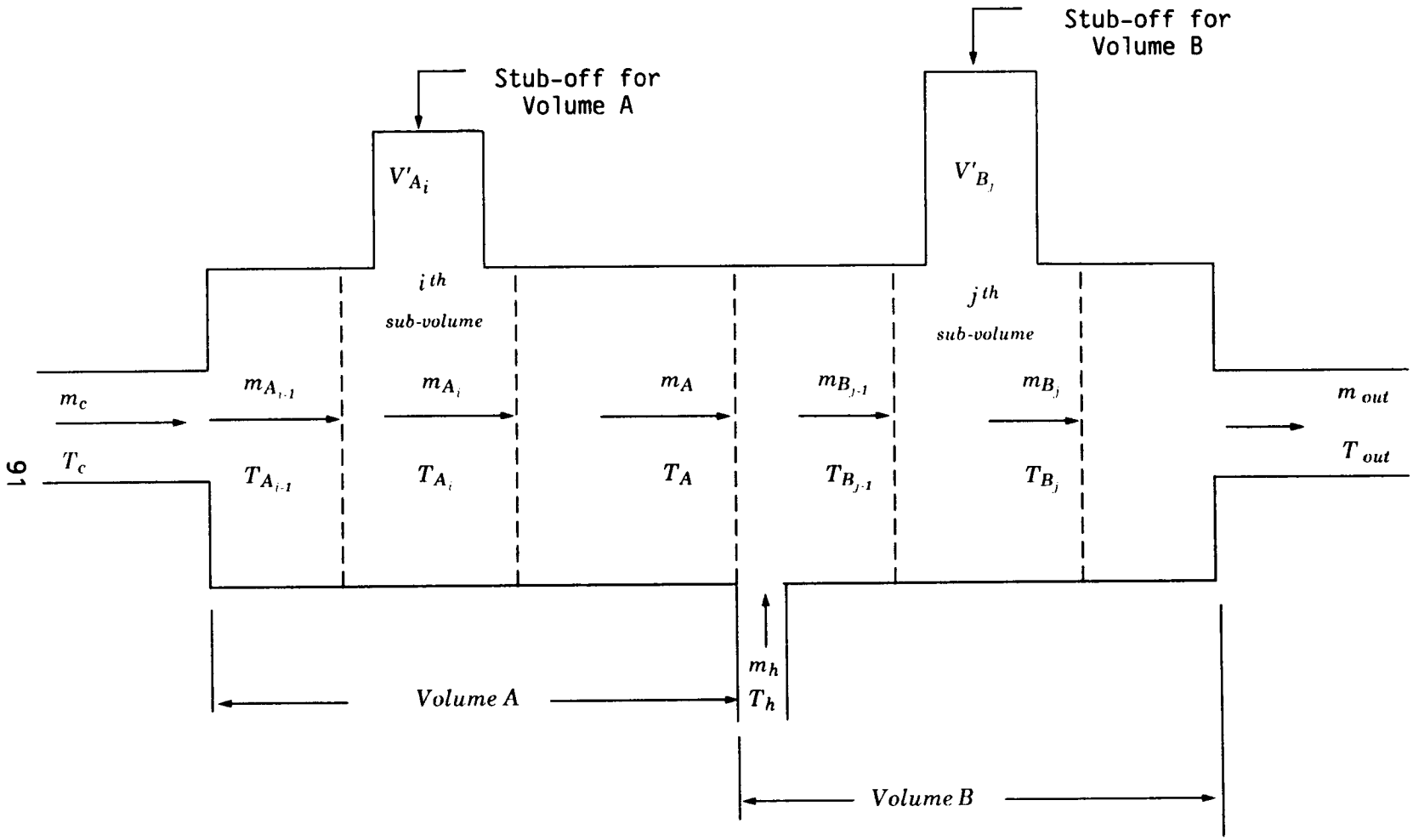


Figure 3.3.2.5.3-1 The "N Sub-Volume Technique:"
Dual Inlets-Single Outlet with Stub-offs

$$m_{A_i} = \frac{1}{T_{A_i}} \left[m_{A_{i-3}} T_{A_{i-3}} - \frac{V_{A_i} + V_{A_{i-1}} + V_{A_{i-2}} + V'_{A_i}}{V_A + V'_{A_i}} \left(m_c T_c - m_A T_A \right) \right]$$

$$\vdots$$

$$m_{A_i} = \frac{1}{T_{A_i}} \left[m_c T_c - \frac{V_{A_i} + V_{A_{i-1}} + V_{A_{i-2}} + \ldots + V_1 + V'_{A_i}}{V_A + V'_{A_i}} \left(m_c T_c - m_A T_A \right) \right].$$

For equal sub-volumes in Volume A,

$$m_{A_i} = \frac{1}{T_{A_i}} \left[m_c T_c - \frac{i V_{A_i} + V'_{A_i}}{N_A V_{A_i} + V'_A} \left(m_c T_c - m_A T_A \right) \right]$$

or,

$$m_{A_i} = \frac{1}{T_{A_i}} \left[m_c T_c - \frac{i + V'_{A_i}/V_{A_i}}{N_A + V'_{A_i}/V_{A_i}} \left(m_c T_c - m_A T_A \right) \right]. \qquad (3.3.2.5.3\text{-}1)$$

Since,

$$\dot{P}_A = \frac{\gamma R}{V_A + V'_{A_i}} \left(m_c T_c - m_A T_A \right)$$

or

$$\left(m_c T_c - m_A T_A \right) = \frac{\left(V_A + V'_{A_i} \right)}{\gamma R} \dot{P}_A .$$

Equation (3.3.2.5.3-1) becomes

$$m_{A_i} = \frac{1}{T_{A_i}} \left[m_c T_c - \frac{i + V'_{A_i}/V_{A_i}}{N_A + V'_{A_i}/V_{A_i}} \frac{\left(V_A + V'_{A_i}\right)\dot{P}_A}{\gamma R} \right].$$

Or, in general, since Volume A may have many stub-offs,

$$m_{A_i} = \frac{1}{T_{A_i}} \left[m_c T_c - \frac{i + \frac{\sum_{k=1}^{i} V'_{A_k}}{V_{A_i}}}{N_A + \frac{\sum_{k=1}^{i} V'_{A_k}}{V_{A_i}}} \frac{\left(V_A + \sum_{k=1}^{i} V'_{A_k}\right)\dot{P}_A}{\gamma R} \right]. \qquad (3.3.2.5.3\text{-}2)$$

Introducing conservation of mass to Volume A results in

$$M_{A_i} = m_{A_{i-1}} - m_{A_i} - m'_{A_i} . \qquad (3.3.2.5.3\text{-}3)$$

The problem here becomes one of determining a relationship for $\dot{m}'_{A_i}$, the mass flow into the stub-off volume. Assuming this flow is adiabatic, the First Law of Thermodynamics for the stub-off volume reduces to

$$\dot{P}'_{A_i} = \frac{\gamma R}{V'_{A_i}} m'_{A_i} T'_{A_i} .$$

Assuming $T'_{A_i} = T_{A_i}$ (an approximation) and noting that $\dot{P}'_{A_i} = \dot{P}_A$,

$$m'_{A_i} = \frac{V'_{A_i} \dot{P}_A}{\gamma R T_{A_i}} . \qquad (3.3.2.5.3\text{-}4)$$

(Note that when P_A is negative, m_{A_i} is negative and the contribution to Equation (3.3.2.5.3-3) is positive. When P_A is positive, the opposite

is true. This is, of course, the desired behavior.) Equations (3.3.2.5.3-2), (3.3.2.5.3-3), and (3.3.2.5.3-4), coupled with the equation of state

$$T_{A_i} = \frac{P_A V_{A_i}}{R M_{A_i}}$$

completely define the system.

Similarly for Volume B, the defining equations become

$$m_{B_j} = \frac{1}{T_{B_j}} \left[m_A T_A + m_h T_h - \frac{j + \frac{\sum_{m=1}^{j} V'_{B_m}}{V_{B_j}} \left(V_B + \sum_{m=1}^{j} V'_{B_m} \right) \dot{P}_B}{N_B + \frac{\sum_{m=1}^{j} V'_{B_m}}{V_{B_j}}} \right] \quad (3.3.2.5.3\text{-}5)$$

$$\dot{M}_{B_j} = m_{B_{j-1}} - m_{B_j} - m'_{B_j}$$

$$m'_{B_j} = \frac{V'_{B_j} \dot{P}_B}{\gamma R T_{B_j}}$$

$$T_{B_j} = \frac{P_B V_{B_j}}{R T_{B_j}}.$$

But, since

$$\dot{P}_A = \frac{\gamma R}{V_A + V'_A}\left(m_c T_c - m_A T_A\right)$$

or,

$$m_A T_A = m_c T_c - \frac{\dot{P}_A\left(V_A + V'_A\right)}{\gamma R}$$

and

$$\dot{P}_A = \dot{P}_B$$

Equation (3.3.2.5.3-5) becomes

$$m_{B_j} = \frac{1}{T_{B_j}}\left[m_c T_c + m_h T_h - \left[\frac{j + \dfrac{\sum_{n=1}^{j} V'_{B_j}}{V_{B_j}}}{N_B + \dfrac{\sum_{n=1}^{j} V'_{B_n}}{V_{B_j}}}\left(V_B + \sum_{n=1}^{j} V'_{B_j}\right)\right.\right.$$

$$\left.\left. + \left(V_A + \sum_{k=1}^{N_A} V'_{A_i}\right)\right]\frac{\dot{P}}{\gamma R}\right]. \qquad \text{(3.3.2.5.3-8)}$$

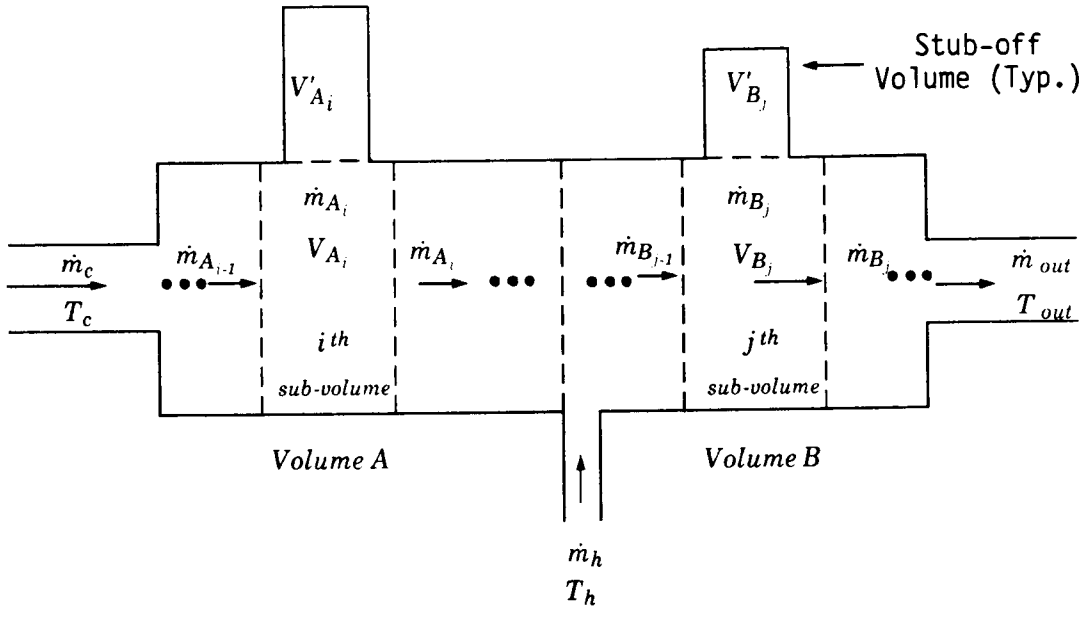
It is easily seen that, if the stub-off volumes are small compared to the primary volumes, Equation (3.3.2.5.3-6) reduces to

$$m_{B_j} = \frac{1}{T_{B_j}}\left[m_c T_c + m_h T_h - \left(\frac{j}{N_B} V_B + V_A\right)\frac{\dot{P}}{\gamma R}\right]$$

which is identical to the equation previously developed for the case without stub-offs.

Figure 3.3.2.5.3-2 provides the general summary of the N Sub-volume technique where Equations (3.3.2.5.3-2) and (3.3.2.5.3-6) have been expressed in a slightly different form for convenience.

With the N sub-volume technique, the value of N becomes a model input. Ideally, experimental data are first obtained. Then, the value of N is selected to specifically tailor the prediction of the outlet temperature as a function of time from the model to the actual experimental results. This tailoring process is discussed in Section 4, Validation.



$$\dot{M}_{A_i} = m_{A_{i-1}} - m_{A_i} - m'_{A_i}; \quad m'_{A_i} = \frac{V'_{A_i}\dot{P}}{\gamma R T_{A_i}} \qquad \text{Volume } A$$

$$T_{A_i} = P V_{A_i} / R M_{A_i}$$

$$m_{A_i} = \frac{1}{T_{A_i}} \left[m_c T_c - \left[\frac{i V_{A_i} + \sum_{k=1}^{i} V'_{A_k}}{N_A V_{A_i} + \sum_{k=1}^{i} V'_{A_k}} \right] \frac{\dot{P}\left(\sum_{k=1}^{N_A} \left(V_{A_k} + V'_{A_k} \right) \right)}{\gamma R} \right]$$

$$\dot{M}_{B_j} = m_{B_{j-1}} - m_{B_j} - m'_{B_j}; \quad m'_{B_j} = \frac{V'_{B_j}\dot{P}}{\gamma R T_{B_j}} \qquad \text{Volume } B$$

$$T_{B_j} = P V_{B_j} / R M_{B_j}$$

$$m_{B_j} = \frac{1}{T_{B_j}} \left[m_c T_c + m_h T_h - \left[\frac{\left(j V_{B_j} + \sum_{m=1}^{j} V'_{B_m} \right) \left(\sum_{m=1}^{j} \left(V_{B_m} + V'_{B_m} \right) \right)}{N_B V_{B_j} + \sum_{m=1}^{j} V'_{B_m}} + \left(V_A + \sum_{k=1}^{N_A} V'_{A_k} \right) \right] \frac{\dot{P}}{\gamma R} \right]$$

Figure 3.3.2.5.3-2 The "N Sub-Volume Technique": Dual Inlets-Single Outlet with Stub-offs—Summary

CHAPTER 4

VALIDATION

4.1 General

4.1.1 Definition of Math Model Validation. There are four basic steps in producing a credible math model:

1. Develop the equations that represent the actual system.
2. Program these equations on a computer to produce a simulation.
3. Compare the computer program that represents the simulation to the equations.
4. Compare the results of simulation runs to experimental data from the actual facility.

Steps 3 and 4 are commonly termed (e.g. [12], [13], and [14]) verification and validation (V&V), respectively, and are formally defined as follows:

Verification - The process of determining that a computer program causes the computer to operate as intended by the programmer.

Validation - The process of determining that the computer simulation behaves like the actual system under study in all pertinent respects.

The relationship among the actual system, the math model, the computer simulation, and the V&V activity is shown in Figure 4.1.1-1.

If the computer simulation does, indeed, accurately represent the math model (i.e., the simulation has been verified), then the

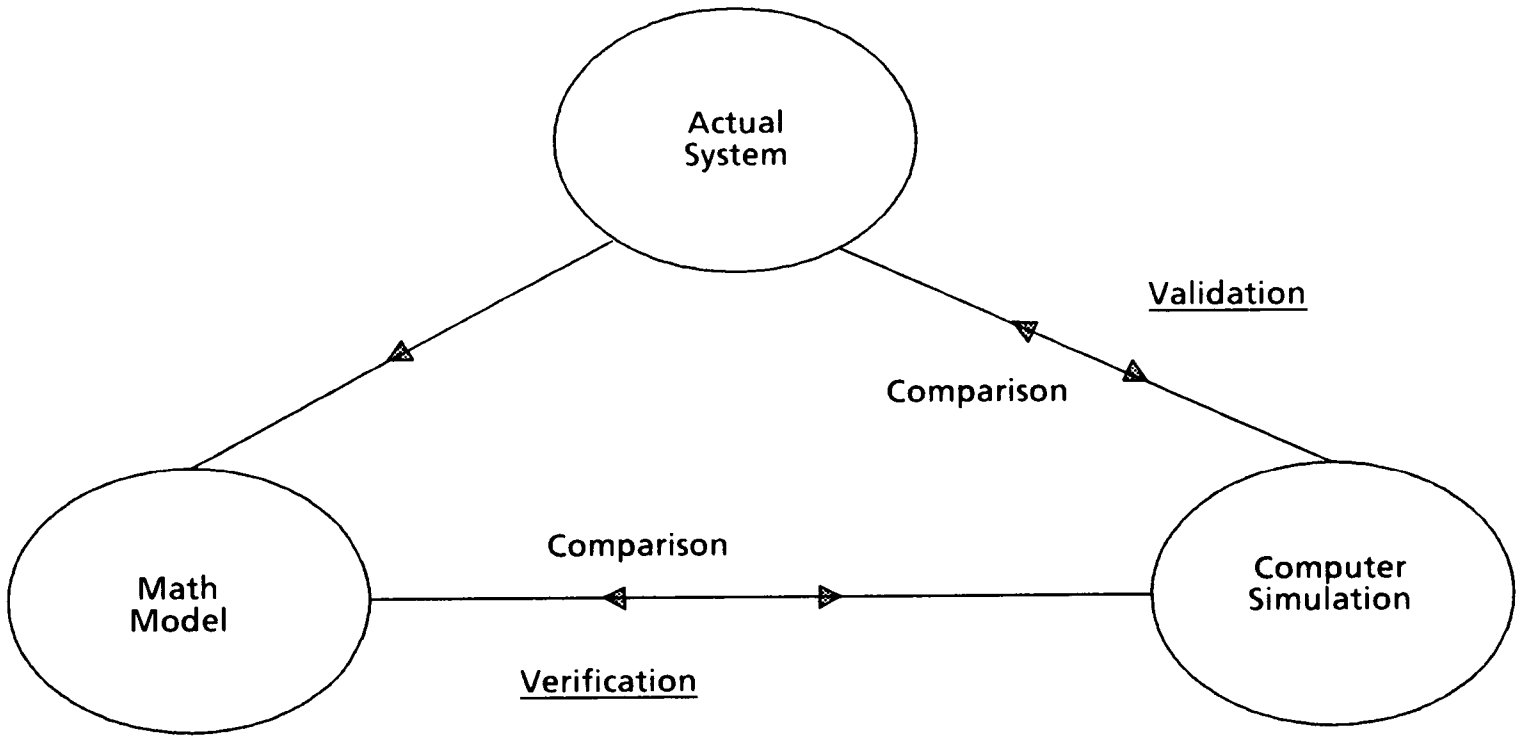


Figure 4.1.1-1 Relationship Among System, Model, Simulation, and V&V

simulation becomes transparent in the math model validation effort. Simulation results can then be compared with actual data with a high degree of confidence that the comparison to the math model is valid.

4.1.2 The Validation Process. The validation process basically consists of:

a. Determining that appropriate simulation data are within accuracy thresholds of the actual data from the facility, and

b. If not, modifying the equations (and the simulation) to whatever degree is necessary to provide the accuracy required.

A more detailed description is shown in Figure 4.1.2-1. If the initial comparison between simulation and actual data is outside the accuracy threshold, the first step in modifying the equations is to conduct a parametric study. This study could range from a task as simple as adjusting a constant in one steady-state relationship to conducting a sensitivity study on a dynamic simulation. If the results of the parametric study do not produce acceptable results, a functional study must be undertaken. This study could range from a task as simple as slightly modifying the dependency of one variable already included in the equation to the addition of new variables not previously considered.

The parametric study is cycled until acceptable results are obtained or until it is evident that a functional study is required. The functional study is also cycled, if required; however, it should be noted that given sufficient resources, the functional study will always

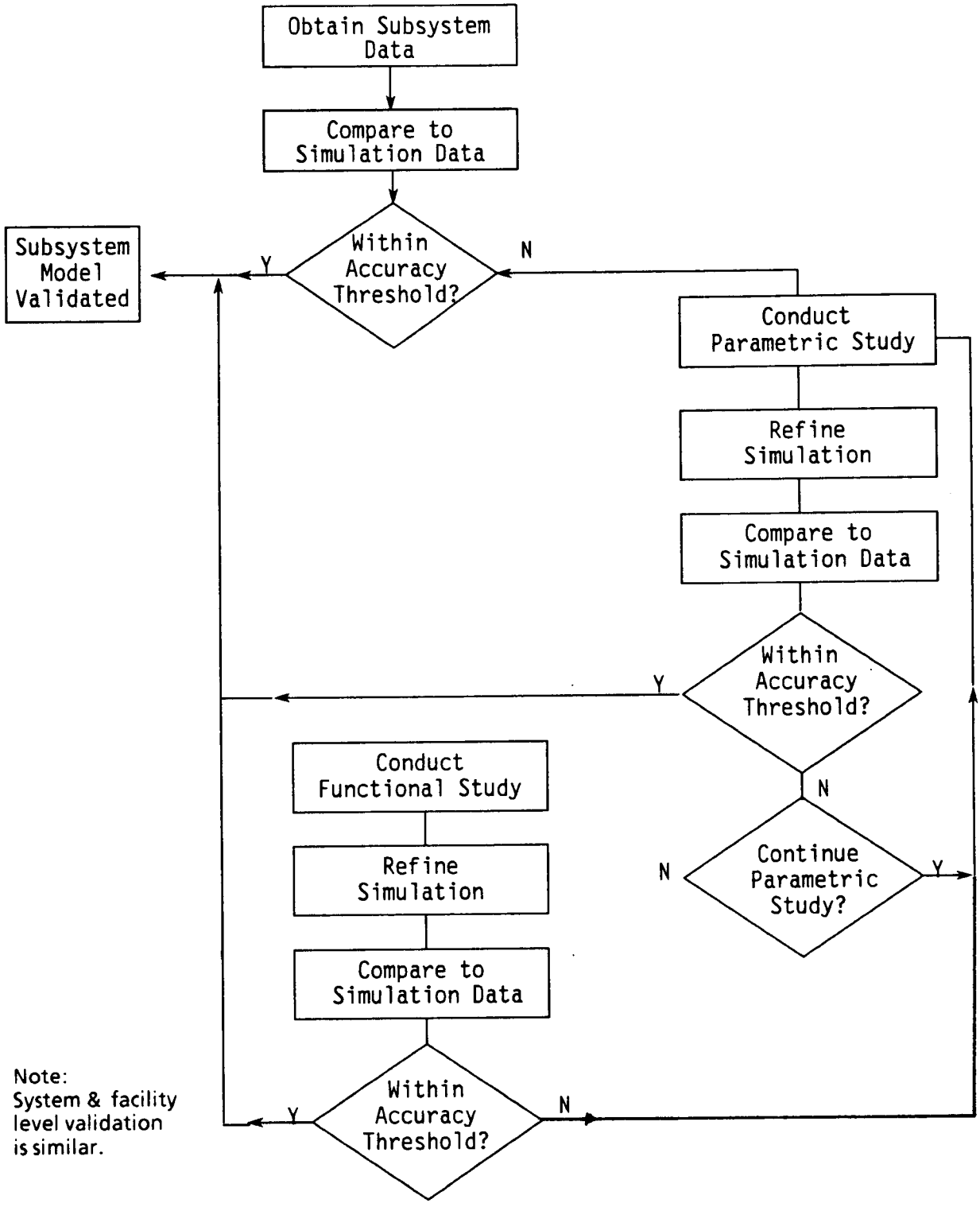


Figure 4.1.2-1 Flow Chart for Subsystem Validation

produce a validated model. In other words, if sufficient data are available, if sufficient time is allocated, if sufficient manhours for engineering analyses are allocated, etc., relationships based on the fundamental laws of science can always be formulated to describe any gas flow phenomena.

Two exceptions exist with regard to the validation process just described. First, if the mathematical model is the result of the application of dimensional analysis, no parametric or functional study is required because the experimental data directly become the validated math model. Second, if the model is merely a simple, steady-state relationship, the simulation would not necessarily require execution because manual calculations could easily provide the model outputs required for the comparison to experimental data.

4.1.3 Hierarchy of Validation. The hierarchy of validation is shown in Figure 4.1.3-1. The lowest level of validation for ASTF involves the various subsystems such as compressors, valves, coolers, engines, etc. The next level is the system level consisting of the air supply and exhaust systems. The highest level is the facility which is produced by coupling the air supply and exhaust systems with a test article in either test cell.

In general, the hierarchy of validation also corresponds to the sequence of validation. That is, subsystems are validated first, followed by systems, and then the facility.

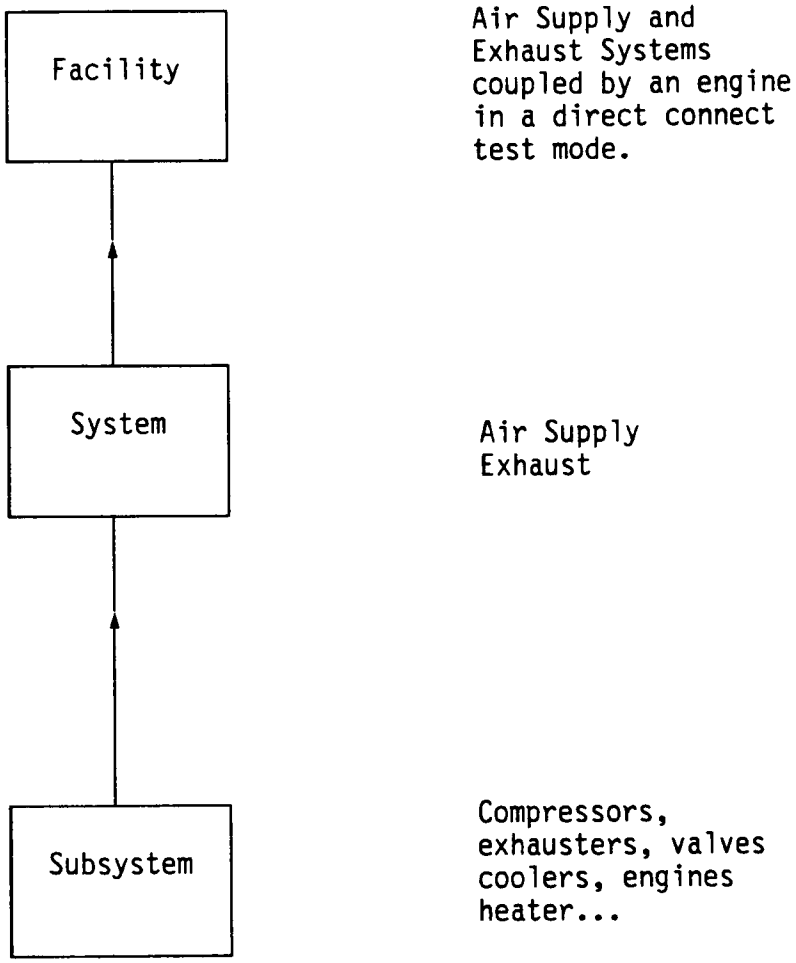


Figure 4.1.3-1 Hierarchy of Validation Using ASTF as an Example

4.1.4 Validation Criteria. A successful math model validation effort requires criteria to determine when a model is acceptably accurate. In relation to Figure 4.1.2-1, the decision statement "within accuracy thresholds?" must be made with quantitative information. The accuracy thresholds cannot be extremely tight because of the large amount of resources required for validation. On the other hand, accuracy thresholds that are too liberal will result in a validation effort that is relatively easy to accomplish, but the resulting "validated" model may be worthless. The key to establishing the proper criteria is a determination of the accuracy required to meet the purposes for which the validated model is to be used. This will, of course, vary with each modeling project. It can also vary within each project as the specific objectives dictate.

4.2 ASTF Validation

In the remainder of this chapter, the ASTF validation effort for those components most common to other industrial facilities is presented. The presentation parallels the math models developed and discussed in Chapter 3 -- first for the selected ASTF subsystems, then for certain portions of the model at the system level.

It should be noted that, in some cases, the model may be validated with experimental data form the facility in sub-scale. One key to the success of this process invovles how accurate the scaling laws are known as compared to the specific validation criteria. In the case of the ASTF, this concept was not implemented due to the lack of a specific need to do so. Although incomplete, sufficient validation

data were available from manual operation of the full-scale facility components to permit successful hardware-in-the-loop testing of the ATCS and to train the ATCS operators. Since ATCS was activated, additional data were obtained as a by-product of normal testing activities. However, large gaps still exist in the data sets required for complete validation.

4.2.1 Subsystems

4.2.1.1 Compressors and Exhausters. Experimental data were obtained for all six air supply compressors and the second- and third-stage exhausters. All data were for a corrected speed characteristic,

$$N_c = \frac{N}{N_d \sqrt{\theta}} \approx 1$$

where $\theta = T_{01}/T_{ref}$. The data for all ten machines plotted very smoothly on a plot of pressure ratio versus corrected mass flow rate with corrected speed as a parameter (see Figure 3.2.1-2, page 45), thus indicating the adequacy of the assumed parameters in the dimensional analysis.

4.2.1.2 Butterfly Valves. Sufficient data were available to partially validate the gas flow through 30 of the ASTF butterfly valves. The validation process was conducted as follows:

a. Data were taken for P_1, P_2, T_1, m, and Φ.

b. The flow coefficient was calculated using Equation (3.2.2.2-3, page 53:

$$C_F = \frac{m\sqrt{\frac{R(\gamma-1)}{2g_c\gamma}}\sqrt{T_1}}{P_1 f_1\left(\frac{P_2}{P_1}\right)\left(\frac{\pi}{4}\right)D_d^2 f_2(\Phi)}$$

c. C_F was found to vary outside the required ±5 percent.

d. A functional study on $f_2(\Phi)$ (see Figure 4.1.2-1, page 101) was then successfully conducted.

e. Some examples of the required functional forms of $f_2(\Phi)$ are

$1 - \cos \Phi$,

$\sin^2 \Phi$, and

$\sin^{1.4} \Phi$.

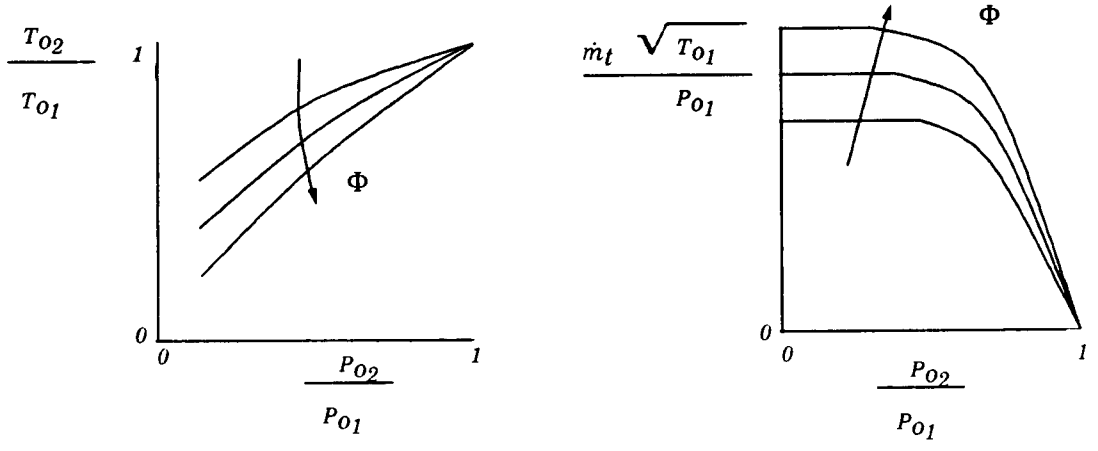
All of the valve models were validated to within ±5 percent on mass flow rate for choked operation in the 20 to 80 percent open range. Average maximum error on mass flowrate outside the 20 to 80 percent range and for unchoked conditions was less than 20 percent.

4.2.1.3 Turboexpanders. As noted in the previous chapter (Section 3.2.3.2), the turboexpander model as determined by dimensional analysis is

$$\frac{m_t\sqrt{R\,T_{o_1}}}{P_{o_1}D_t^2} = g_6\left(\frac{P_{o_2}}{P_{o_1}}, \frac{\rho_{c_1}}{\rho_{t_1}}, \Phi\right)$$

$$\frac{T_{o_2}}{T_{o_1}} = g_7\left(\frac{P_{o_2}}{P_{o_1}}, \frac{\rho_{c_1}}{\rho_{t_1}}, \Phi\right)$$

It was discovered during the validation process that the dependency on the above noted density ratio was very weak; therefore, it was dropped from consideration. Two plots were constructed



Because R and D_t are constants, they could only influence the "scale factor" for the data. Therefore,

$$\frac{m_t \sqrt{R T_{o_1}}}{P_{o_1} D_t^2}$$

was expressed simply as

$$\frac{m_t \sqrt{T_{o_1}}}{P_{o_1}} .$$

The data plotted smoothly, without significant scatter, and was within the required accuracy thresholds of 5 percent on discharge temperature, T_{o2}, and 10 percent on mass flowrate, m_t.

4.2.1.4 Heaters and Coolers. Experimental data taken during facility activation indicated that all heaters and coolers (except Cooler EC1) operated in "near steady state" and the assumption that the discharge temperature is equal to the setpoint value was, indeed, adequate. Insufficient data were available to validate the model for Cooler EC1 with regard to downstream temperature.

The validation effort for pressure losses consisted of taking sufficient data to calculate the resistance coefficient in Equation (3.2.4-1, page 59). These coefficients varied from values as low as 1 to over 100.

4.2.1.5 Venturi. The equation for mass flowrate through the venturi (Section 3.2.5, page 59) is

$$m = \frac{P_1 A}{\sqrt{T_1}} f\left(\frac{P_2}{P_1}\right)$$

This equation was validated by simply taking sufficient data to plot

$$f\left(\frac{P_2}{P_1}\right) = \frac{m\sqrt{T_1}}{P_1 A}$$

as a function of pressure ratio, P_2/P_1. In essence, this technique substitutes experimental data for $f(P_2/P_1)$. The data plotted very smoothly, with maximum scatter of generally less than 5 percent.

4.2.2 Systems

4.2.2.1 The "N-Subvolume Technique". The "N-subvolume technique" was applied to the portion of the ASTF air supply system between the mixing header control valves and a point immediately upstream of each of the last flow straightening grids in the test cell inlet ducting (Figure 2.4.5-1, page 18). This is the portion of the facility that does not operate in the "near steady-state" mode.

The validation required special tests using supply Legs 2 and 3 with airflow through test cell C-2. Flow was initially established in the test cell inlet ducting using Leg 2. Flow at a higher temperature was established through Leg 3 out the dump valves (CV.C.4 A, B and C). After flow stabilization, the Leg 2 mixing valves (CV.C.1, A, B, and C) were quickly closed while simultaneously opening the Leg 3 mixing valves (CV.C.3 A, B, and C), throughout this process, trying to maintain constant mass flowrate and pressure in the mixing header. This procedure approximated a step input for temperature while attempting to hold all other parameters constant. Data were obtained for the following test cases:

1) m = Low $T_{Leg\ 2}$ = 550°R; $T_{Leg\ 3}$ = 573°R
2) m = Medium $T_{Leg\ 2}$ = 500°R; $T_{Leg\ 3}$ = 568°R
3) m = Medium $T_{Leg\ 2}$ = 515°R; $T_{Leg\ 3}$ = 783°R
4) m = High $T_{Leg\ 2}$ = 513°R; $T_{Leg\ 3}$ = 587°R

All required pressures and temperatures were recorded and the mass flowrate was measured using the validated C-2 venturi subsystem. Actual variations in mass flowrate, mixing header pressure as well as

the near step change in inlet temperature were input into the simulation and a parametric study (Section 4.1.2) conducted on the value of N in each of the five major lumped volumes between the mixing valves and the last flow straightening grid. The results are presented in Figures 4.2.2.1-1 through 4.2.2.1-4. These comparisons were all generated for N = 1 -- the value of N that produced the closest comparisons. The differences in actual versus calculated temperature at the second flow straightener (T_2), are less than 5 percent at all points.

It should be noted that the actual outlet temperature for each of the four test cases initially decreased slightly prior to resuming a more predictable profile. The reason for this decline was that the pressure could not be held constant during the valve transition -- the pressure initially decreased in all four cases. When these actual pressure decreases were input into the simulation, the predicted outlet temperature also decreased due to the unsteady expansion of the air within the volumes. In each case, the variation in outlet temperature was greater for the calculated values. This difference is believed to be attributable to the finite response time of the temperature transducers except for Case No. 2 (Figure 4.2.2.1-2). The initial "double dip" behavior for this case could not be explained.

It was very surprising that N = 1 produced the best results. It should be restated for emphasis (see previous page) that the ducting had already been divided up into five volumes in the lumped parameter representation of this portion of the facility. Therefore, N = 5 as

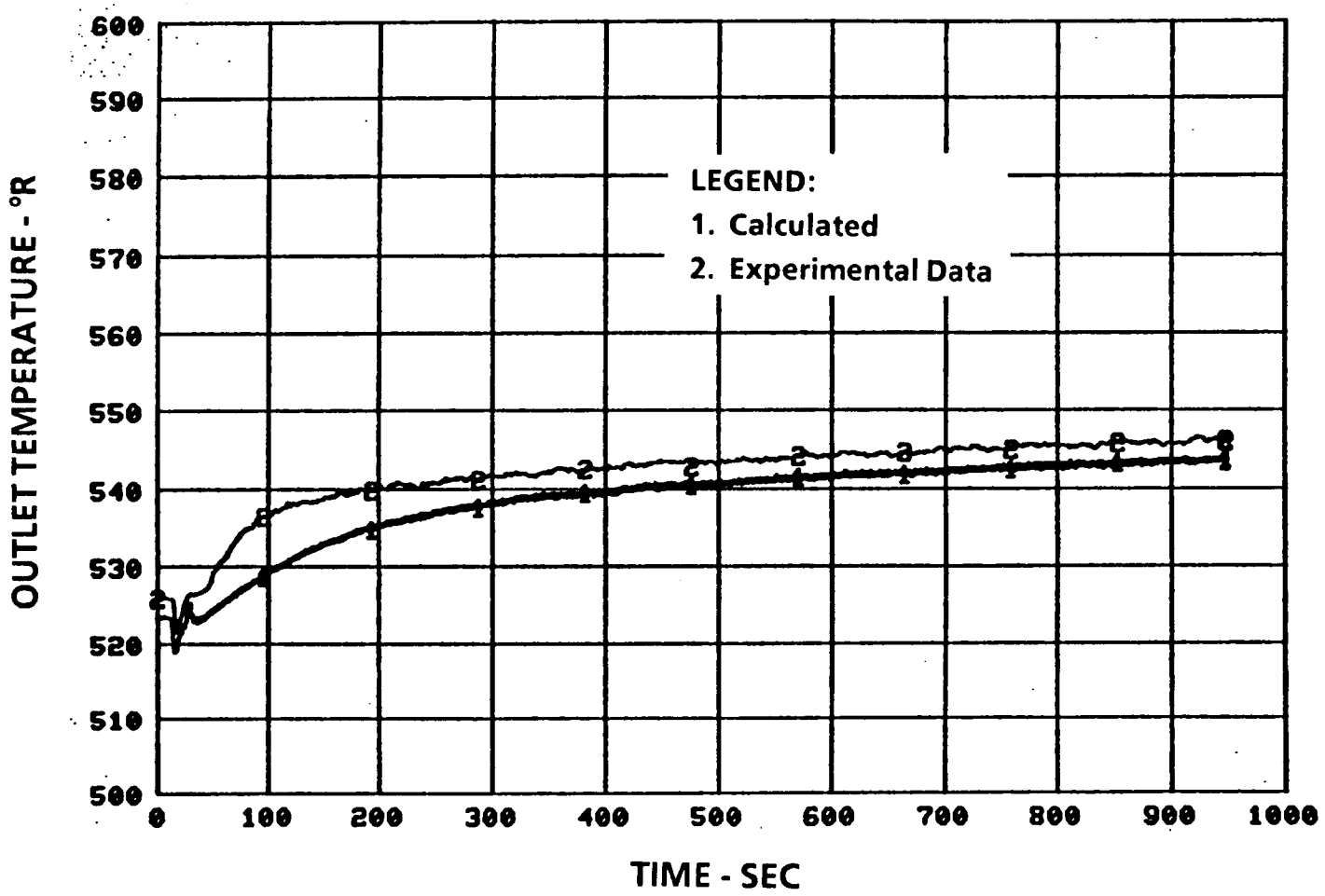


Figure 4.2.2.1-1 "N Sub-volume Technique" Validation - Case 1 - N = 1

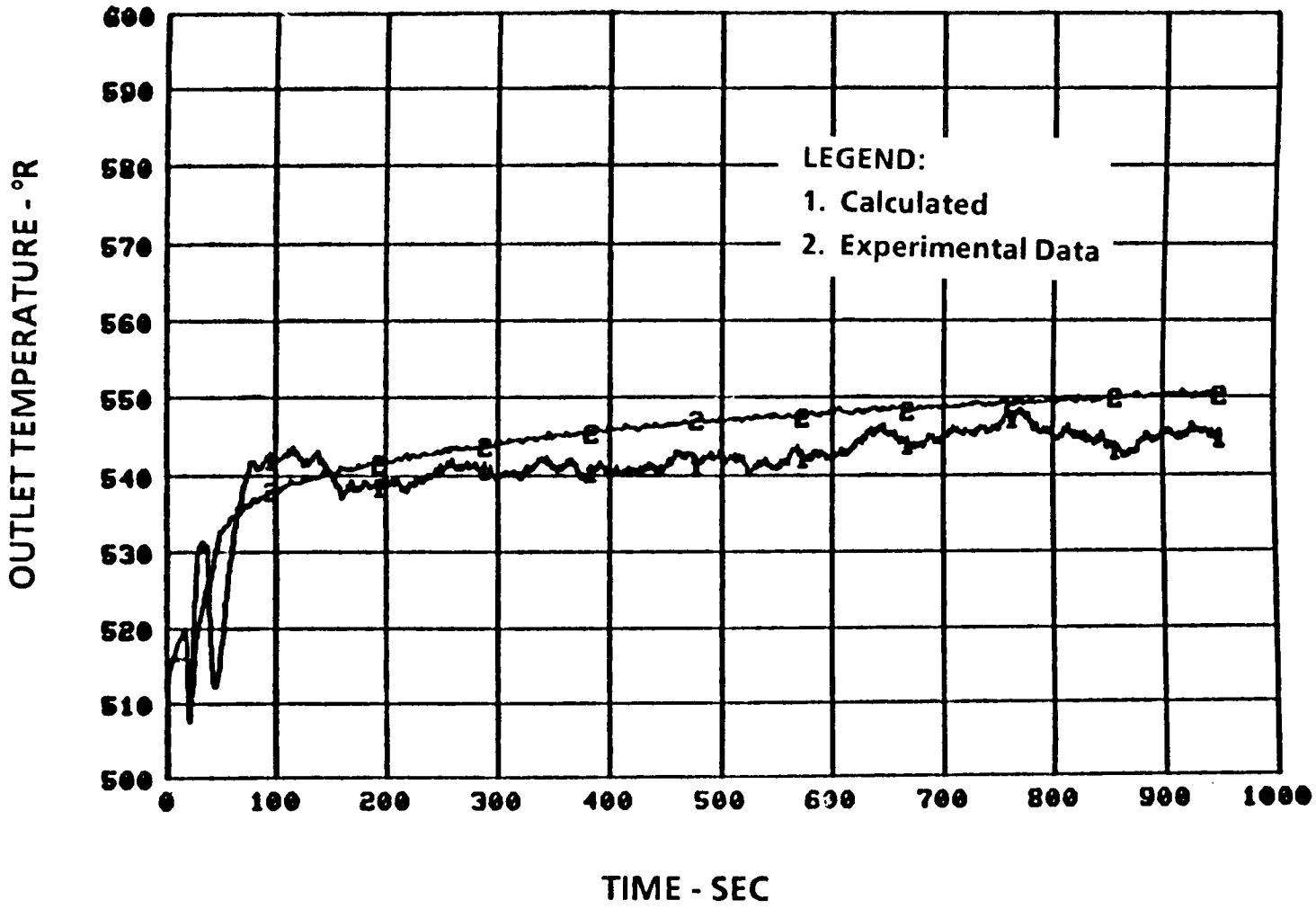


Figure 4.2.2.1-2 "N Sub-volume Technique" Validation - Case 2 - N = 1

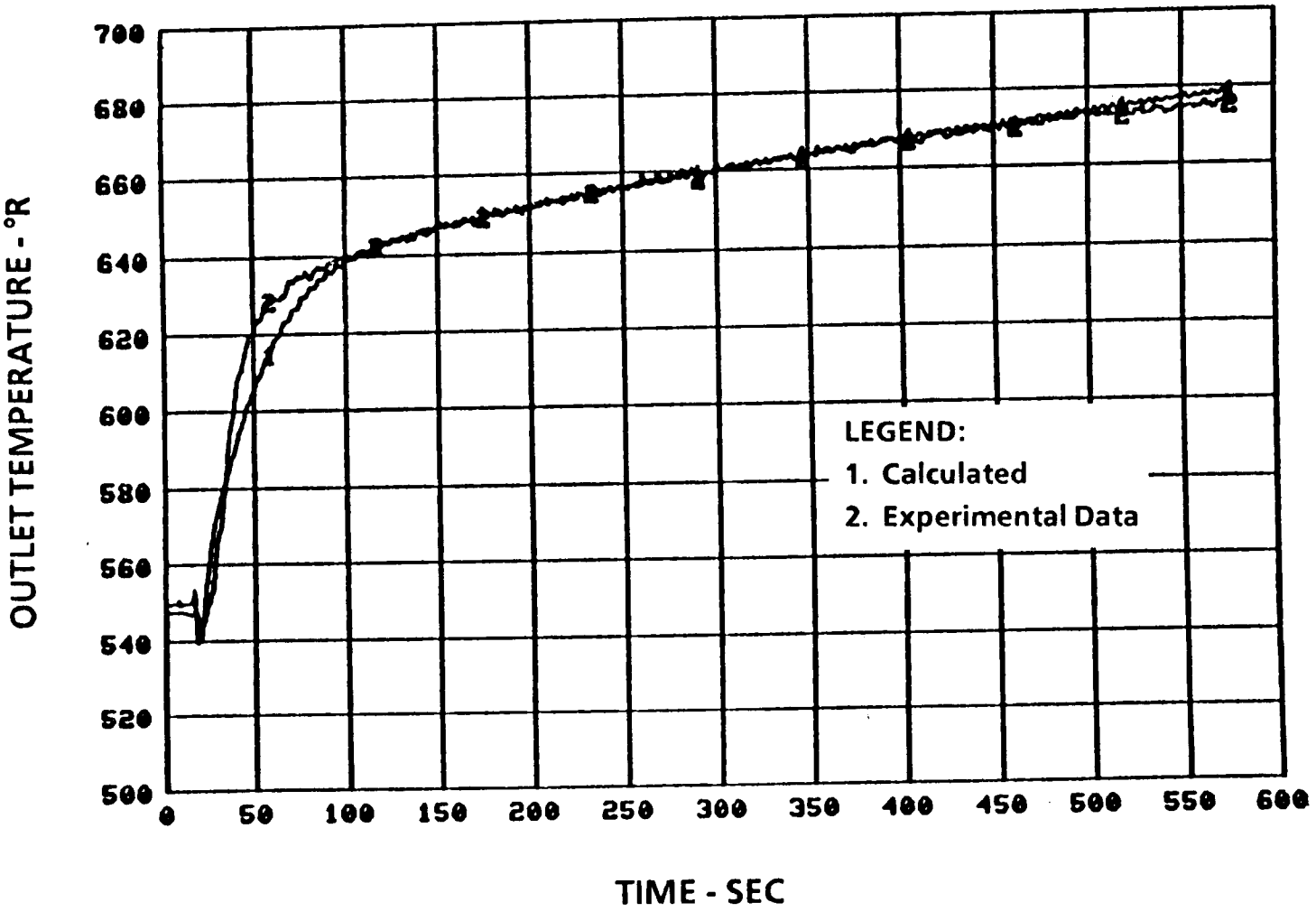


Figure 4.2.2.1-3 "N Sub-volume Technique" Validation - Case 3 - N = 1

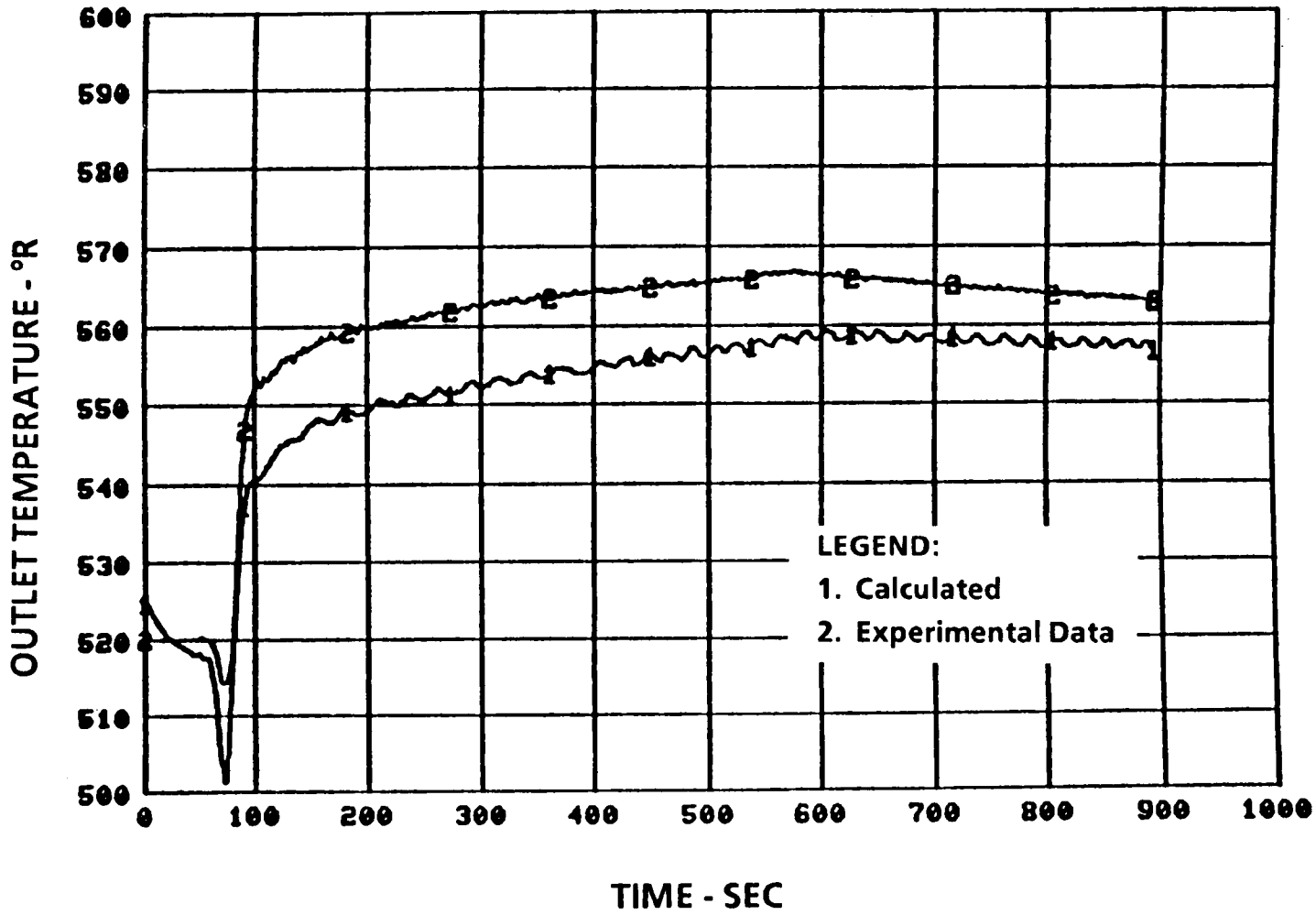


Figure 4.2.2.1-4 "N Sub-volume Technique" Validation - Case 4 - N = 1

parameters constant. Data were collected at strategic locations throughout the system including data from all the metal thermocouples.

4.2.2.2.2 Initial Comparisons. The simulation was then upgraded by replacing the assumption of a constant duct wall temperature with a lumped parameter representation given by

$$\frac{dT_m}{dt} = \frac{Q}{c_m M_m}$$

where

$$Q = m\, c_p \left(T_{B_2} - T_{B_1} \right).$$

The actual inlet temperature to the mixing header was input into the simulation and the predicted values of test cell inlet air temperature, and duct metal, venturi and flow straightener temperatures were calculated and compared to experimental data. Large differences existed. Figure 4.2.2.2.2-1 is an example of the comparison between test cell inlet temperatures. The error greatly exceeds the ±5% criteria.

In order to make the validation task more manageable and because of a very limited number of air temperatures, the system was broken up into two parts. The first part was that portion of the system from the mixing valves to a point immediately upstream of the first flow straightener -- the first location in the air stream past the mixing valves where a temperature measurement was available. The second part encompassed the remainder of the system to the test cell inlet.

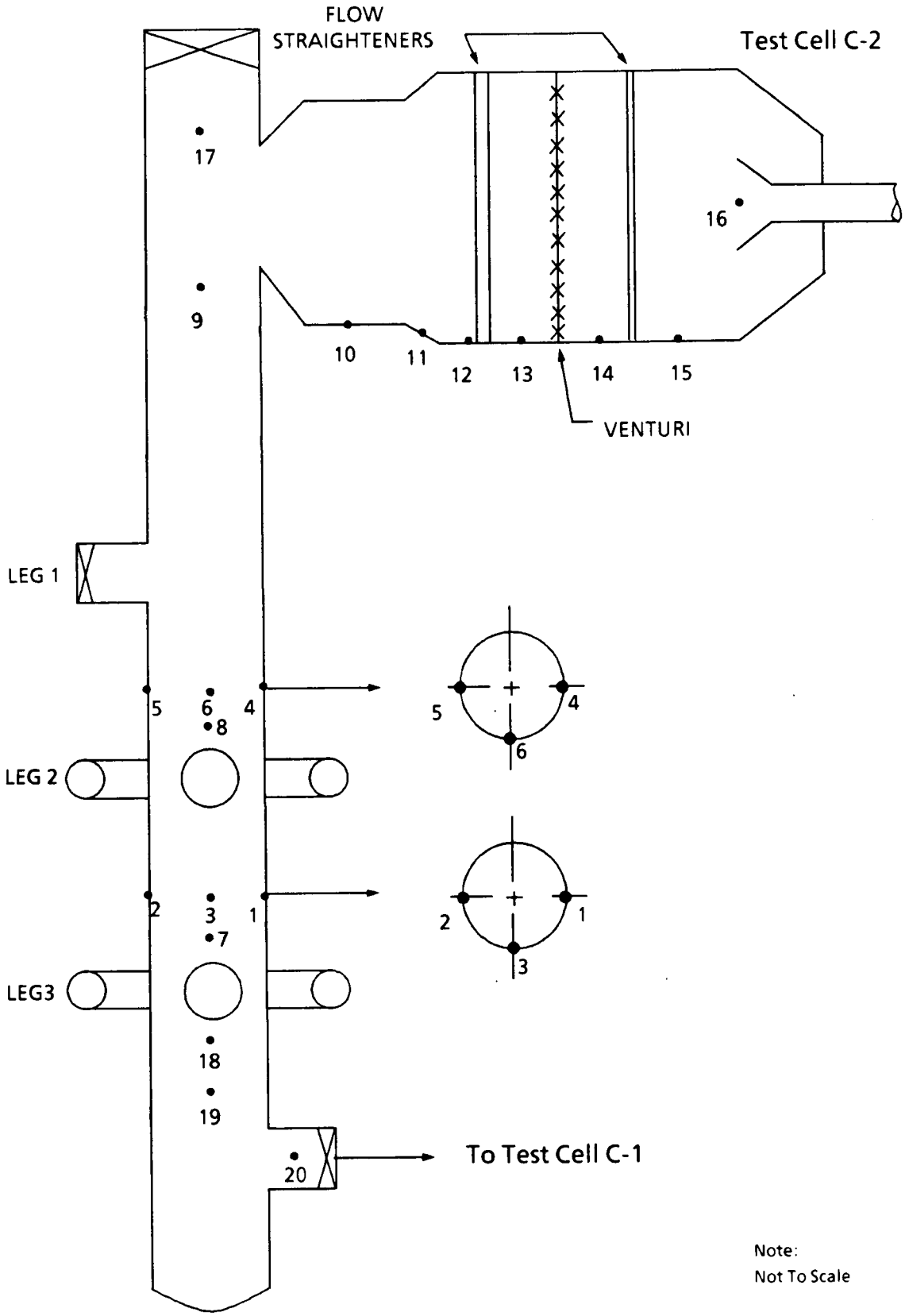


Figure 4.2.2.2.1-1 Duct Metal Temperature Measurement Locations

related to the total duct length. However, this result still indicates that an extremely high degree of longitudinal mixing occurs in this duct segment.

4.2.2.2 Heat Transfer. The heat transfer was validated for that portion of the facility between the mixing valves and the inlet to test cell C-2. During the initial runs of the facility, it was noted that the difference between the temperature of the air in the mixing header and upstream of the first C-2 flow straightening grid was large. There is no internal hardware between these two locations, thus indicating that the heat transfer rate to the duct wall is high.

4.2.2.2.1 Special Test Cases. Thermocouples were then added to the outside duct wall at various locations (Figure 4.2.2.2.1-1) to estimate the heat transfer rates. (Thermocouples for the venturi and flow straighteners were already in place.) A set of four special test cases were then run -- similar to those executed for the validation of the "N-subvolume technique." These cases were:

1. m = Low $\Delta T_{legs} = 70°F$
2. m = Medium $\Delta T_{legs} = 60°F$
3. m = Medium $\Delta T_{legs} = 270°F$
4. m = High $\Delta T_{legs} = 70°F$

Flow was quickly swapped from the Leg 2 mixing valves to the Leg 3 mixing valves for each case thereby producing a near step increase in temperature into the mixing header while attempting to hold all other

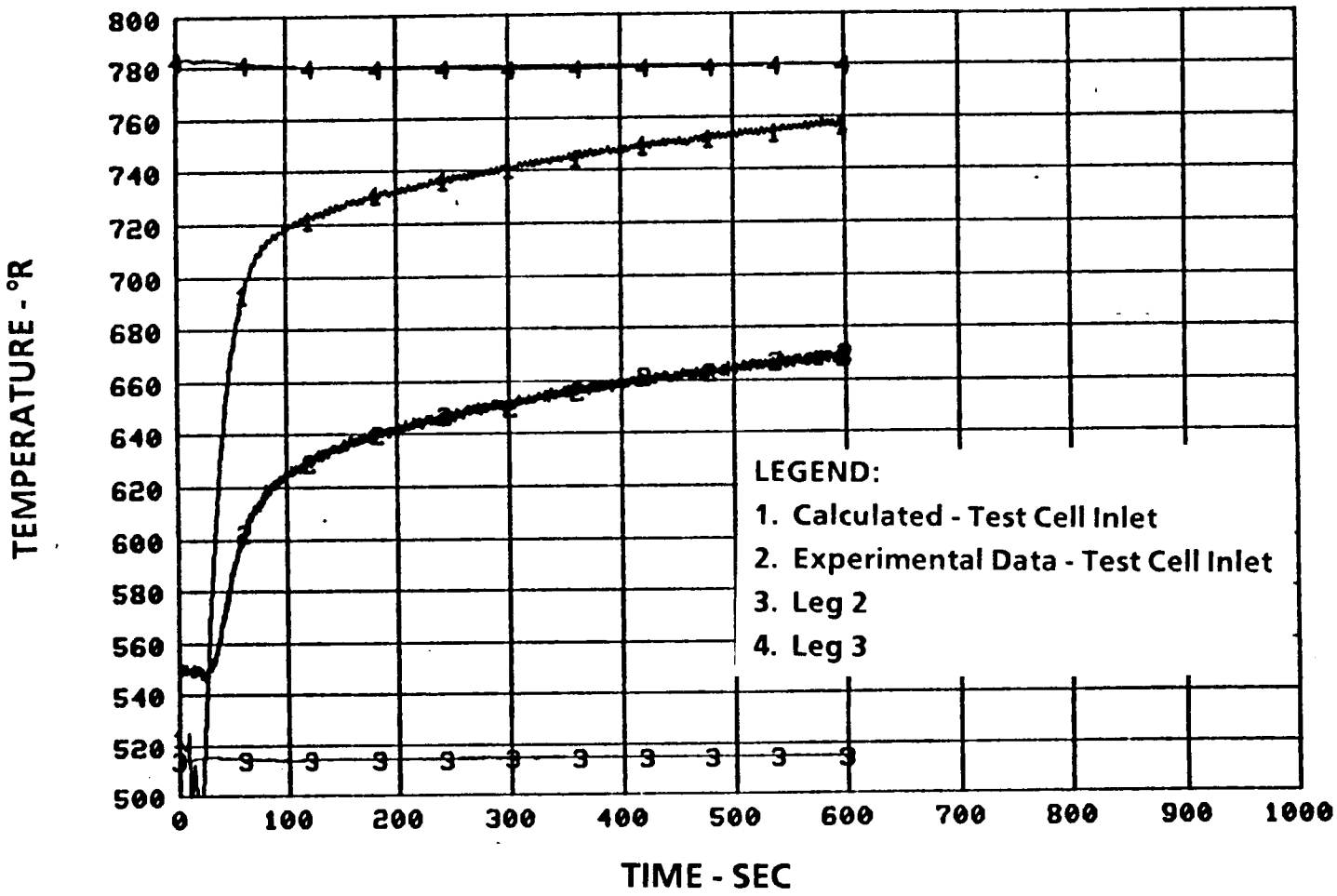


Figure 4.2.2.2.2-1 Example-Heat Transfer Validation - Initial Comparison

4.2.2.2.3 First Parametric Study. A parametric study (see Section 4.1.2) was conducted on the heat transfer coefficients and on the duct temperature for the first part. The duct mass was calculated at several values of time, using actual data from the four test cases, by the following equation

$$M_m = \frac{Q}{c_m \frac{dT_m}{dt}}$$

where

$$Q = m\, c_p \left(T_{B_2} - T_{B_1} \right)$$

and

T_{B_2} = Measured air temperature upstream of the straightener

T_{B_1} = Measured air temperature upstream of the Leg 3 mixing valves

$\frac{dT_m}{dt}$ = Average rates of change for metal temperatures at locations 7, 8, 9, 10, 11, and 12 (see Figure 4.2.2.2.1-1, page 116)

The mass, M_m, was found to vary from point to point but with a maximum deviation of only 20% from the average value of 900,500 lbm. The ducting mass calculated from the facility drawings was only 414,490 lbm. (Of course, the lumped parameter technique is only an approximation, but the major cause for this difference is identified later in this section.)

The inside heat transfer coefficient used for the ducting is given by [15]

$$h = \frac{0.0384\, k_f (Re_d)^{0.75} (Pr)}{D\left(1 + 1.5\,(Pr)^{-1/6} (Re_d)^{-1/8} (Pr-1)\right)}. \qquad (4.2.2.2.3\text{-}1)$$

Because the denominator of Equation (4.2.2.2.3-1), the thermal conductivity and the Prandtl number vary very little over the range of test conditions, the ratio of the product of thermal conductivity and Prandtl number to the denominator was set equal to a constant, C_1, and the parametric study sought to validate the resulting heat transfer coefficient expression

$$h = C_1 C_2 Re_d^x.$$

The heat transfer coefficient was calculated from experimental data using

$$h = \frac{Q}{A_s\left(\frac{T_{B_1} + T_{B_2}}{2} - T_m\right)}$$

where

$$Q = m\, c_p \left(T_{B_2} - T_{B_1}\right).$$

The values of h/C_1 were plotted against Re_d for the four test cases. The result showed a linear relationship on a log-log plot. The slope of line, x, was 0.569 and the value of C_2 was determined to be 4.922. The validated equation for h is, therefore, (approximately)

$$h = \frac{4.922\, k_f\, Re_d^{0.569}\, Pr}{D\left(1 + 1.5\,(Pr)^{-1/6}(Re_d)^{-1/8}(Pr - 1)\right)} .$$

The math model was then changed to reflect the new heat transfer equation and the new value of ducting mass and the simulation was rerun for the four test cases. The results were in excellent agreement with the experimental data with the exception of Case No. 3 which remained slightly out of the ±5% tolerance band on test cell inlet temperature. It was not surprising that at least one of the cases would be outside of tolerance, because the second part of the system was yet to be validated.

4.2.2.2.4 Second Parametric Study. Attention was then focused on the portion of the facility from the first flow straightener to the test cell inlet. Sufficient data were available to conclude that the math model for the venturi subsystem was in error. Validation of this subsystem proceeded along similar lines as for the first part of the system. The mass of each venturi in the venturi subsystem was calculated from experimental data to be 15,000 lbm -- up from the 424 lbm used in math model. (Apparently this difference is due to the venturi bulkhead mass which had not been included in the original theoretical calculations.) The venturi heat transfer coefficient was then validated via a parametric study in a similar manner to that described for part one.

Again the math model was upgraded and the simulation rerun. The results for the four test cases are presented in Figures 4.2.2.2.4-1 through 4.2.2.2.4-4. The test cell inlet temperature is within the ±5% criteria for all four test cases. As was the situation with the validation of the "N-Subvolume Technique", the initial dip in the inlet temperature is due to the inability to hold pressure constant during the initial part of each transient.

4.2.2.2.5 Other Heat Transfer Studies. One of the assumptions built into the math model was that no heat is transferred into a ducting stub-off either by conduction through the duct metal or by convection from the air. It was observed during each of the four test cases that the duct temperature of the stub-off into test cell C-1 (see Figure 4.2.2.2.1-1, page 115) rose almost as rapidly as the "active" part of the ducting into C-2.

A simple calculation was performed to determine the mechanism by which this heat was transferred. For one of the test cases, the rate of heat transfer into the stub-off ducting to C-1 was calculated from

$$Q = M c_m \frac{dT_m}{dt}$$

and found to be 700,000 BTU/hr. It was then assumed that conduction was the responsible transfer mechanism and the heat transfer rate was approximated by the equation

$$Q = \frac{\pi D s \Delta T}{L}$$

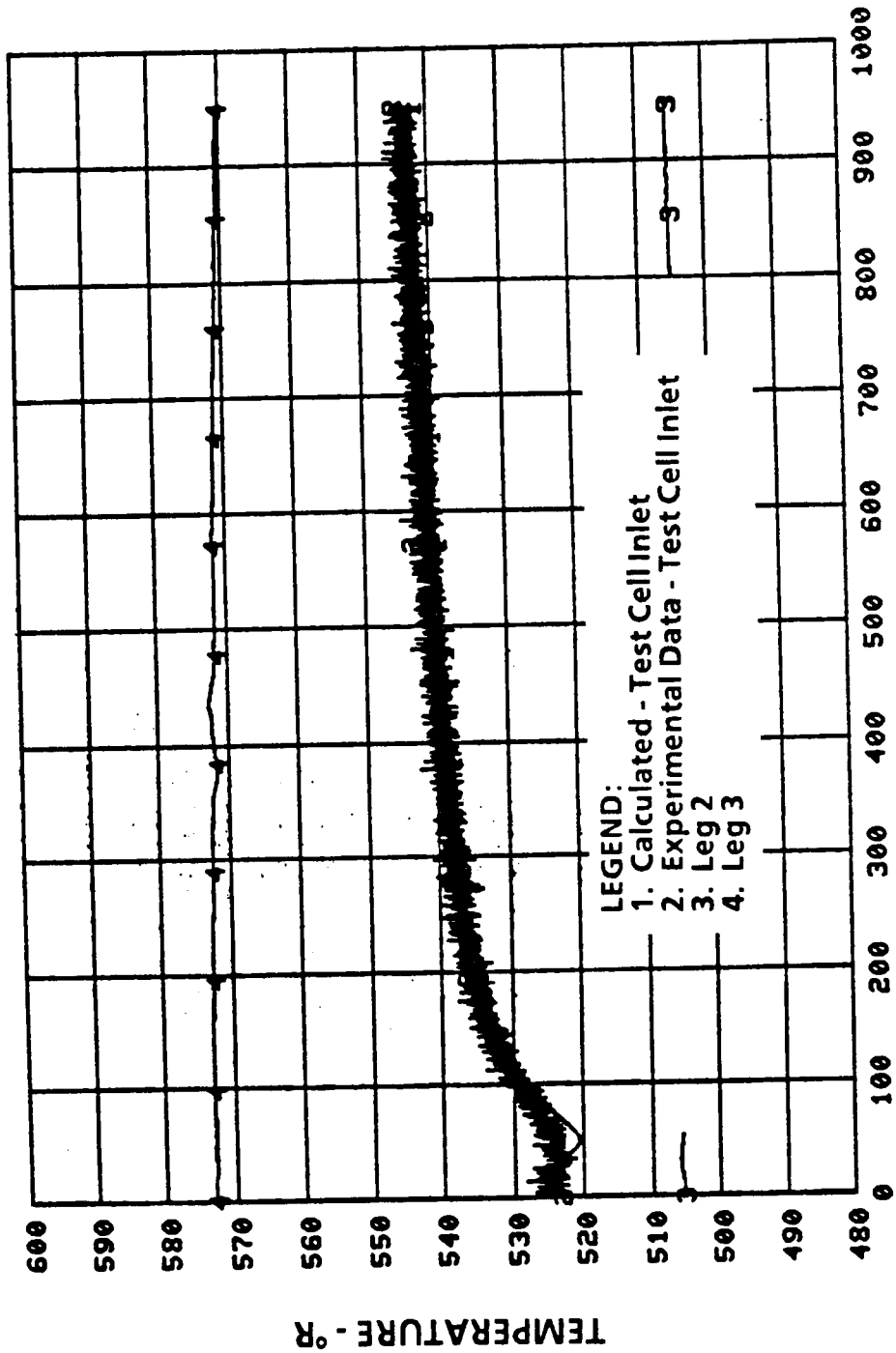


Figure 4.2.2.2.4-1 Heat Transfer Validation - Case 1

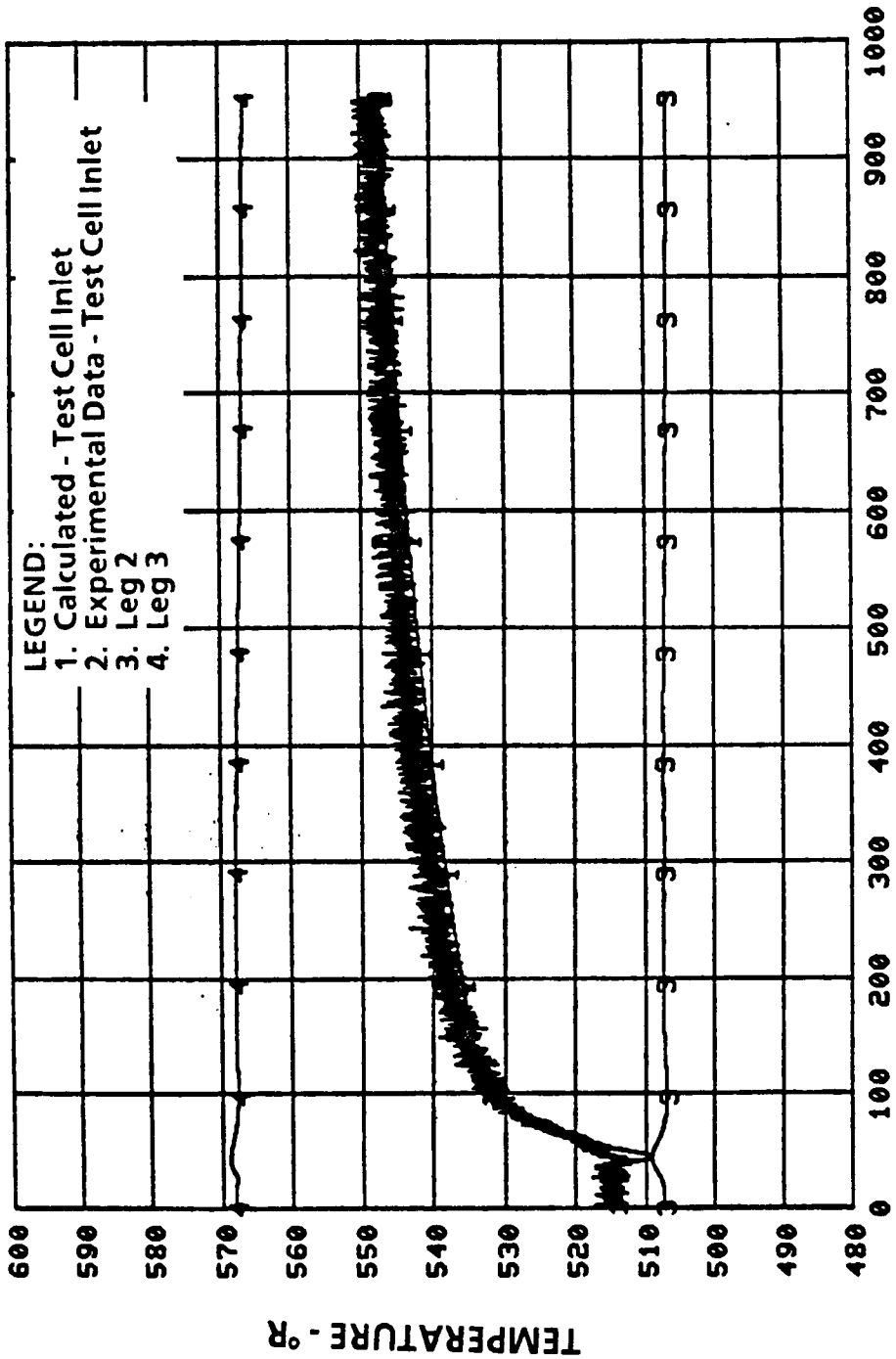


Figure 4.2.2.2.4-2 Heat Transfer Validation - Case 2

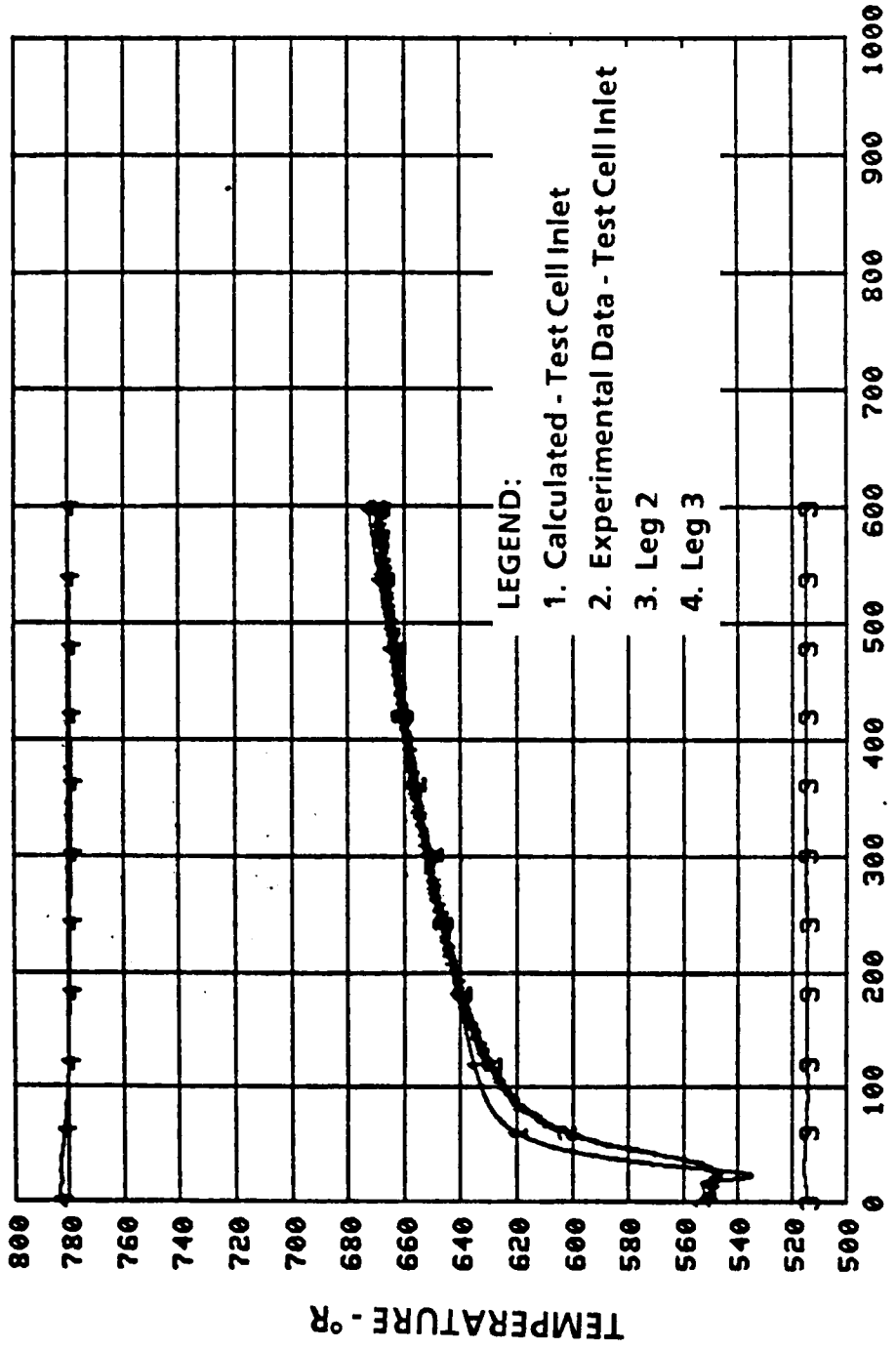


Figure 4.2.2.2.4-3 Heat Transfer Validation - Case 3

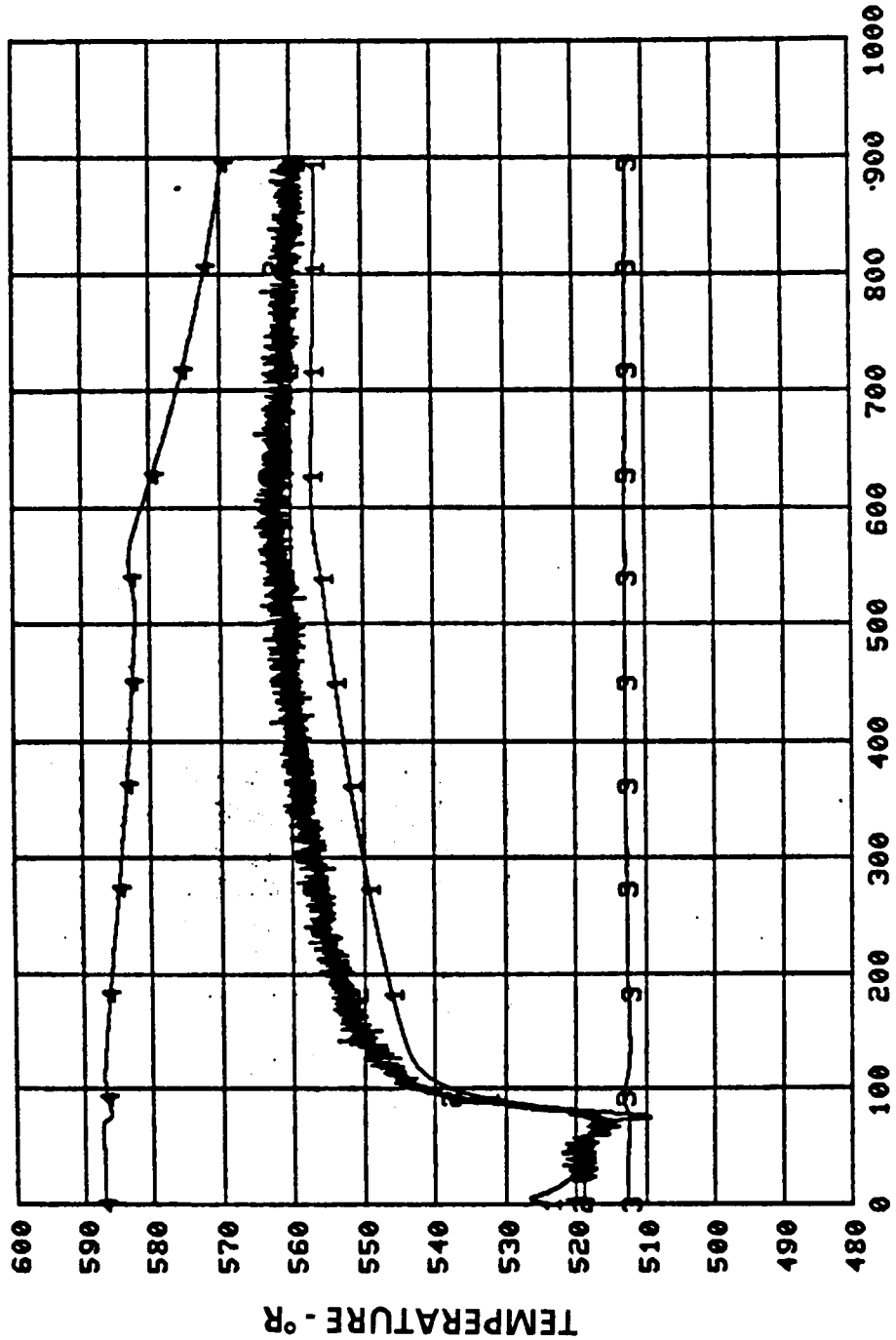


Figure 4.2.2.2.4-4 Heat Transfer Validation - Case 4

where s is the duct wall thickness and $\Delta T/L$ was the linear, transient, temperature gradient obtained from experimental data. It was discovered that in order to conduct only one-tenth of the actual heat transfer rate (70,000 BTU/hr), a temperature difference of over 12,000°F was required! It was therefore concluded that the primary heat transfer mechanism was convection -- not conduction.

The above result implies that a tremendous degree of swirling of the air in the stub-offs existed. It also accounts for why the mass of part of the ducting in the active flow path had to be increased by a factor of two in the validation of the ducting heat transfer between the mixing valves and the first flow straightener.

The validation of the heat transfer for a complex three-dimensional flow field by using a lumped parameter technique for the metal and simple heat transfer coefficient equations for fully developed axisymmetric flow is considered to be one of the most significant achievements of the ASTF modeling project. Without this accomplishment, a real time simulation would have been in serious jeopardy.

It should be emphasized, however, that Equation (4.2.2.2.3-1) is a theoretical relationship valid only for steady, fully developed, turbulent, axisymmetric flow. The flow is neither steady, fully-developed nor axisymmetric in this portion of ASTF. The constant coefficient and, to a lesser degree, the Reynolds number exponent in the validated equation changed so drastically that suspicion exists as to whether this technique can be successfully applied to other similar facilities.

4.2.3 Facility. No facility level validation was accomplished.

CHAPTER 5

A METHODOLOGY FOR THE DEVELOPMENT OF MATH MODELS AND SIMULATIONS

5.1 Background

The team that developed the ASTF math models and simulations has worked on several modeling and simulating projects for many years. It has been noticed that the project generally goes well when the modelers, simulationists and users are the same people. Requirements are clearly understood, approaches to the development are agreed upon easily, everyone is aware of all aspects of the development and the work flows smoothly throughout the duration of the project. User requirements are usually met because the user helped perform the work.

On the other hand, difficulties arise when the modelers, simulationists and users are different people. The difficulties are amplified when different organizations are involved. Communication problems are usually present. Organizational responsibility problems arise. Most workers no longer see "the big picture" because they only have a piece of the project. The actual purpose of the simulation may be forgotten during the course of the project. And, most importantly, too little attention may be given to the user.

Others have also experienced difficulties. McLeod [12] documented the results of a Workshop on Model Acceptance held in Washington, D. C., in April 1981. Thirty-four people, all of whom were well versed in modeling and simulating, attempted to determine what made a modeling project successful. Poor communication was assessed to be the biggest obstacle in developing useful models. Model credibility was noted as

being another major problem area. If the customer, or project sponsor, does not view the model as credible, then any recommendation that comes out of the modeling and simulating effort will not likely be adopted. Questions in the area of ethics were raised and discussed at length. How do modelers and simulationists avoid possible bias throughout the development? Bias can be exhibited by erroneous assumptions, the improper use of "soft" data and by designing simulation experiments that highlight desired aspects and downplay other, less desirable or unfavorable, aspects. Reference [12] addresses the above problems, as well as many others, and offers advice for developing models that are both credible and useful.

Clema, et al. [16] lists ten most common modeling and simulating pitfalls and briefly discusses how to avoid them. Included in the list are:

- Failure to define an achievable goal,
- Inadequate level of user participation,
- Poor communications,
- Obsolete or nonexistent documentation
- Using an unverified or invalid model, and
- Poor presentation of results.

Although References [12] and [16] point out many of the problems which occur in an extensive simulation project and offer useful advice toward avoiding them, they do not provide a complete framework to support such a project. During the course of the work covered by this dissertation, a project management structure evolved which was of great

benefit to the project. It is believed that this management structure plus other applicable project features (a methodology) could be applied directly to other large projects, and, suitably scaled down, to even very small projects.

For such a methodology to be useful it must address all important aspects of modeling and simulating. It must be sufficiently general that it would, when properly tailored, be applicable to any modeling and simulating project. It must include adequate documentation, and must have provisions for proper planning, project organization and project management. It must include user participation from project inception. It must contain adequate reviews and employ configuration management. It must, overall, provide for a structured, disciplined and highly visible development.

Prior to introducing the methodology, a brief review of the modeling and simulating process is presented such that the methodology may be more thoroughly understood.

5.2 Brief Review of the Modeling and Simulating Process

5.2.1 Fundamental Technical Components. There are several fundamental technical components of a modeling and simulating project. The most notable are:

1. Determine the requirements which the final simulation must satisfy.
2. Develop the equations that represent the actual system and transmit to the simulation organization.

3. Program these equations on a computer to produce a simulation.

4. Compare the computer program that represents the simulation to the equations and modify the simulation when mistakes are found.

5. Compare the results of simulation runs to experimental data from the actual system or facility and modify the model when excessive differences are discovered.

6. Assemble and transmit deliverables to the project sponsor.

Components 4 and 5 are of particular importance due to the confusion that sometimes exists in these areas. These components are commonly termed verification and validation, respectively, as defined in 4.1, page 97, and are repeated here for convenience:

Verification - The process of determining that a computer program causes the computer to operate as intended by the programmer (i.e., the equations have been programmed correctly).

Validation - The process of determining that the computer simulation behaves like the actual system under study in all pertinent respects.

The relationship among the actual system, the math model, the computer simulation, and the "V&V" activity is shown in Figure 4.1.1-1, page 99.

As previously noted in Section 4.1.1, if the computer simulation does, indeed, accurately represent the math model (i.e., the simulation has been verified), then the simulation becomes transparent in the math

model validation effort. Simulation results can then be compared with actual data with a high degree of confidence that the comparison to the math model is valid.

5.2.2 Fundamental Project Management Components. Many fundamental project management components exist. The most important are:

1. A documented plan for the development
2. Other documentation
3. Reviews and audits
4. Quality assurance
5. Configuration management
6. Schedule (with milestones)
7. Project organization
8. Resource allocation and management

Of particular importance are components 1, 2, and 3. Documentation, which is always important to any development project, becomes crucial when different organizations are involved in the development. It represents the only way of communicating requirements, allocating and authorizing organizational responsibilities and transmitting the results of the development. Reviews and audits become a vital component necessary for interagency understanding and approval of the work as the development progresses.

5.3 The Methodology

The major features of the methodology fall into two categories - those that are general in nature and those that are specific to the

development at hand. The general features are presented first. These are:

A project management structure which includes:

Documentation,

Design Reviews and Configuration Audits,

A Quality Assurance Program, and

A Configuration Management Activity.

An identification of the steps to be performed during the development process.

A test philosophy which includes:

Types of Testing to be Performed,

Goals of Testing, and

Approach to Testing.

An Independent Technical Review Activity.

Each of these features are discussed in turn.

5.3.1 Documentation. The following specifications and baseline documents should be written (in order of publication):

- Model and Simulation Specification (MSS)
- Initial Model Baseline (IMB)
- Program Performance Specification (PPS)
- Initial Simulation Baseline (ISB)
- Model Validation Specification (MVS)
- Simulation Verification Specification (SVS)
- Model Validation Report (MVR)
- Simulation Verification Report (SVR)

- Final Model Baseline (FMB)
- Final Simulation Baseline (FSB)
- Users Manual (UM)

The Model and Simulation Specification contains the technical requirements for the development effort. It contains every requirement which is essential to the success of the project and no requirement which is non-essential. Some examples of the topics that should be covered are:

The objective(s) of the model and simulation development.

A detailed description of the facility or system to be modeled and simulated.

Selection of Modeling Technique: Bottom-Up or Top-Down.

Requirements for a "Discussion" Model. (In general, it is recommended that such a high-level, simplified model be developed.)

The approach to the modeling effort. Included in this topic should be:

Governing Modeling Techniques and Assumptions (e.g., for continuous systems, considerations of lumped versus distributed parameter).

System Effects Incorporated (e.g., transport lag phenomena, heat transfer considerations, individual versus combined components, approximations of valve dynamics, etc.)

Treatment of Existing Experimental Data, if any.

Relationship to Previously Developed Models, if any.

System Level Model Accuracy Requirements (This should be quantitative).

Model Inputs.

Model Outputs.

Simulation Hardware Considerations (Analog, Digital or Hybrid; Timing Requirements).

Simulation Accuracy Requirements.

Treatment of how all requirements are to be confirmed (e.g., inspection, analysis or test).

The Initial Model Baseline is an interim document that describes the completed model. It contains all the equations and logic that mathematically define the system. It also identifies and justifies the various assumptions utilized in the development and contains sufficient narrative for easy understanding by the reader.

The Program Performance Specification states the detailed requirements for the software that constitutes the simulation. It primarily consists of all the model equations and logic. It also contains specific programming guidelines and quality assurance provisions for the software. The specific format and contents of this document are contained in MIL-STD-1679.

The Initial Simulation Baseline is an interim document that describes the completed simulation. It contains all the software which fulfills the requirements of the PPS. It describes all pertinent aspects of software implementation (e.g., choice of numerical integration technique) which may impact fulfillment of PPS requirements. It

also contains sufficient narrative for easy understanding by the reader. The specific format and contents of this document are also contained in MIL-STD-1679 (under the title "Program Description Document").

The Model Validation Specification documents, in detail, the requirements for the validation effort. It defines the validation process, describes how validation is to be applied, identifies the required test cases, assesses data requirements and allocates the system level model accuracy requirements in the MSS to the subsystem level. This document may be very voluminous because all measurement locations must be identified and discussed. The Model Validation Specifications for a large facility could be in excess of 100 pages in length.

The Simulation Verification Specification documents, in detail, the requirements for the verification effort. It defines the verification process, describes how verification is to be applied, and delineates the specific software verification activities (code walkthroughs, software test cases, etc.) that will be applied at both system and subsystem levels.

The Model Validation and Simulation Verification Reports document the validation and verification efforts, respectively. They should contain a brief description and results of each test or analysis that was conducted. Any deviations from the associated specification should be noted and explained. A summary should also be prepared which

addresses the overall degree of success in the validation and verification efforts.

The Final Model Baseline documents the validated model. This document can be most conveniently generated by simply revising the IMB to reflect the changes to the equations that resulted from the validation effort.

The Final Simulation Baseline documents the verified simulation. The ISB can simply be revised to reflect changes to the simulation that resulted from the verification effort. However, this document must also reflect changes to the model that resulted form the validation effort. The requirements for these latter changes are documented in a revision to the PPS.

The Users Manual documents user interface requirements. It contains short, descriptive summaries of the model, provides instructions on executing the simulation, identifies responsible organizations and individuals, and delineates all inputs and outputs for the user. It also references the MSS, the FMB, and the FSB for more detailed information. This document should be written in easy-to-read, non-technical terms.

5.3.2 Design Reviews and Configuration Audits. A total of six design reviews and one configuration audit should be held in the course of the development. Four of these should be formal, two should be internal, and one should be informal. The formal reviews or audit should be convened, have agendas and should be attended by representatives from all organizational functions. An internal review involves only model or

simulation development personnel and their immediate technical supervision. An informal review involves all organizational functions but does not require convening.

The following reviews and audit should be held:

Review/Audit	Document Reviewed	Internal	Formal	Informal
Model and Simulation Requirements Review (MSRR)	MSS		X	
Program Performance Specification Review (PPSR)	PPS			X
Model Critical Design Review (MCDR)	IMB MVS		X	
Simulation Critical Design Review (SCDR)	ISB SVS		X	
Simulation Verification Review (SVR)	Revisions to ISB	X		
Model Validation Review (MVR)	Revisions to IMB	X		
Verification and Validation Audit (VVA)	FMB, FSB MSS		X	

Figure 5.3.2-1 presents a summary of work phases, documentation, reviews and audit in relation to the various development work phases.

In addition, to the reviews and audit noted above, two other types of meetings should be conducted. First, Monthly Review Meetings should be held throughout the course of the development. The primary purpose of these meetings is to keep all agencies abreast of the progress of the development so that the various reviews can be based on a complete understanding of the project. Second, it is advisable, especially for

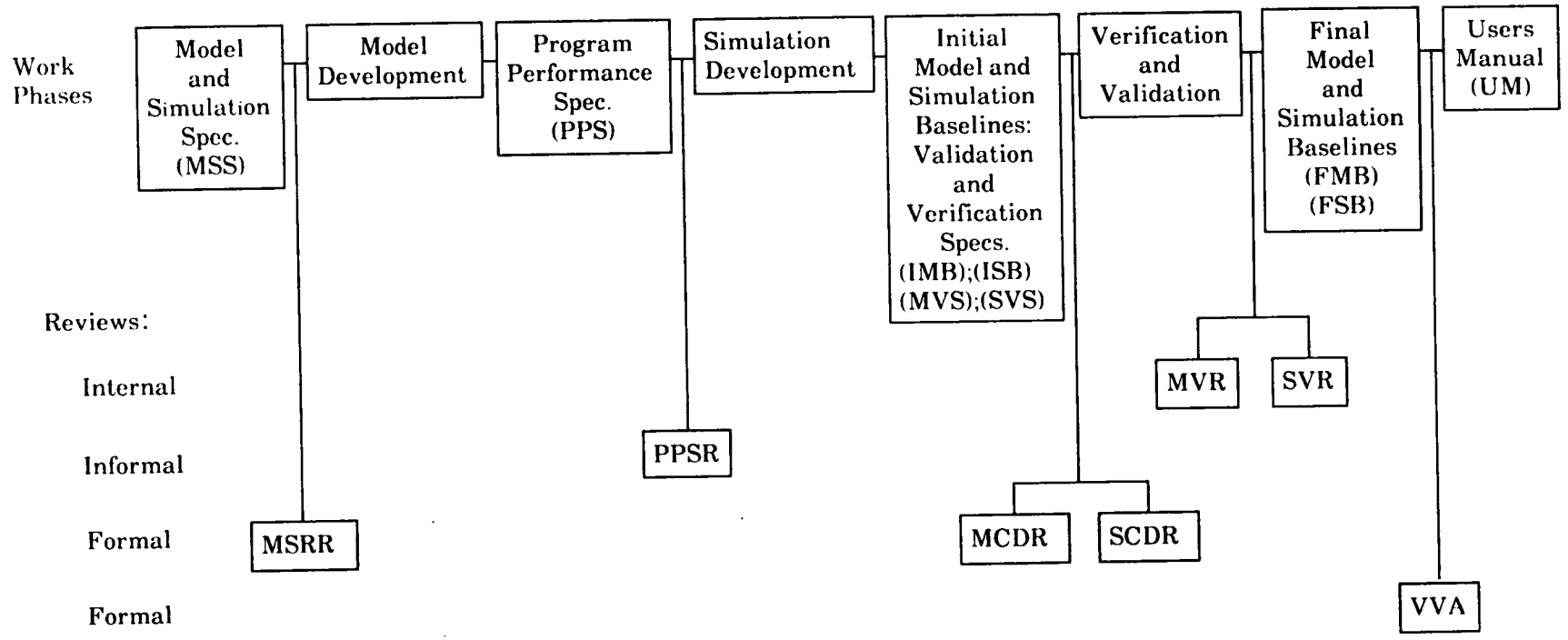


Figure 5.3.2-1 Summary of Work Phases, Documentation, Reviews and Audits

large and complex developments, to have the equivalent of a "Preliminary Design Review" for both the model and the simulation early in their development. This ensures that the requirements have been properly understood and are being correctly implemented.

5.3.3 Quality Assurance. Quality Assurance (QA) should be conducted at two different levels: system and development. The system level QA function is responsible for ensuring that the system level requirements contained in the MSS have been correctly identified and documented. System level QA is also responsible for ensuring that these requirements have been met at the end of the development (at the VVA). A QA panel, consisting of recognized experts, should be assembled for these tasks. The QA panel chairman should sign-off on the MSS, FMB, and the FSB.

The development level QA function should ensure that all formal structured activities and controls are properly invoked and executed. Of particular importance are the following tasks:

Ensure that the writing of all formal documents is conducted in a timely and professional manner.

Properly plan, coordinate and conduct all formal meetings, reviews and audits.

Ensure that all configuration management requirements are properly invoked.

Ensure that all testing conforms to applicable specifications.

Coordinate all important activities and progress with all agencies.

The responsibility for development level QA should be assigned to a single individual with sufficient authority to carry out the above tasks.

5.3.4 Configuration Management. The Configuration Management (CM) disciplines of configuration identification, configuration control and configuration status accounting should be imposed throughout the development process. The CM activity should address basically two different areas: documentation and simulation code. All the documents identified above and the simulation code associated with the ISB should be baselined under CM at publication. Changes to the documents and code should not be permitted unless approved by a Configuration Control Board (CCB).

The CCB should be composed of representation from all agencies and chaired by the individual who has first level responsibility for the entire project. A detailed treatment of CM can be found in MIL-STD-483 or in numerous textbooks.

5.3.5 Steps in Modeling and Simulating. The steps involved in model and simulation development are presented in network form in Figure 5.3.5-1. As can be noted, the model and simulation development are shown in parallel. In the ideal case, the model should be developed first, the PPS then written and, finally, the simulation developed based on the PPS requirements. However, most projects cannot afford the calendar time required to perform these steps consecutively. The

concurrent development shown in Figure 5.3.5-1 involves developing and transmitting the PPS in a piecemeal manner as the model is developed. (All official requirements would still be contained in the final, complete version of the PPS.) Some risk is involved here because changes to the model may be required as the model development progresses. However, this risk should be taken for time-critical development in order to start the simulation work as soon as possible.

It is important to recognize that a verified simulation is usually required for the validation process. The actual system or facility and the verified simulation are exercised for identical test cases and the outputs are compared. Changes are then made to the equations and the simulation; and, the simulation is rerun. This process continues until the outputs from the simulation and the actual facility are within predefined accuracy tolerances. (Changes to the model equations are most conveniently documented by simply revising the PPS.) If the simulation has not been verified, it will not be possible to determine if disagreements in outputs are caused by an erroneous model or errors in the simulation. There are cases, however, when exercising the simulation is not required. These cases exist when, for example, the model (or a submodel) is composed entirely of experimental data. A dimensional analysis representation of a facility component fits this category. Another example is when the submodel is so simple that the outputs can be determined without exercising the simulation.

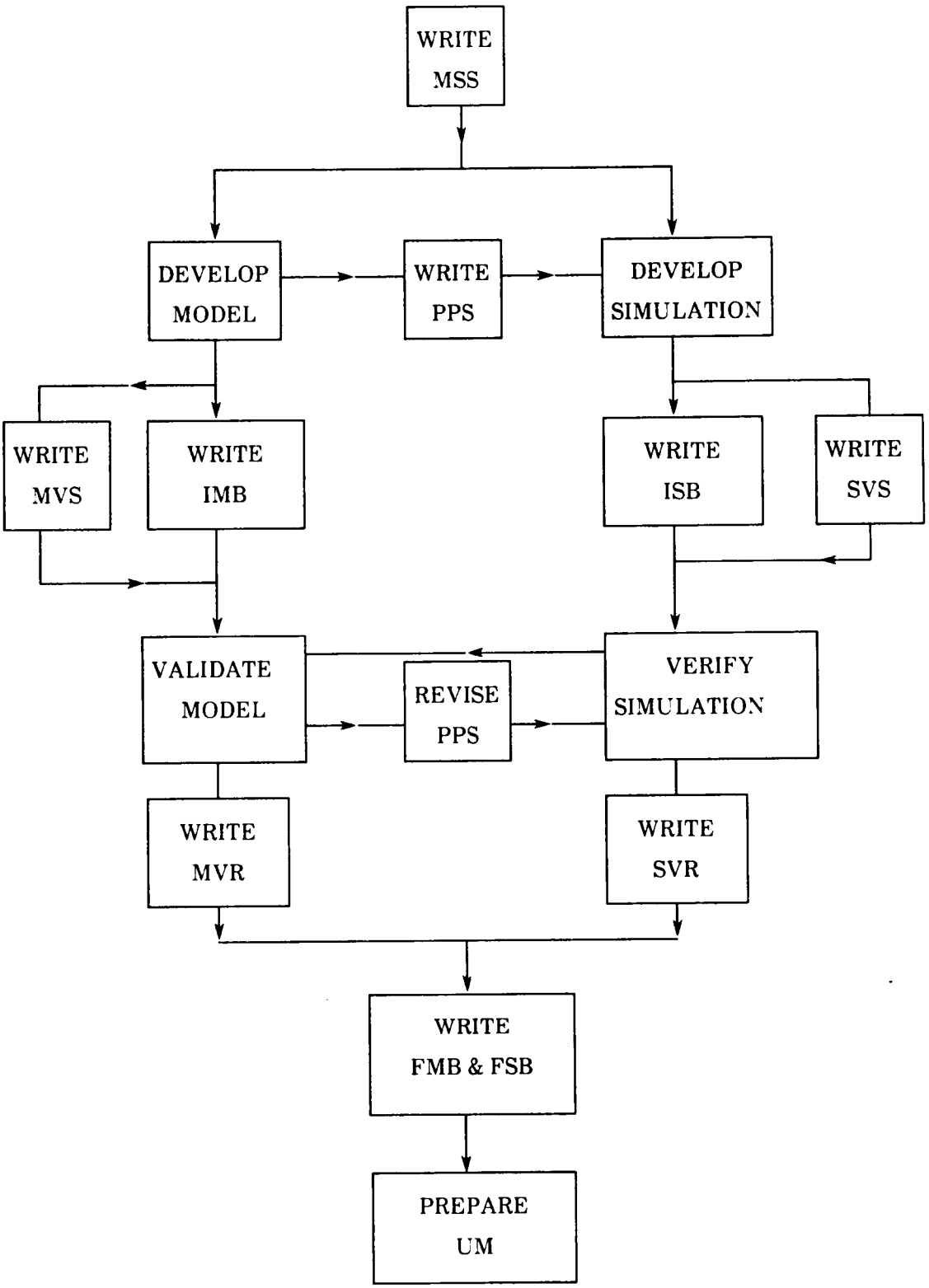


Figure 5.3.5-1 Steps in Model and Simulation Development

5.3.6 Types of Testing. There are basically two different types of testing associated with modeling and simulating: validation testing and verification testing. Validation testing involves testing the facility being modeled (i.e., collecting experimental data) for comparison with simulation predictions and is part of the overall validation process. Verification testing involves testing the software (simulation) for compliance with the specified model, and is a part of the overall verification process.

5.3.7 Goals of Testing. The goal of validation testing is to collect sufficient data such that the validation effort, as specified in the MVS, can be successfully applied. In some cases sufficient data may already exist and, therefore, no additional testing is required.

The goal of the simulation testing is to demonstrate that the software is reasonably free from errors and that the simulation will perform as specified in the SVS.

5.3.8 Approach to Testing. The approach to validation testing should be detailed in the MVS. First, a hierarchy of validation should be established. "Subsystems" typically comprise the lowest level. A subsystem is the smallest portion of the facility for which a math model has been derived. A "system" is composed of two or more subsystems. The "facility" is composed of two or more systems. Specific test cases should be established for each level in the hierarchy. Test cases at the system and facility levels typically relate to the validation of equations utilized to couple and otherwise integrate the various subsystems and systems. Instrumentation requirements in terms of loca-

tion, accuracy and response must be assessed. Finally, careful planning should be directed toward the conduct of each test such that resource expenditures can be minimized.

The approach to verification testing should be detailed in the SVS. In a general sense, this testing is very similar to validation testing. The hierarchy of verification would typically include "modules," "subprograms," and "system." Test cases should be generated for each level. Expected outputs and overall pass/fail criteria should also be generated. Further details of software testing are beyond the scope of this dissertation. However, the interested reader can find these details in MIL-STD-1679, MIL-STD-2167, or in any of several textbooks on the subject.

5.3.9 Independent Technical Review. An independent technical review team should be assembled, especially for complex development efforts. The team should be composed of recognized experts in the fields of math modeling and computer simulation. The team's primary responsibility is to act in an advisory capacity to the project sponsor. Team members should have "hands on" participation in the development by reviewing requirements, evaluating approaches and final designs, suggesting alternate approaches, and evaluating the adequacy and results of the validation and verification efforts. It is important that this team have complete freedom in exercising their responsibility. For this reason, team members should be selected from outside agencies and report directly to the project sponsor. (This portion of the

methodology was strictly enforced for the ASTF modeling effort and proved to be very beneficial to the overall project.)

5.3.10 The Development Plan. The features discussed to this point correspond to the more general parts of the methodology. These features should be tailored to the specific development at hand in much the same manner that MIL-STDs are tailored for software development. Once tailored, these more general features should be included in a Model and Simulation Development Plan (MSDP) - a document to be written at project inception. Additional features, which are much more peculiar to the specific development effort, should also be included in the MSDP. Figure 5.3.10-1 shows the MSDP outline in order that these additional features may be identified and discussed. Sections, 1, 2.1, 4, 6, 7, 8, 9, 10, 11 and 12 represent these additional features. Each is discussed in turn.

Introduction

Background

This section should contain all background information relevant to the development effort. As a minimum, a brief description on how the development fits into other ongoing work, especially in the modeling and simulating area, should be included.

Purpose

The purpose of the development effort should be stated as concisely as possible.

1.0 ..... INTRODUCTION
1.1 ..... BACKGROUND
1.2 ..... PURPOSE
1.3 ..... SCOPE
1.4 ..... OVERVIEW OF MANAGEMENT PHILOSOPHY
1.5 ..... AUTHORITY
1.6 ..... DEFINITIONS
2.0 ..... PROJECT ORGANIZATION AND MANAGEMENT
2.1 .... PROJECT ORGANIZATION
2.1.1 ... CONTRACTUAL RELATIONSHIPS
2.1.2 ... MODEL AND SIMULATION ORGANIZATION
2.2 .... PROJECT MANAGEMENT
2.2.1 ... DOCUMENTATION
2.2.1.1 .. SPECIFICATIONS
2.2.1.2 .. MODEL AND SIMULATION BASELINES
2.2.1.3 .. REPORTS
2.2.1.4 .. USERS MANUAL
2.2.2 ... DESIGN REVIEWS AND AUDITS
2.2.3 ... QUALITY ASSURANCE
2.2.4 ... CONFIGURATION MANAGEMENT
3.0 ..... STEPS IN MODELING AND SIMULATIING
4.0 ..... COMPUTER RESOURCE CONTROL
5.0 ..... TEST PHILOSOPHY
6.0 ..... USER RELATIONSHIPS
7.0 ..... DEVEOLPMENT SUPPORT FACILITIES
8.0 ..... OTHER AGENCY FURNISHED EQUIPMENT AND SERVICES
9.0 ..... RISK AREAS
9.1 .... TECHNOLOGICAL RISKS
9.2 .... SCHEDULE RISKS
9.3 .... COST RISKS
10.0 ..... SCHEDULE AND MILESTONES
11.0 ..... RESOURCE ALLOCATION AND MANAGEMENT
11.1 ... PLANNED ALLOCATION
11.1.1 .... PERSONNEL
11.1.2 .... SERVICES
11.1.3 .... MATERIAL
11.1.4 .... TRAVEL
11.2 ... MANAGEMENT OF RESOURCES
12.0 ..... DELIVERABLES

Figure 5.3.10-1 MSDP Table of Contents

Scope

The development effort should be scoped as carefully as possible. Describe the model and associated simulation that is to be developed. State precisely what is to be done so as to avoid misunderstandings later. If needed for clarity, also state what is not going to be done.

Overview of Management Philosophy

Give a synopsis of how the project should be managed. For example,

Specifications shall be written.

A series of design reviews and configuration audits shall be conducted.

A Quality Assurance Team shall be assembled.

A Technical Review Panel shall be assembled.

A network with scheduled milestones shall be constructed and followed.

Other pertinent features, as required.

Authority

The individual or agency that authorized the development effort should be stated. (Also, it is important that the MSDP approval page or approval form contain the signatures commensurate with the level of authority required.)

Definitions

Include whatever definitions are appropriate.

Project Organization

Contractual Relationships

All contractual relationships to be implemented should be identified and discussed. A discussion which is centered around a contractual organizational chart is ideal.

Modeling and Simulating Organization

The development organization should be identified and discussed. It is important that all assigned individuals be identified. This paragraph should also specifically identify the responsibility of each function in the organization. For large projects, it is a good idea to form functional teams with assigned team leaders.

Computer Resource Control

This topic applies to the simulation and is most important when the simulation must execute in "real time." If real time execution is required, or if for any other reason computer resources are to be minimized, techniques should be identified for accomplishing this requirement. Resource control not only implies efficient programming but may also have implications on model simplifications.

User Relationships

The simulation user(s) is a very special individual (or agency) in any model and simulation development. Too often

user requirements are de-emphasized. Too often a simulation is developed that does not totally meet user needs. It is imperative that the ultimate user be brought into the development effort in the planning stage. This paragraph should identify the user, summarize user requirements and detail the relationship with the user that will exist throughout the development.

Development Support Facilities

All facilities to be used in support of the development effort should be identified and discussed. These facilities can range from the computer system in which the final simulation will be executed to interactive terminals used in the simulation development.

Other Agency Furnished Equipment and Services

The work discussed in the MSDP typically is to be done by the developing organization utilizing its own resources. This paragraph provides a means by which services and equipment to be furnished by other agencies can be identified. Such identification minimizes subsequent misunderstandings.

Risk Areas

All risk areas should be specifically identified. These risks typically fall into three categories: technological, schedule, and cost. Examples of technological risks include missing the accuracy requirements of the model and simulation, and other unachieveable performance criteria. Schedule risks

involve such areas as technical difficulties with the equation development, problems with the simulation, and inadequate manning by any organization. Cost risks are closely coupled to schedule risks, complexity of the development effort, and to the ability to accurately scope the work.

Schedule and Milestones

The successful management of every major project requires a detailed schedule with meaningful milestones. In the case of model and simulation development, the steps in the development shown in Figure 5.3.5-1, page 141, can be used as the basis for formulating the schedule and milestones.

Resource Allocation

The planned resource allocation should be specifically stated. The manhours demanded from each individual in the organizational chart should be documented. All required services, material, and travel should be identified. A paragraph dealing with the management of resources should also be included. Finally, it is important to document what alternatives are available if additional resources are required.

Deliverables

This paragraph should state precisely what is to be delivered to the project sponsor. It is suggested that all documents previously identified be declared as deliverables.

5.4 Application of Methodology at the AEDC

The methodology, in its entirety, has yet to be applied at AEDC to any one project. However, two partial applications have been made. The first application relates to the modeling and simulating activity addressed by this dissertation -- the ASTF. The IMB and MVS were written, and the validation effort formally applied and documented. The second application involves the coordinated development of several independent modeling and simulating projects relating to a turbine engine test facility.

5.5 Application To Other Development Efforts

Sufficient portions of the methodology have been applied at AEDC to recognize that it can, and should, be applied to other development efforts. The key to the application is in the tailoring process. For very large and complex developments, the full methodology should be applied. However, for smaller and less complex efforts, some reviews, monthly meetings and perhaps the Technical Review Panel could be eliminated. (It should also be pointed out that the documents become very short for a simple development project.) For other projects it might be advisable to keep the Technical Review Panel due to the complexity of the work but delete or refine other features. The important point is that refinements to the methodology should be based on the details of the specific development at hand.

5.6 Summary

A new, perhaps first, general methodology for developing math models and simulations has been devised. The methodology introduces structure, discipline and visibility into the development process such that the work can be conducted in a more orderly, effective and efficient manner.

Plans and technical requirements are well documented. The model and associated simulation are baselined under configuration management; and, verification and validation are formally applied based upon detailed specifications. After the verification and validation efforts are completed, the final model and simulation baselines are audited for conformity to project requirements. A users manual is then published.

The development effort is overseen by a Technical Review Panel to ensure that technical requirements are being properly implemented. A formal Quality Assurance program is invoked. Timely reviews are conducted throughout the development to ensure conformance to requirements and coordination of the development among all appropriate agencies. Finally, provisions for active participation by the user are included and strongly encouraged such that the finished product does, indeed, meet user requirements.

The result of these planned and structured activities -- documentation of plans and technical requirements, conduction of verification and validation on detailed specifications, incorporation of timely reviews and audits, the oversight by a Technical Review

Panel, and the conduction of QA and CM activities -- is that model and simulation credibility are maximized and conformance to user requirements is ensured.

It is believed that, with proper tailoring, the methodology can be meaningfully applied to any modeling and simulating project. The tailoring process involves reviewing the specific development at hand and refining the methodology accordingly. Typically, for large and complex developments, the entire methodology should be applied. For smaller and less complex projects certain features can be simplified or eliminated. Once tailored, application of that methodology maximizes the probability that the development

will be completed on or ahead of schedule and within or below budget, and

will produce a credible model and simulation that meet user requirements.

CHAPTER 6

SUMMARY AND RECOMMENDATIONS

The successful mathematical modeling and real time computer simulation of a large industrial facility characterized by gas pumping and conditioning equipment may be a very challenging task, especially if some of the facility operates in a transient operational mode. The mathematical relationships must be kept as simple as possible in order to minimize the required computational resources yet sufficiently accurate to meet what may be very tight validation criteria. The idea of implementing sets of partial differential equations in the independent variables of spatial coordinates and time can usually be immediately dismissed because such an approach can easily overtax the capability of any existing computer system. Even if a real time simulation is not required, the additional complexity of partial differential equations may be unnecessarily expensive in terms of equation development, programming, verification, and computer execution costs.

The gas flow processes for the facility addressed by this study -- the ASTF -- were mathematically modeled utilizing steady state and ordinary differential equations. Recent advances in digital computational state-of-the-art, coupled with the success achieved in keeping the mathematical relationships simple, led to the implementation of a real time simulation on an off-the-shelf SEL 32/67® minicomputer. This is a 32 bit machine rated at four mips (AEDC estimate) with two mbytes of main memory. The simulation consisted of 10,600 lines of FORTRAN source code with an execution cycle time of 50 ms. The system that

controls test conditions in ASTF -- the ATCS -- was interfaced to the minicomputer and the facility operators were trained and the ATCS hardware and software were operationally checked prior to ATCS control of the facility.

Several key technical issues were addressed and resolved during the course of the project. First, based on previous experience with the modeling of a smaller, yet functionally similar facility, it was assumed that the lumped parameter technique could be utilized -- a technique that freed the basic mathematical model from partial differential equations. This technique is applicable only to low Mach number flow (to at least M = 0.2) and yields approximations to thermodynamic properties as a function of spatial coordinates only between each successive lump. Second, the dimensional analysis technique was heavily emphasized. This very simple, yet powerful modeling method, results in one of the easiest tasks that a digital computer can execute -- a table look-up. Third, a special, original technique was developed to approximate temperature transport lag when a variable degree of longitudinal mixing in the ducting is present. Again, no partial differential equations are involved.

Even though the original ducting heat transfer model seriously underestimated the heat transfer rates, the subsequent validation effort was successfully completed via a parametric study of a lumped parameter model for the ducting with associated heat transfer coefficients determined by simple equations for axisymmetric flow. This was accomplished in spite of the fact that the air flow in the portion of

the facility between the mixing valves and the inlets to the test cells experiences a high degree of longitudinal mixing in the active ducting and swirling in the dead leg "stub-offs" -- truly a three-dimensional phenomena.

All the above techniques are believed to be applicable to other industrial facilities characterized by gas pumping and conditioning equipment. It is strongly recommended that these techniques be investigated for suitability to other, similar modeling and simulating projects. The material is presented at a level sufficiently general to facilitate such an investigation.

Finally, there were many "lessons learned" throughout the duration of the ASTF modeling and simulating effort. Rather than simply provide an itemized listing and discuss how these mistakes may be avoided, a comprehensive modeling and simulating methodology is presented and thoroughly discussed. When properly tailored, it is believed that this methodology is applicable to essentially any modeling and simulating project. Consequently, it is recommended for general use.

BIBLIOGRAPHY

BIBLIOGRAPHY

1. "The United States Air Force's Arnold Engineering Development Center Aeropropulsion Systems Test Facility," Office of Public Affairs, Arnold Engineering Development Center, Arnold Air Force Base, Tennessee, December 1987.

2. Polce, Ronald L., "A Systems Description of the Aeropropulsion Systems Test Facility (ASTF)," AEDC-TMR-82-E59, October 1982.

3. Clouse, Ron L., "A Methodology for Control Algorithm Development," 1984 Proceedings of the Summer Computer Simulation Conference, July 1984.

4. Cunningham, J. W. and Bang, Major C. J., "Fault-Tolerant Control System for Jet Engine Testing," Presented to the "Spring Compcon - 1983," The IEEE Computer Society, February 1983.

5. McGregor, W. K., Jr., et al., "Analysis of Gas Flow Systems for Dynamic Control Purposes," AEDC-TR-55-11, April 1956.

6. Zuker, Robert D., Fundamental of Gas Dynamics, Matrix Publishers, Inc., Champaign, Illinois, 1977.

7. Albertson, Maurice L., et al., Fluid Mechanics for Engineers, Prentice Hall, Inc., Englewood Cliffs, New Jersey, 1960.

8. Suiec, James, Heat Transfer, Simon and Schuster, New York, New York, 1975.

9. Buckingham, E., "Model Experiments and the Forms of Empirical Equations," Presented at the Spring Meeting of the American Society of Mechanical Engineers, Buffalo, New York, June 1915.

10. Obert, Edward F., Concepts of Thermodynamics, McGraw-Hill Book Company, New York, New York, 1960.

11. Huang, Francis F., Engineering Thermodynamics Fundamentals and Applications, Second Edition, Macmillan Publishing Company, New York and Collier Macmillan Publishers, London, 1988.

12. McLeod, John, P. E., Computer Modeling and Simulation - Principles of Good Practice, A Society for Computer Simulation Publication, 1982.

13. Kheir, Naim A., "On the Credibility of Models," Proceedings of the 1981 Summer Computer Simulation Conference, July 1981.

14. Lalwani, C. S., "Verification and Validation of Simulation in Social Sciences," Proceedings of the 1982 Summer Computer Simulation Conference, July 1982.

15. Eckert, E. R. G., Heat and Mass Transfer, McGraw-Hill Book Company, Inc., New York, New York, 1959.

16. Clema, Joe, Delfosse, Claude, and Russell, Ed, "The Ten Most Frequent Causes of Simulation Analysis Failure ... and How to Avoid Them!," CACI, Inc., Federal, 1983.

VITA

Ronald L. Clouse was born in a two room, rural farmhouse in Coffee County, Tennessee on June 23, 1940. He first attended school in a weather-boarded, log cabin with no electricity, pot-bellied stoves and with drinking water that was carried from a spring about one-quarter of a mile away. The cracks in the floor were so numerous and wide that the teacher periodically sent some of the older boys crawling under the floor to retrieve pencils, erasers, and other supplies. He was graduated from the same elementary school in 1955, but in a new four room building.

He was graduated from Manchester, Tennessee Central High School and after a brief period working at odd jobs, entered the University of Tennessee at Knoxville. After a year at the university, he was awarded a cooperative engineering scholarship with Sverdrup Technology, Inc. at the Arnold Engineering Development Center near Manchester, Tennessee. He was graduated from the University of Tennessee, with honors, in Mechanical Engineering in June 1963. He began his part-time graduate student career in September 1963 while working for Sverdrup and was awarded a Master of Science degree from the University of Tennessee in March 1977. He was awarded the Doctor of Philosophy degree in August 1990.

The author is a registered professional engineer and is a member of numerous professional, honorary, and civic organizations. He is

also a member of the Hillsboro, Tennessee congregation of the Church of Christ where he serves as song director.

He is married to the former Francis Diane Alexander of Florence, Alabama. They have two children, Mrs. Renee Holt and Miss Mysty Clouse, both of Manchester.